



University
of Glasgow

<https://theses.gla.ac.uk/>

Theses Digitisation:

<https://www.gla.ac.uk/myglasgow/research/enlighten/theses/digitisation/>

This is a digitised version of the original print thesis.

Copyright and moral rights for this work are retained by the author

A copy can be downloaded for personal non-commercial research or study,
without prior permission or charge

This work cannot be reproduced or quoted extensively from without first
obtaining permission in writing from the author

The content must not be changed in any way or sold commercially in any
format or medium without the formal permission of the author

When referring to this work, full bibliographic details including the author,
title, awarding institution and date of the thesis must be given

Enlighten: Theses

<https://theses.gla.ac.uk/>
research-enlighten@glasgow.ac.uk

ULTIMATE STRENGTH DESIGN
OF PERFORATED DEEP BEAMS

A thesis submitted to the University of Glasgow
for the degree of Master of Science

by

GUL HASSAN MEMON, B.E.

Department of Civil Engineering
University of Glasgow.

May, 1982

J. S. HERON LTD
5 QUEENS CRESCENT
ST. GEORGES CROSS
GLASGOW 041 332 1883

ProQuest Number: 10646837

All rights reserved

INFORMATION TO ALL USERS

The quality of this reproduction is dependent upon the quality of the copy submitted.

In the unlikely event that the author did not send a complete manuscript and there are missing pages, these will be noted. Also, if material had to be removed, a note will indicate the deletion.



ProQuest 10646837

Published by ProQuest LLC (2017). Copyright of the Dissertation is held by the Author.

All rights reserved.

This work is protected against unauthorized copying under Title 17, United States Code
Microform Edition © ProQuest LLC.

ProQuest LLC.
789 East Eisenhower Parkway
P.O. Box 1346
Ann Arbor, MI 48106 – 1346

To
my Parents
and
my Teachers

ACKNOWLEDGMENTS

The work described in this thesis was carried out in the Department of Civil Engineering at the University of Glasgow under the general direction of Professor A. Coull, to whom the author is indebted for his help and interest.

The author wishes to express his deep sense of gratitude to his supervisor Dr. D.R. Green, for his valuable guidance, active interest and constant encouragement during all phases of this work.

The author is grateful to Dr. P. Bhatt for his valuable proposals and advices on various aspects of the work.

For their support and encouragement, the author would like to thank all the staff members of the Civil Engineering Department. Many thanks are also due to his research colleagues who have contributed in various ways with their helpful discussion and assistance.

The author wishes to thank the staff of Engineering Department workshops and in particular Messrs. J. Thomson and J. Coleman for their help in conducting the experimental work.

Thanks are due to Ms. Carol John for her assistance with computer work.

Sincere thanks are expressed to Mrs. J. Lawn for her neat and diligent typing of this manuscript.

Thanks are due to the Government of Pakistan for financial support and to Mehran University of Engineering & Technology for granting study leave.

Finally the author expresses special thanks to his family for their great support and patience.

SUMMARY

The design of deep beams with or without openings is not yet covered by the new British Code CP110 (1972). The CIRIA guide does contain some design guidance for solid deep beams but the design of deep beams with openings is only briefly covered. In both cases the design procedures follow an empirical approach.

The current trend in reinforced concrete design is towards the ultimate limit state methods. In recent years proposals have been made for a more rational approach to reinforcement design for in-plane forces. For a given ultimate load, a stress field in equilibrium with external loads is obtained by a linear elastic stress analysis, e.g. finite element analysis. Reinforcement is provided such that the combined resistance of steel and concrete at every point is equal to or greater than the applied stresses. If the equilibrium and yield criteria are satisfied exactly at every point then the entire structure will be converted to a mechanism at ultimate load. In order for this to happen the structure should have sufficient ductility so that redistribution of stresses takes place as cracking occurs.

This thesis is concerned with an experimental study of the proposed design method applied to deep beams with openings and in general with the effect of the opening on beam behaviour.

The test series comprised of seven specimens of deep beams with and without an opening having different concrete strengths and varying span to depth ratios. The effects of an opening on/

deflections, crack widths, crack patterns, failure mode and ultimate shear strengths were studied. All the beams were simply supported and under two concentrated top loads except one. The beams were loaded in increments without unloading until collapse occurred.

The test results indicate that the ultimate loads were higher in beams where an opening is near the beam soffit than in beams where an opening is at mid-depth. In all the tests the experimental ultimate load greatly exceeded the design load. Why this is so is discussed and by using an empirical factor experimental ultimate load predictions are improved. Further analytical and experimental study is recommended.

CONTENTS

	<u>Page</u>
Acknowledgments	iii
Summary	iv
Contents	vi
List of Tables and Figures.	ix
Symbols and Units of Measurements.	xii
<u>CHAPTER ONE</u> <u>INTRODUCTION</u>	1
1.1 General.	1
1.2 Objective and Scope.	3
<u>CHAPTER TWO</u> <u>LITERATURE REVIEW</u>	4
2.1 Introduction.	4
2.2 Review of Previous Work.	4
2.2.1. Reinforced concrete solid Deep Beams.	5
Theoretical Investigation.	5
Experimental Investigation.	6
2.3 Estimates of the Ultimate Shear Strength of Deep Beam.	13
2.4 Deep Beam with Openings.	16
Theoretical Investigation.	17
Experimental Investigation.	19
Conclusions.	27
2.5 Outlines of Design Methods for solid Deep Beams.	28

<u>CHAPTER THREE</u>	<u>DESIGN PHILOSOPHY</u>	<u>Page</u> 36
3.1	Introduction	36
3.2	Object of Limit State Design.	37
3.3	Limit State Design.	38
3.3.1.	Equilibrium Criterion.	41
3.3.2.	Yield Criterion.	42
3.3.3.	Mechanism Criterion.	46
3.4	Serviceability Limit State.	46
3.5	Practical Constraints.	47
3.5.1.	The Application of the Finite Element Programme.	47
3.6	Design Consideration for Reinforced Concrete Deep Beams with Web Opening.	48
3.6.1.	Design for Reinforcement.	48
3.6.2.	Bearing Capacity.	49
3.6.3.	Bond and Anchorage.	51
<u>CHAPTER FOUR</u>	<u>TEST PROGRAMME</u>	52
4.1	Introduction	52
4.2	Test Programme.	52
4.2.1.	Test Specimens.	52
4.2.2.	Beam Notation.	53
4.3	Materials.	54
4.3.1.	Concrete.	54
4.3.2.	Reinforcement.	54
4.3.3.	Fabrication and Curing.	55

	<u>Page</u>
4.4 Test Procedure.	56
4.4.1. Test Apparatus.	56
4.4.2. Test Method.	57
4.5 Instrumentation.	57
<u>CHAPTER FIVE</u> <u>TEST RESULTS</u>	59
5.1 Presentation of the Test Data and Results.	59
5.1.1. Crack Pattern and Modes of Failures.	59
5.1.2. Crack Width.	61
5.1.3. Load-Deflection.	63
5.1.4. Concrete Surface Strains.	64
5.1.5. Steel Strains.	65
5.1.6. Ultimate loads.	66
5.2 Factors Affecting the Behaviour of Deep Beams with Openings.	67
5.3 Analysis of Test results.	70
A) Serviceability limit state.	70
B) Ultimate limit state.	71
<u>CHAPTER SIX</u> <u>CONCLUSIONS</u>	76
6.1 Introduction.	76
6.2 Conclusions.	76
6.3 Suggestions for Further Work.	79
APPENDICES.	
1. Concrete Surface Strain. Distribution at Section 1-1 and 2-2.	80
2. Steel Strain Distribution along the bottom row of bars above and below the opening.	98
REFERENCES.	109

LIST OF FIGURES AND TABLES

CHAPTER 2.

- Figure 2.1. Development of arch-action in deep beam.
- Figure 2.2. Meaning of symbols.
- Figure 2.3. Location of opening in an unperforated stress field.
- Figure 2.4. Different failure modes observed by Sharp.
- Figure 2.5. The structural idealization (Truss model).
- Figure 2.6. Typical crack pattern in deep beam with opening.
- Figure 2.7. Failure modes for deep beam with opening (observed by Kubik).
- Figure 2.8. Idealization for deformation of beams with web opening.
- Figure 2.9. Typical planes of failure.

CHAPTER 3.

- Figure 3.1. Yield criteria for concrete in plane stress.
- Figure 3.2. Sign convention for in-plane Direct and shear stresses.
- Figure 3.3(a) Applied stresses.
- 3.3(b) Stress resisted by concrete.
- 3.3(c) Position of steel.
- Table 3.1. Various possible combinations of reinforcement.
- Table 3.2. Design equations for reinforcement.
- Table 3.3. Boundary curves.
- Figure 3.4. Boundary equation graph.
- Figure 3.5. Finite element mesh.
- Figure 3.6. Flow Chart for reinforcement design.

Table 3.4. Modified boundary equations corresponding to
table (3.3).

Figure 3.7. Conditions for chosen cases of boundary curves.

Table 3.5. The theoretical steel ratios required at each
element for beam B4/0.95/0.22/2.

Figure 3.8. Design for reinforcement for beam B4/0.95/0.22/2.

CHAPTER 4.

Figure 4.1. Details of size and position of the openings.

Table 4.1. Details of the dimensions and properties of the
beams.

Figure 4.2. Arrangement of reinforcement.
(a-g)

Table 4.2. Concrete mix proportions used for the test beams.

Figure 4.3. Uniaxial stress strain curve for plain concrete.

Figure 4.4. Typical stress-strain relationship for various
sizes of bars.

Table 4.3. Properties of Reinforcement.

CHAPTER 5.

Figure 5.1. Crack pattern at failure of the beams.

Figure 5.2. Maximum crack width curves.

Table 5.1. Comparision of service cracking loads and Measured
loads.

Figure 5.3. Central deflection curves.

Table 5.2. Design loads. Yield loads above and below the
opening and Measured loads.

Table 5.3. The relationship between the Measured Ultimate load
and the concrete strength.

Table 5.4. The relationship between the Measured Ultimate load and the steel ratios.

Table 5.5. Measured service load, Design ultimate load and the Measured ultimate load.

Figure 5.4. Comparison of service load and design ultimate load.

Figure 5.5. Load-transmission paths.

Figure 5.6. Comparison of predicted and Measured strength.

Table 5.6. Measured and Computed ultimate load.

Table 5.7. Design Load, Measured ultimate load and theoretical load.

SYMBOLS AND UNITS OF MEASUREMENT

A	area of individual web bar, for the purpose of equation (2.3), (2.4), (2.8), (2.9), (2.10), (5.1), (5.2) and (5.3), the main longitudinal bars are also regarded as web bar.
A_c	area of concrete (CP 110).
A_r	used in equation (2.20a), see symbol A.
A_s	area of main longitudinal reinforcement.
A_{sc}	area of compressive reinforcement.
A_{sh}	area of the horizontal web steel (ACI Code).
A_{sv}	area of the vertical web steel (ACI Code).
A_x, A_y	reinforcement areas per unit thickness in the directions x and y.
a	shear span.
a_L	shear span below web opening.
a_u	shear span above web opening.
B	beam notation.
b	breadth (thickness) of beam.
c_1	empirical coefficient in equation (2.3), (2.4), (2.8), (2.9), (2.10), (5.1), (5.2) and (5.3), (for normal weight concrete, $c_1 = 1.4$, for light weight concrete $c_1 = 1.35$).

c_2	empirical coefficient in equation (2.3), (2.4), (2.8), (2.9), (2.10), (5.1), (5.2) and (5.3). (for deformed bars $c_2 = 300 \text{ N/mm}^2$, for plain round bars $c_2 = 130 \text{ N/mm}^2$).
c_3	0.35 in equation (2.3).
D	overall beam depth.
d	effective depth.
E_c	Young's modulus of concrete.
f'_c	specified compressive strength of concrete.
f_{cu}	characteristic concrete cube strength.
f'_s, f'_s	specified yield strength of tension and compression reinforcement respectively.
f_t	characteristic cylinder splitting strength of concrete.
\bar{f}_x, \bar{f}_y	reinforcement stresses in the directions x and y respectively.
f_y	characteristic (or specified) yield strength of reinforcement.
H	horizontal force induced around a web opening in the model (fig.2.8).
H_F	value of H corresponding to rotational failure of the model.
H_s	value of H corresponding to shear failure in the region between the beam end and the web opening.

h	used in equation (2.5) and Fig. (2.8), see symbol D.
h_a	effective height of the beam.
h_L	depth of beam web below an opening.
h_o	depth of a web opening (Fig. 2.8).
h_u	depth of beam web above an opening.
h_1	depth of an opening (Fig. 4.1).
h_2	coefficient defining the position of an opening.
k	splitting coefficient according to Ramakrishnan and Ananthanarayana.
k_1, k_2, \bar{k}	coefficients defining the position of an opening used in equation (2.4), (5.1) (5.2) and fig. (5.5).
L	simple span of beam, generally refer to a distance between centre lines of supports.
l_n	clear span measured face to face of supports.
M	design moment at ultimate limit state.
M_u	ultimate moment at section (ACI Code).
M_1, M_2, M_3, M_4	hinge moments (Fig. 2.8).
n	total number of bars.
P_c	ultimate load used in equation (2.2).
P''_s	ultimate load used in equation (2.1).

Q	shear force.
Q_B	shear transmitted below a web opening.
$(Q_B)_F$	value of Q_B corresponding to rotational failure of the load path below the opening.
$(Q_B)_S$	value of Q_B corresponding to shear failure of the load path below the web opening.
Q_T	shear transmitted above a web opening.
$(Q_T)_F$	value of Q_T corresponding to rotational failure of the load path above the opening.
$(Q_T)_S$	value of Q_T corresponding to shear failure of the load path above the web opening.
$(Q_T)_{S1}$	value of Q_T corresponding to shear failure of the beam in the region above the web opening.
$(Q_T)_{S2}$	value of Q_T corresponding to shear failure of the beam in the region between the beam end and the web opening.
Q_{ult}	ultimate shear strength ($Q_{ult} = \frac{W_c}{2}$)
s_h	spacing of horizontal web reinforcement (ACI Code)
s_v	spacing of vertical web reinforcement (ACI Code).
T	total tensile force resisted by A_s .
t	distance between web opening and beam end (fig. 2.8).
V_c	shear capacity of a beam.

V_u design shear force at critical section.

v_c ultimate concrete shear stress, in equation (2.15),
 v_c = nominal shear stress carried by the concrete.

v_u limiting concrete shear stress in equation (2.14)
 v_u = nominal shear stress at critical section.

v_x, v_{ms} , shear stress parameters and steel shear stress
 v_{wh}, v_{wv} , parameters equation (2.21 a & b).
 v_{max}

W total load on beam.

W_c computed ultimate load according to equation (5.1).

W_d the design ultimate load.

W_s the service load from tests.

W_{sc} the service-cracking load at which the maximum crack width exceeds 0.3 mm.

W_{th} the theoretical calculated load from finite element analysis.

W_u the measured ultimate load from tests.

W_{ya} the yield load above the opening.

W_{yb} the yield load below the opening.

x clear shear span.

x_L clear shear span below a web opening.

x_o length of a web opening.

x_u clear shear span above a web opening.
 x_1 length of opening (Fig. 4.1).
 x_2 coefficient defining the position of an opening.
 y the depth, at which typical bar intersects the potential critical diagonal crack in deep beam which is approximately the line joining the loading and reaction points.
 y_L, y_r , used in equation (2.8), (2.10) and (2.20a), see symbol y
 y_u
 y_t horizontal distance measured from the web opening at which a reinforcing bar intersects a defined plane.
 Z lever arm.
 α acute angle between a typical bar and the potential critical diagonal crack described in definition Y above.
 α_L, α_t , used in equations (2.10), (2.9) and (2.8) respectively,
 α_u see symbol α .
 β shear span coefficient used in equation 2.2
 β_1, β_2 , constants.
 β_3
 γ_m partial safety factor for material.
 σ_1, σ_2 principal concrete stresses.
 σ_x, σ_y in-plane direct and shear stresses.
 τ_{xy}

ρ_s total steel ratio.
 ρ_t steel ratio used in de-Paiva and Siess formula.
 ρ_w $A_s/bw.d$.
 ρ_x, ρ_y reinforcement ratios in the directions of x and y.
 θ orientation of major principal concrete stress to y-axis.
 θ_r used in equation (2.20a) see symbol α .
 λ empirical factor (1.0 for main reinforcement, 1.5 for web reinforcement).
 λ_1, λ_2 constants.
 η $(Q_B)_s / (Q_B)_F$.
 μ $(Q_T)_s / (Q_T)_F$.

The SI system of measurements is used throughout this thesis.

CHAPTER ONE

INTRODUCTION

1.1 GENERAL

Deep beams are most frequently employed in modern construction and have useful applications in a variety of structures. In modern construction, e.g. in departmental stores, hotels, municipal buildings and so on, it is often desirable to have the lower floor entirely free of columns. It may be simpler to utilize the external and partition walls as deep beams to span across the column free space and carry the whole building above them instead of heavy frame construction, the use of virodeal trusses in concrete or even structural steel trusses.

It is only during the last decade or so that the research in reinforced concrete deep beams with openings has been carried out on a practical scale. The design of reinforced concrete deep beams with web openings is not yet covered by the major design codes of practice, namely the American building code ACI (Ref.1), the European recommendation CEB-FIP (Ref.2) and the British Code CP(110)(Ref.3)

In 1970, Committee European de Beton (CEB) and Federation Internationale de la Precontrainte (FIP) included the recommendation for solid deep beams in their international code. In 1971, the American building Code ACI, for the first time include recommendations for solid deep beams. Recently construction Industry research and Information Association (CIRIA) published a guide "The design of deep beams in reinforced concrete" which is the only design guide/

currently available in United Kingdom. (Ref. 4)

The design methods, which were based on the prediction of internal forces in deep beams from elastic theory, were at the time of their introduction consistent with the accepted design criteria of service load requirements.

The trend in current design thinking is towards the ultimate limit state methods. In recent years proposals have been made for a more rational approach to reinforcement design for in-plane forces. This is the direct design approach. Both the direct design approach and the more empirical methods based on elastic theory can only be verified by comparing the predicted force/deformation response with the measured experimental response of models of realistic size.

A survey of the literature shows that while many experimental programmes have considered solid deep beams little information and experimental data is available on reinforced concrete deep beams with openings. No codes of practice include recommendations for the design of reinforced concrete deep beams with openings. However CIRIA has published a guide on the design of deep beams which includes a section on the provision of web openings. Because of the lack of experimental evidence this recommendation which is also based upon elastic theory tends to be rather cautious and a more comprehensive method of design of deep beams with opening is still needed. The purpose of this investigation is to provide some experimental evidence by which the design of deep beams with openings can be assessed and to/

consider if the design process can be based on the more rational direct design approach.

1.2 OBJECTIVE AND SCOPE

This thesis is aimed at proposing a method for the ultimate strength design of perforated deep beams with the help of observed behaviour of such beams during experimental study.

The design of deep beams with openings is based on the stress field obtained by a linear elastic analysis e.g. finite element analysis. The procedure to reinforce the beam, using the calculated stress field is presented in Chapter 3.

In view of the fact that verification can be achieved by comparing the predicted response with the measured experimental response of realistic models, an experimental programme consisting of seven rectangular deep beams with openings was carried out. All the beams were simply supported and were tested under two point top loading except one. Load deflection graphs, concrete and steel strain distribution at various sections were plotted. Crack pattern, ultimate strength and failure type were studied by subjecting each beam to its ultimate load capacity. A detailed description of the experiments and analysis of results are given in Chapter 4 and 5 respectively. Based on the experimental results, the design procedure seem to be feasible.

C H A P T E R T W O

LITERATURE REVIEW

2.1 INTRODUCTION

Deep beams are found in various types of the structures. The provision of an opening to give access from one part to another part of the structure is a common feature in these beams. A knowledge of the behaviour of beams with openings is therefore essential for design.

A major contribution in this area has been made by University of Nottingham (Ref. 5-10) where several research projects on reinforced concrete deep beams without web openings, have shown that their post cracking behaviour is so complex that, at least for sometime yet empirical design procedures must be used.

Little practical design guidance is available for deep beams with web openings and a survey of the literature shows that little information and experimental data is available on reinforced concrete deep beams with web openings.

2.2. REVIEW OF PREVIOUS WORK

Most previous investigations have been concerned with solid reinforced concrete deep beams. Very few investigations have been carried out for reinforced concrete deep beams with openings, and limited experimental data is available for such cases (Ref.11). A review of literature of both solid deep/

beams and deep beams with openings, as a background to the present investigation is given below.

2.2.1. Reinforced Concrete Solid deep beams:

Theoretical Investigation

Much of the early theoretical work on deep beams was performed as examination of the change in stresses from engineer's theory of bending as span to depth ratio increases.

The pioneering work in this field was done by Franz Dischinger (Ref.12), who used trigonometric series to determine the stresses in deep beams on a number of supports. In the same paper, he also proposed an approximate solution for simply supported girders.

Analysis of single-span deep beams, in comparison to continuous ones presents more difficulties because of the increased number of boundary conditions to be satisfied. Several investigators have proposed approximate solutions for the analysis of single span deep beams. Li chow, Conway and Morgan (Ref.13) have solved the problem of single span deep beams using Fourier series and principle of least work, while Bay, Chow, Conway and Winter (Ref.14) and Uhlman (Ref.15) have given a solution using the finite difference method. Guzman and Luisoni (Ref.16) and Archer and Kitchen (Ref.17) have obtained the solution to this problem by using the strain energy method. An exact solution for single span deep beams using Fourier series has been given by Sundara Raja Iyengar (Ref.18).

Experimental verification of the results was provided/

by Casewell, Kaar and Lambart (Ref.19 and 20) who tested models of deep beams made from elastic materials. The authors concluded that when the span to depth ratio is below 1.5, the application of the ordinary flexural formula was inaccurate. The stresses in deep beams computed by ordinary flexural formulae (Euler-Bernoulli theory) were seriously in error and were so affected by localized stresses caused by the applied loading and support reactions that the relative positions of loading and support were of great importance.

Most theoretical models of deep beam behaviour have assumed that reinforced concrete is homogeneous and isotropic material (Ref.21). The stress-strain response of reinforced concrete in situations where cracking occurs is more complicated than these simple elastic homogeneous models predict. Some investigators, namely Chow, Conway and Winter (Ref.14) and Uhlman (Ref.15) have based recommendations for reinforcing deep beams on this simplified model, however cracking of the beam may lead to a redistribution of stresses which may invalidate the results of the elastic analysis upon which the design was based.

The effect of the redistribution of stresses is best determined by experimental studies of reinforced concrete beam behaviour. These are reviewed in the following section.

Experimental Investigation

Leonhart & Walther

A series of deep beams were tested by Leonhart and Walther at the University of Stuttgart (Ref.22). In 1970 the/

European Concrete Committee CEB-FIP (Ref.2) formulated design rules for deep beams based upon their findings. Their work dealt with simply supported deep beams under top loads. The experiments were designed to explore the detailing requirements and other aspects of deep beams behaviour.

Five of the twelve beams were tested under top uniform loading having span-depth ($\frac{L}{D}$) ratio equal to one and different arrangement of reinforcement including bent up bars and inclined stirrup shear reinforcement. In some beams the main steel was concentrated near the bottom, and in others it was distributed over one-fifth of the height of the beam from bottom.

They concluded that the main tension steel to resist bending moment should be calculated on the basis of moment arm

$$Z = 0.6D \quad \text{for} \quad \frac{L}{D} \gg 1$$

$$Z = 0.6L \quad \text{for} \quad \frac{L}{D} \leq 1$$

the steel area so calculated should be distributed over the bottom fifth of the depth of the beam.

The arch action behaviour was apparent from concrete and steel strain measurements in all the tests. Concrete strains measured on the beam surface were converted to stresses, found to agree reasonably well with the theoretical elastic prediction at low levels but not at loads approaching the ultimate load. The reinforcement stresses calculated from the measured strains indicated that the tension chord was weakened if the longitudinal reinforcement near bottom of the beam was bent up. In addition/

bent-up bars and diagonal stirrups, which were inclined to horizontal axis near the support region, were largely ineffective as shear reinforcement.

The beams failed either in flexure or by local failure at support. The authors believed that a well anchored tension chord continuous from support to support provides the best type of reinforcement for a deep beam.

The crack widths were noticeably reduced by distributing the reinforcement of main tension chord over the bottom part of the beam. Due to the inefficiency of bent-up bars and diagonal stirrups the authors suggested that the use of light orthogonal reinforcing mesh was adequate.

De Paiva & P. Siess:

Tests on nineteen simply supported reinforced concrete deep beams were carried out by the authors at the University of Illinois (Ref.23). The span-depth ($\frac{L}{D}$) ratio varied between the range two to six. The beams were reinforced with straight tensile reinforcement which was well anchored by welding steel plates to the ends. The beams were also provided with compression reinforcement and in some cases with vertical and inclined stirrups.

At failure, all of the beams tested had well developed vertical cracks at the section of the maximum moment and had typical inclined cracks, originating near the support and propagating upwards towards mid span. In beams without web reinforcement the cracking load was considered to be a measure of the useful capacity.

The authors found that the presence of the web reinforcement had no effect on the formation of the cracks, or on the failure load of the deep beams tested. However, the presence of such web reinforcement did significantly reduce the amount of visible damage to the beam.

The condition for tied-arch behaviour (see fig.2.1) previously suggested by Kani (Ref.24) was developed when the inclined cracking load was reached. They calculated the load from the measurements of strains along the tension reinforcement and along the top concrete surface of the beam.

From tests, three modes of failures were identified. Flexural failure occurred in nine beams, involving yielding of the tensile reinforcement. Shearing failure occurred in five beams. This involved the formation of the second parallel inclined crack outside the first and failure was due to the destruction of the portion of the concrete between these two cracks in compression. The third type of failure was flexure-shear failure and this occurred in five beams. Here the final collapse was due to shearing once the full flexural capacity of the beam had been reached.

The effect of the type and amount of web reinforcement provided was found to be not significant in changing the failure modes. But it was observed that the increasing quantity of main steel changed the mode of failure from flexural to shear. Also an increase in concrete strength increased the shear capacity but did not increase flexural capacity.

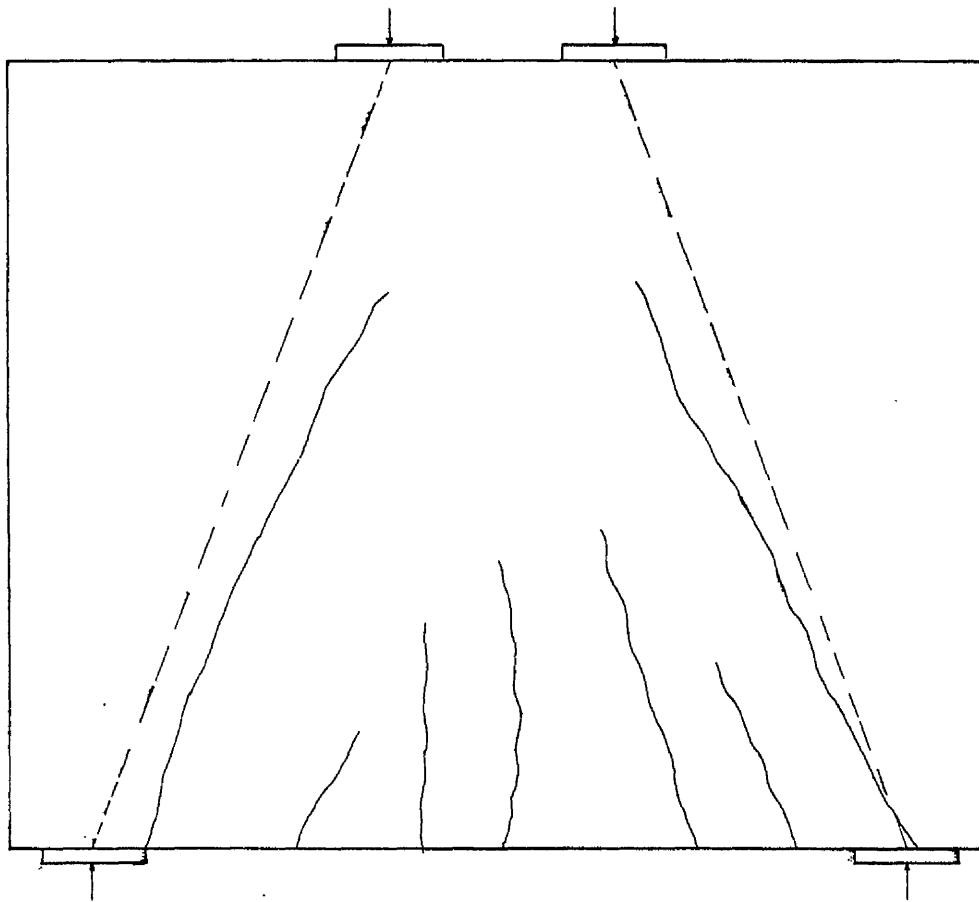


FIG.2.1. DEVELOPMENT OF ARCH-ACTION IN DEEP BEAM:

The most valuable experimental study so far for deep beams has been completed by Kong et al at the University of Nottingham (Ref.8). In two series of tests 135 beams were tested. The first series covered seventy eight simply supported deep beams under two top point loading. Span to depth ($\frac{L}{D}$) ratios ranged from 1 to 3 and clear shear-span to depth ($\frac{x}{D}$) ratios ranged from 0.23 to 0.7. Forty of these beams were made of normal weight concrete and tested by Kong, Robin and Cole (Ref.9) and Kong, Robin, Kirby and Short (Ref.25) while thirty eight were made of lightweight concrete and were tested by Kong and Robin (Ref.26).

From the results of these tests the authors showed that the presence of web reinforcement has a great influence on the development of inclined cracks whereas De-paiva and Siess found that the presence of web reinforcement has no effect on the inclined cracks.

Eight different types of the web reinforcement were used and found that the most effective web reinforcement for controlling the crack width was the "inclined" reinforcement. The effectiveness of the other types of web reinforcement was found to depend upon either one, or both of the span depth ($\frac{L}{D}$) ratio and clear shear-span-depth ($\frac{x}{D}$) ratios. These ratios were not varied independently in the tests so it was not possible to determine which was the important parameter.

In the second series of tests fifty seven (57) deep beams were tested, to isolate the effect of span-depth and clear/

shear-span-depth ratio by keeping beam depth constant.

Forty five (45) beams were made with lightweight concrete and twelve (12) with normal weight concrete. It was observed that the clear shear-span-depth ($\frac{x}{D}$) ratio was an important parameter while span-depth ($\frac{L}{D}$) was not.

For all the tested beams, the crack pattern and the mode of failure was similar. The most common type of failure involved propagation of inclined cracks which split the beam approximately along the line joining the loading and supporting points. Failures involving crushing of the strut between two such inclined cracks were also reported.

Chun Keung Lin:

Chun Keung Lin tested a series of 11 simply supported normal weight concrete deep beams at the University of Glasgow (Ref.27). The beams were divided into two groups to study the major variables, i.e. the concrete strength, the orientation of web reinforcement and span to depth ratio. All the beams were loaded under central concentrated top load and were reinforced following the stress field obtained by linear elastic stress analysis.

Following conclusions were drawn from the test results:

- 1) Increasing the amount of reinforcement does not have important influence on the load at which the diagonal crack appears but has the advantage of restricting the crack width and thus increasing the ultimate load.

2) Concrete strength is very important in deep beams. An increase in concrete strength produce an increase of ultimate strength in deep beams.

3) The inclined reinforcement was found more effective at controlling the crack widths, central deflections and for raising the ultimate shear capacity. For beams having span to depth ($\frac{L}{D}$) ratio of 0.9 horizontal reinforcement at close spacing near the beam soffit was quite effective as observed by Leonhart and Walther in 1966 (Ref.22). In the upper portion of the beam the use of inclined reinforcement was much better than orthogonal reinforcement because:

- a) Considerable saving of reinforcement can be obtained.
- b) It gives better control over deflection and maximum crack width and as a result increases the service load and ultimate strength of the deep beams.

4) The failure modes were diagonal tension/compression failure, splitting failure and shear compression failure. Six out of eleven beams failed a diagonal failure (three in diagonal tension and three in diagonal compression). Four beams failed in splitting failure mode. The main cause of such splitting was probably due to high compression force in support region and the lack of confinement of concrete beyond the region where reinforcement was terminated.

The test results have shown that the design ultimate load based upon an elastic analysis is in good agreement with the actual ultimate load of the beam. The techniques adopted to/

reinforce the beams in the present study of deep beams with openings are similar to those of Lin.

2.3. ESTIMATION OF THE ULTIMATE SHEAR STRENGTH OF DEEP BEAM

Since the current trend in structural reinforced concrete design is towards ultimate load methods, there is a need to know the ultimate behaviour and strength of such beams. Since experimental studies have shown that deep beams mostly fail under shear or diagonal cracking. The commonly used methods for predicting the shear strength of deep beams are outlined below.

De-Paiva & Siess:

De Paiva and Siess (Ref.23) have extended the work of Lupa and found that Lupa's equation (Ref.28) can be used if a correction factor, to take into account the clear shear-span to depth ($\frac{x}{D}$) ratio is included. They suggested that the following equation can be used to predict the ultimate shear.

$$P_s'' = 1.6(1 - 0.6 \frac{x}{D}) (200 + 0.188 f'_c + 21,000 \rho_t) b.D \quad (2.1)$$

where P_s'' = ultimate shear strength.

x = clear shear-span distance between load blocks.

f'_c = concrete strength in pounds per square inch.

b = beam width.

D = overall beam depth.

$\rho_t = A_s (1 + \sin\alpha / b.d)$

Where the quantity $A_s (1 + \sin\alpha)$ refers to the total steel area crossing a vertical section between the load point and the support and α is the angle of inclination of the bent up/

reinforcement to the axis of the beam.

Ramakrishnan and Ananthanarayana:

Results of 26 single span rectangular deep beams which they tested in their investigation (Ref.29) showed that the shear failure was actually a diagonal tensile failure initiated by the splitting action and there was little sign of any shear or sliding taking place during the process. Based upon the diagonal splitting strength of concrete in the shear span they proposed the following shear strength formula.

$$P_c = \beta k f_t b d \quad (2.2)$$

where P_c = ultimate load for a deep beam.

β shear span coefficient ($\beta = 2$ for symmetrical two point, single point and uniform loadings).

k = splitting coefficient.

f_t = splitting strength of 6 in x 12 in cylinder.

b = beam width.

d = overall beam depth.

Kong and Robin:

The shear strength formula proposed by Kong, Robin, Singh and Sharp is based on a number of deep beam tests carried out at the University of Nottingham (Ref.30). Although the formula contains empirical constant, it is based on an assumed diagonal tension failure model i.e. failure occurs as a splitting failure between the load and support points (see fig. 2.2). The formula is given below.

$$Q_{ult} = c_1 \left(1 - c_3 \frac{x}{D}\right) f_t b.D + c_2 \sum^n \frac{A_y}{D} \sin^2 \alpha \quad (2.3)$$

where Q_{ult} = ultimate shear strength.

c_1 = 1.0 for light weight concrete.

1.4 for normal weight concrete.

c_2 = 130 N/mm² for plain round reinforced bars.

300 N/mm² for deformed reinforced bars.

c_3 = 0.35

f_t = cylinder splitting tensile strength of concrete.

x = clear shear span.

b = beam width.

D = overall depth of beam.

A = cross-sectional area of typical bar (including main longitudinal bar) intersects the line joining the inside edge of the support block to the outside edge of the load bearing block.

y = the depth, measured from the top of the beam, at which an individual web bar intersects the line joining the inside edge of the bearing block at the support to the outside edge of that at the loading point.

α = the angle between the reinforcing bar being considered and the line described above.

n = total number of web bars including the main longitudinal bars, that cross the line described in definition of y . Thus the quantity $A(y/D) \sin^2 \alpha$ is to be summed for all n bars.

The above equation proposed by Kong, Robin, Singh and Sharp (Ref.30) has gained general acceptance and has been used in the recently published CIRIA guide (Ref.4) for deep beams.

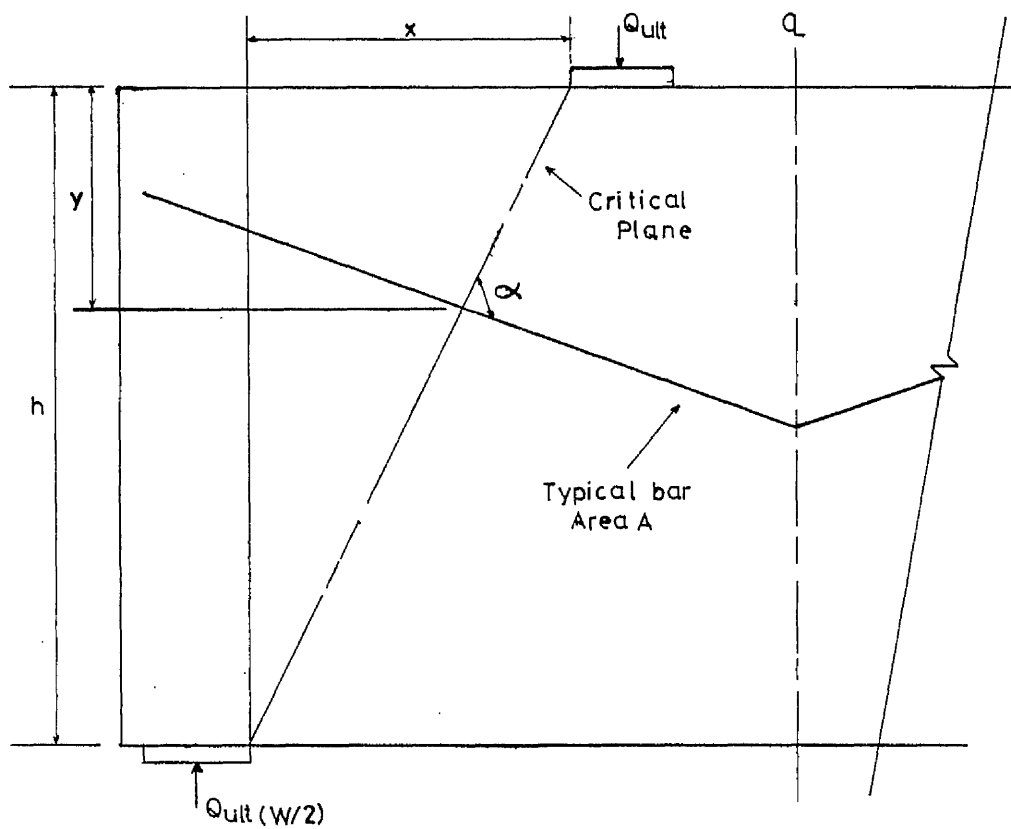


FIG.2.2. MEANING OF SYMBOLS.

It should only be applied to deep beams under top loading and its application is restricted to beams for which the shear-span-depth ($\frac{x}{D}$) ratio should not depart widely from the range of 0.23 - 0.70.

The first term in equation (2.3) is the measure of the inclined cracking load capacity of the beam. It mainly depends upon the tensile strength of the concrete and the beam geometry but not upon the reinforcement. The second term of equation (2.3) represents the contribution of the reinforcement which crosses the inclined cracks including main reinforcement.

2.4 DEEP BEAMS WITH OPENINGS

Deep beams are frequently used in structures and incorporate the openings to give access from one part to another part of the structure.

Very little information is available regarding the behaviour of deep beams with openings. This lack of experimental information is also reflected in the absence of design guidance in the three main codes of practice, the British Code CP110 (Ref. 3 1972), American code ACI (Ref. 1, 1971) and the European Recommendation CEB-FIP (Ref. 2, 1970). The CIRIA guide "the design of deep beams in Reinforced concrete" published by Construction Industry research and Information Association (Ref. 4) is the most comprehensive design guide does include a section on the provision of web opening.

The elastic method of analysis applied to beams with web openings to assess the behaviour of such beams are those of/

Uhlman (Ref.15) and CIRIA guide (Ref. 4) and are reviewed in the following section.

Theoretical Investigation:

Uhlman (1952) studied the state of stresses near the rectangular opening (see fig.2.3) by running a series of tests on simply supported reinforced concrete girder wall models with opening.

Typical state of stresses in such girder wall is shown in fig. 2.3. Let OX and OY be the original directions of the maximum and minimum principal stresses respectively in the region of the opening when the member is regarded as unperforated. The effect of an opening on the unperforated stresses is as follows:

a) It produces an increase in the magnitude of the stresses along those edges of the opening which are approximately tangential to the unperforated lines of stress (near corner A and A').

b) A force of opposite sign is induced along the edge of the opening approximately perpendicular to the unperforated lines of stress (near corner B and B').

Uhlman used photo elastic methods to determine the design tensile force for which the required amount of reinforcement would be calculated. This was obtained by considering the values of increases force parallel to the original stress direction and the induced force perpendicular to the original stress direction in terms of total force intercepted by the opening. He suggested/

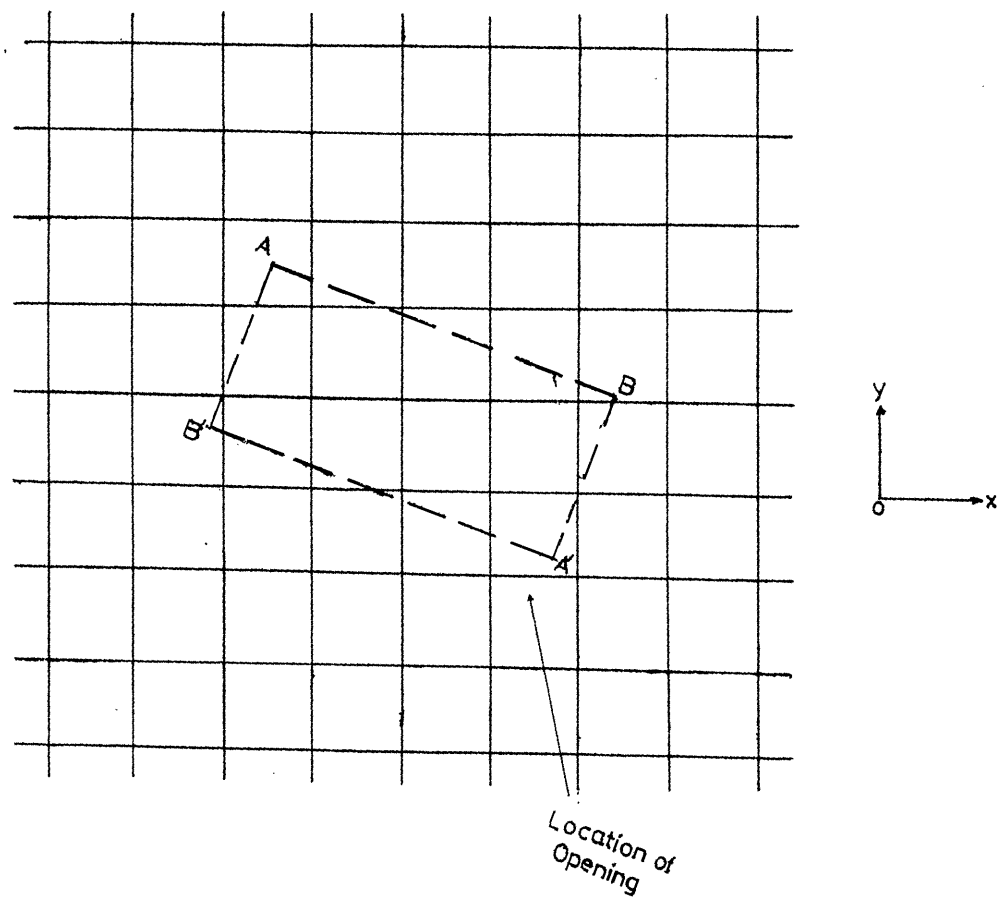


FIG.2.3. LOCATION OF OPENING IN AN UNPERFORATED STRESS FIELD.

that the reinforcement be proportioned according to the predicted tensile force and gave no limit to the size of the opening and imposed no restriction on its location.

The origin of the theoretical elastic basis of the CIRIA guide (Ref.4) for the provision of opening is similar to the method described by Uhlman. The analysis proposed by CIRIA does consider the effect of the size and location of the opening on the stress distribution.

Any opening which is likely to significantly disturb the stress pattern that would be obtained in a solid deep beam (beam without opening) is deemed inadmissible under the guide rules. Openings, that are admissible under the rules are assumed by the guide to be unlikely to disturb the overall behaviour of the beam.

The guide requires that the dimension of the opening are not greater than 0.2 times the width of the band in which the stress is locally concentrated. If the web opening satisfies the admissibility criterion, the amount of reinforcement is to be determined by considering the opening surrounded by the four simply supported deep beams subjected to the resolved forces set up within the primary deep beam. The loads are calculated by the use of a number of principal stress diagrams.

The proposed methods of Uhlman and CIRIA guide are based upon the elastic theory. It can be considered valid in understanding the way in which the reinforced concrete structures carry the loads but it does not predict the behaviour of such structures after cracking or as the ultimate load is approached.

Experimental Investigation

There have been only a few experimental investigations which study the behaviour of deep beams with openings. These are reviewed here.

The most systematic study of the behaviour of reinforced concrete deep beams with web openings has been undertaken by Kong and Sharp (Ref.31) at the University of Nottingham.

Sharp tested a series of seventy two simply supported deep beams of which 16 beams were made with normal weight concrete and 56 beams were made with lightweight concrete. The test beams were of span L 1500 mm, overall depth D 750 and width b 100 mm. A wide range of the opening sizes and locations were used with several different arrangements of web reinforcement. The effect of the opening on beam behaviour was found to depend upon the extent to which the opening intersected a "load path" which was considered to exist between the loading and supporting points. When the opening intersected the above mentioned load path the strength of beam was reduced, the extent of reduction depends upon the size and location of the opening.

Three different type of failure modes were observed (see fig.2.4). Failure mode 1 occurred when the web opening was clear of the load path or when there was no web opening. This is a typical failure mode of solid deep beams and this type of failure has been reported by a number of other investigators like Kong and Robin (Ref.8-26) and Ramakrishnan and Ananthanayaran. (Ref.29).

When the opening intercepted the load path between loading and supporting points either failure mode 2 or mode 3 occurred. Below the opening failure was caused by the propagation of a diagonal crack from the inside edge of support bearing block to the bottom inside edge of the web opening (see fig. 2.4). Above the opening failure occurred by the propagation of a diagonal crack between the outside edge of the load bearing block and the top outside edge of the web opening (see fig. 2.4).

It was found that the web reinforcement was highly effective on controlling crack width and must protect both the diagonal regions above and below the opening. Inclined web reinforcement was found to be particularly effective for crack width control and for increasing ultimate shear strength.

The order of the formation of cracks was found to depend upon the size and the location of the opening and crack widths were increased when the web opening intercepted the load path. The best way of controlling the crack widths is to provide either inclined reinforcement or horizontal reinforcement and vertical stirrups.

Based upon the test results, a truss model was proposed to explain the effect of the web opening on deep beam behaviour. The truss model is shown in fig. 2.5.

The load is transmitted to the support mainly by the lower path ABC and partly by an upper path AEC. In the absence of the web opening the upper and lower path become one, which is the natural load path joining the loading and reaction points.

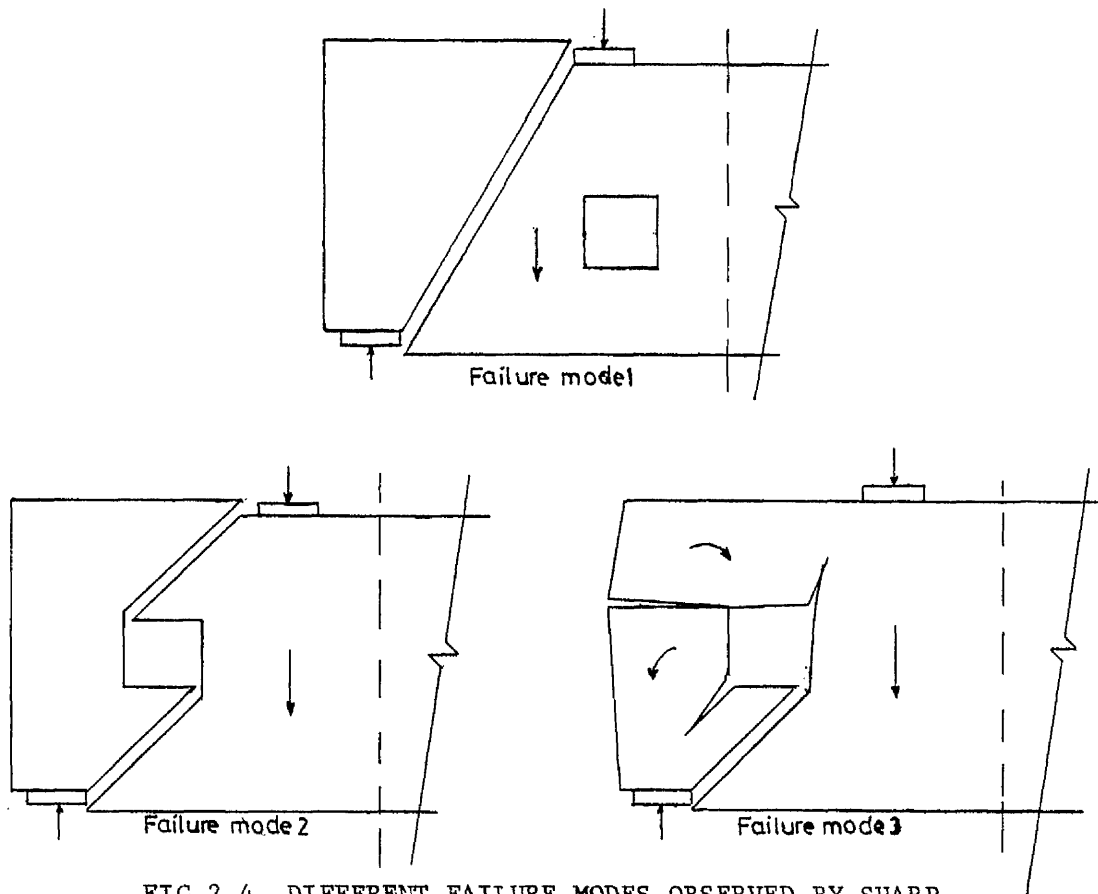


FIG.2.4. DIFFERENT FAILURE MODES OBSERVED BY SHARP,

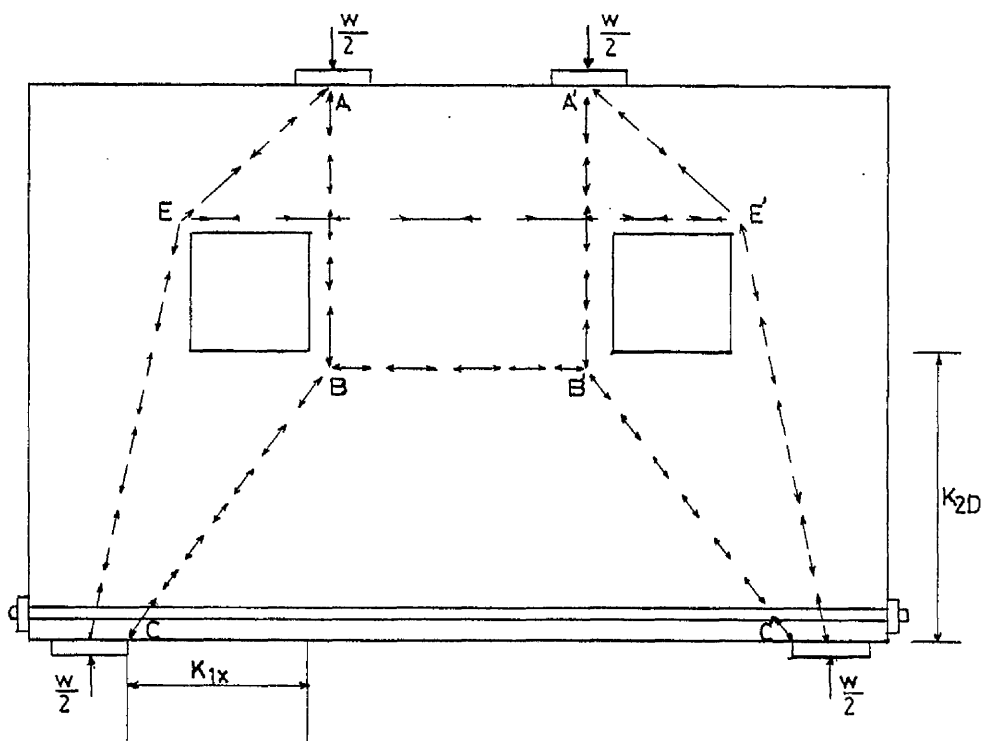


FIG.2.5. THE STRUCTURAL IDEALIZATION (TRUSS MODEL).

An empirical equation was suggested to predict the ultimate strength in shear, which is the modified form of the previously suggested equation (see equation 2.3) for solid deep beams or beams with no opening.

$$Q_{ult} = c_1 \left(1 - 0.35 \frac{k_1 x}{k_2 D}\right) f_t b k_2 D + \sum \lambda c_2 \frac{A_y}{D} \sin^2 \alpha \quad (2.4)$$

where Q_{ult} is the ultimate shear strength of the beam.

c_1 is the empirical coefficient equal to 1.4 for normal weight concrete and 1.0 for lightweight concrete.

c_2 is the empirical coefficient equal to 130 N/mm^2 for plain bars and 300 N/mm^2 for deformed bars.

λ is the empirical coefficient equal to 1.5 for web bars and 1.0 for main bars.

x is the clear shear-span distance.

k_1, k_2 are coefficients defining the position of an opening.

b is the breadth (thickness) of beam.

f_t is the cylinder splitting tensile strength of concrete.

A is the cross-sectional area of a typical reinforcing bar.

y is the depth at which a typical bar intersects the typical diagonal crack - as AE of the upper path and BC of the lower path.

α is the angle of intersection between the reinforcing bar and the strut AE or BC.

The first term on the right hand side of the equation 2.4, the quantity $c_1 f_t b k_2 D$ gives the resistance of the concrete in the lower path to the diagonal cracking. The second term on the right hand side represents the contribution of the reinforcement to shear strength of the beam.

The concrete contribution, as represented by the first term on the right hand side of equation 2.4 is based on the capacity of the lower path. Under certain circumstances, however, the lower load path might be much weaker than the upper load path. In such cases the strength prediction may be conservative hence it is suggested that in design k_2 should be kept not less than 0.2.

Kong and Kubik:

Tests on eighteen lightweight and eight normal weight concrete deep beams were carried out by Kubik at the University of Cambridge (Ref.32).

The normal weight concrete beams were 4000 x 1800 x 250 mm with a clear span (centre to centre of supports) of 3500 mm. The specimens were therefore approximately $2\frac{1}{2}$ times the size of the beams tested by Sharp. (Ref.31).

The volume of reinforcement used in large beams have been scaled up approximately from the small scale specimens of Sharp. Four 20 mm deformed reinforcing bars were used as flexural reinforcement. This was anchored at the ends by 90° bends, where in small specimens of Sharp one 20 mm diameter deformed bar was used as main longitudinal steel and was anchored to external steel blocks at the ends.

A single size of web opening in the two different locations was used. It was observed that, deep beam with web opening which interrupt the flow of stresses due to intersection of load path with opening deform mainly by the rotation of the three blocks of the beam. One above the opening, another below the opening and third between the opening and the end of the beam.

The cracks were on the whole similar to those reported by Sharp and depend also upon the location of the web opening. The new crack types 7, 8 and 9 formed within the web of the beam. shown in fig. 2.6 had an important influence on the failure of the beam were not identified by Sharp. These were the widest at the point close to mid length of crack, reducing to zero at both ends and referred as splitting cracks. In general the cracks were originating in the corners of the web opening followed by crack type 3 and 4a (see fig.2.6) and by splitting cracks above and below the opening.

It was found that the inclined web reinforcement was more effective at controlling the maximum crack width than the orthogonal reinforcement of horizontal bars and vertical stirrups. Using inclined reinforcement in the web of the beam the splitting cracks above and below the opening were more effectively restrained. This observation agrees reasonably well with Sharp who also emphasises the contribution of the web reinforcement in the region above and below the opening.

The different failure modes observed in the tests are shown in fig.2.4 and fig.2.7. Fig. (2.4a) shows that failure/

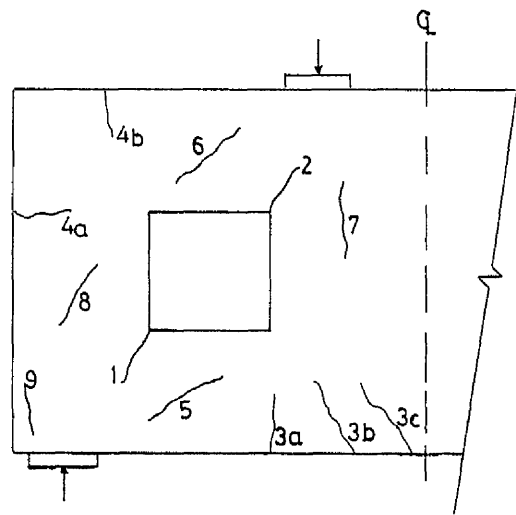
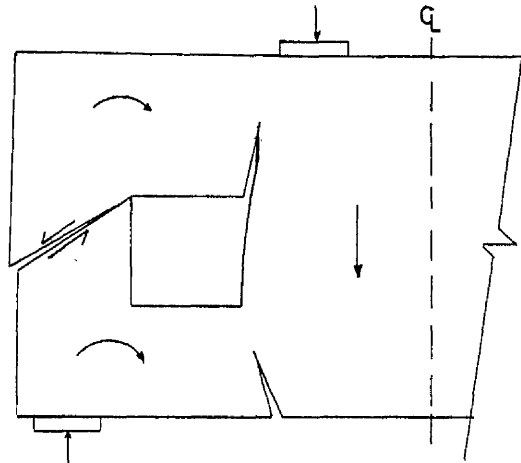
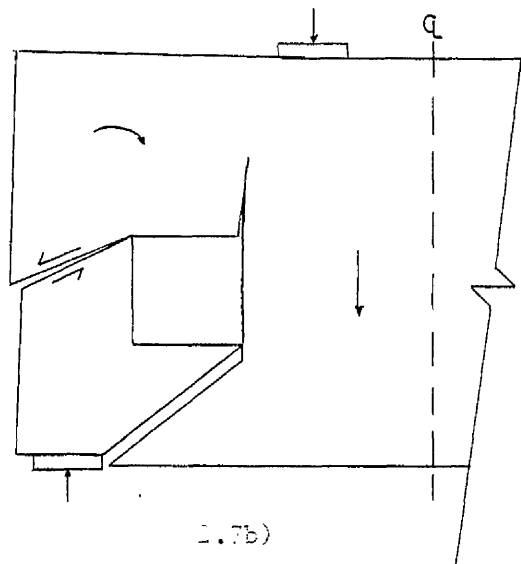


FIG.2.6. TYPICAL CRACK PATTERN IN DEEP BEAM WITH OPENING.



(2.7a)



(2.7b)

FIG.2.7. FAILURE MODES FOR DEEP BEAM WITH OPENING (OBSERVED BY KUBIK)

occurred by separation along the planes above and below the opening which is similar to the shearing failure of deep beam without opening. The other failure modes shown in fig. (2.4b) and (2.4c) were observed when the opening intercepted the load path. The pattern of failure was similar to those failure modes reported by Sharp. A special type of failure occurred along a plane between the top outside corner of the web opening and the end of the beam, either with the opening of the flexural cracks from the top inside corner of the web opening and from the beam soffit (see fig. 2.7a) or with separation along a plane roughly aligned with the splitting crack below the opening (see fig. 2.7b).

A deformation model was proposed for simply supported deep beam with openings and was used in the derivation of the equations for ultimate strength. It was found that all the deformations took place by the rotations of the three blocks A, B and C with downward displacement of the fourth block D, shown in fig. 2.8. Considering the force interaction between the blocks, which occurred through the hinges 1-4 (see fig. 2.8) the load carried above and below the opening in terms of hinge moments were calculated as follows.

$$Q_T = \frac{M_1(h_o + h_L) + M_2h + M_3h_u}{a_u(h_o + h_L) - h_u(a_L - x_o)} \quad (2.5)$$

$$Q_B = \frac{M_3 + M_4}{a_L} - \frac{h_L M_1(a_L - x_o) + M_2a + M_3a_u}{a_L a_u(h_o + h_L) - h_u(a_L - x_o)} \quad (2.6)$$

$$H = \frac{M_1(a_L - x_o) + M_2a + M_3a_u}{a_u(h_o + h_L) - h_u(a_L - x_o)} \quad (2.7)$$

Tests on deep beams with openings indicated that the shearing failure was the predominant mode of failure and the possible locations of shear failure were in the region above the opening, between the end of the beam and web opening and below the opening. It must be considered in these regions. The proposed equation of Kong (see equation 2.3) was used to predict the ultimate shear strength given by:

$$(Q_T)_{s1} = c_1 \left(1 - 0.35 \frac{x_u}{h_u}\right) f_t b h_u + c_2 \sum A \frac{y_u}{h_u} \sin^2 \alpha_u \quad (2.8)$$

above the opening.

$$H_s = c_1 \left(1 - 0.35 \left(\frac{h_o}{t}\right)\right) f_t b t + c_2 \sum A \left(\frac{y_t}{t}\right) \sin^2 \alpha_t \quad (2.9)$$

between the end of the beam and the web opening.

$$(Q_B)_s = c_1 \left(1 - 0.35 \frac{x_L}{h_L}\right) f_t b h_L + c_2 \sum A \left(\frac{y_L}{h_L}\right) \sin^2 \alpha_L \quad (2.10)$$

Below the opening.

The shear strength between the end of the beam and web opening given by equation (2.9) is also related to the load in the path above the opening $(Q_T)_{s2}$.

$$(Q_T)_{s2} = \frac{H_s}{H_F} (Q_T)_F \quad (2.11)$$

where $(Q_T)_F$ and H_F are given by equations (2.5) and (2.7) respectively.

When the load (Flexural load) carried above and below the opening given by equation (2.5) - (2.7) exceeded the corresponding shear strength above and below the opening given by (2.8) - (2.11) failure occurred along the assumed failure planes, shown in fig. 2.9.

The ultimate strength will be calculated from the strength of the load paths above and below the opening. The load carried in the paths above and below the opening increases linearly with central deflection of the beam in the absence of the premature shearing failure. If the premature shearing failure occurs in the upper load path the ultimate strength at which this failure occurs will be:

$$Q_{ult} = (Q_T)_s + \mu (Q_B)_F \quad (2.12)$$

where $\mu = (Q_T)_s / (Q_T)_F$ is the ratio between ultimate shear strength above the opening and the load carried in the upper path.

Similarly if the premature shearing failure occurs in the lower path, the ultimate strength at which this failure occurs will be

$$Q_{ult} = (Q_B)_s + \eta (Q_T)_F \quad (2.13)$$

where $\eta = (Q_B)_s / (Q_B)_F$ is the ratio between the ultimate shear strength below the opening and the load carried in the lower path. If the shear failure is predicted in both upper and lower load paths equation (2.12) will be used if $\mu < \eta$ and equation (2.13) will be used if $\eta < \mu$.

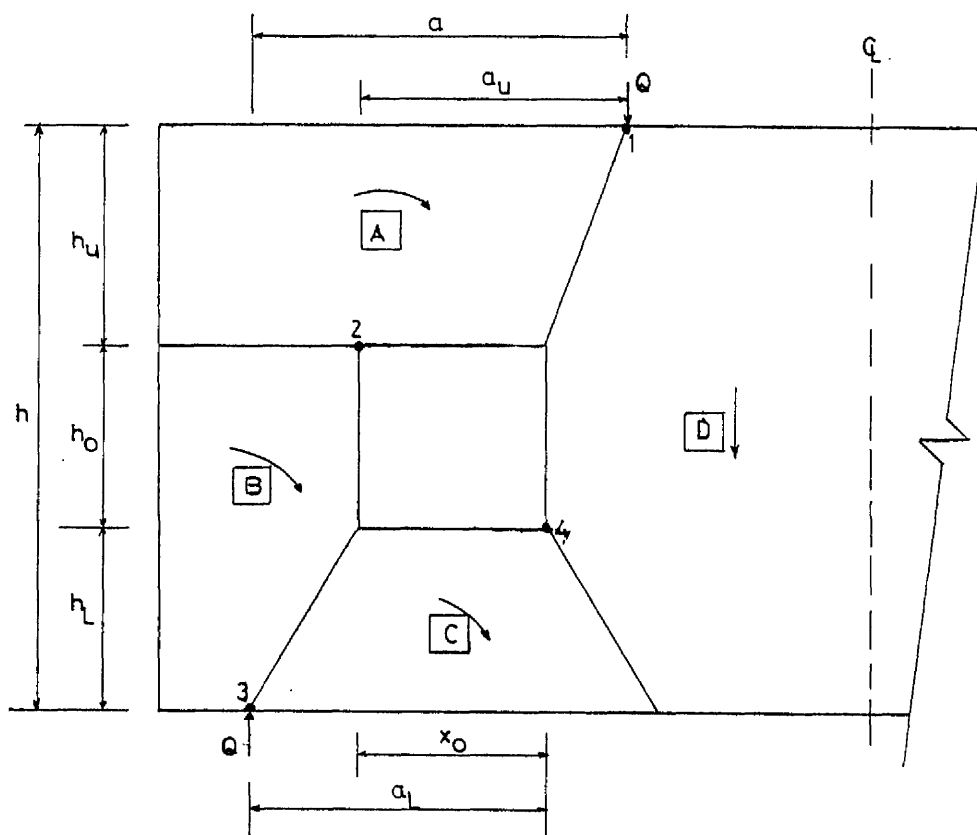
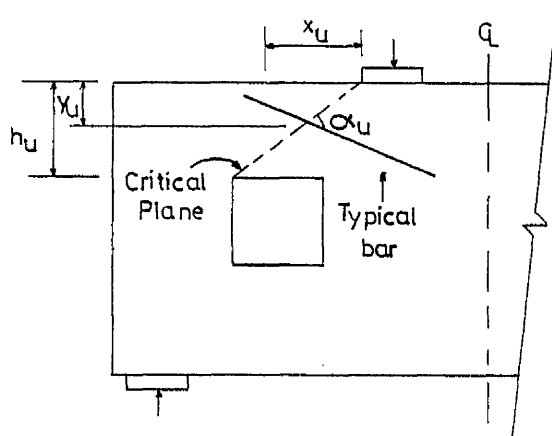
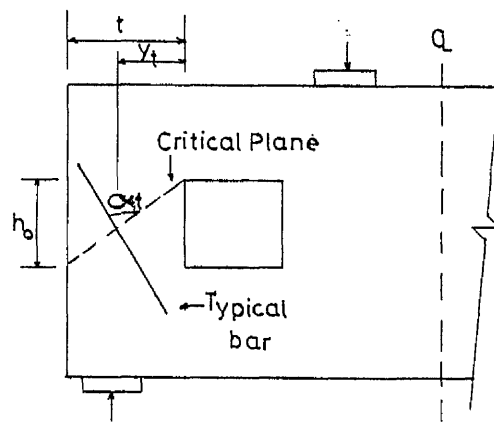


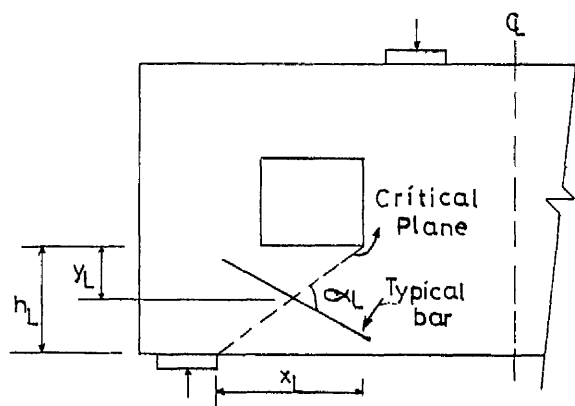
FIG.2.8. IDEALIZATION FOR DEFORMATION OF BEAMS WITH WEB OPENING.



(2.9a)



(2.9b)



(2.9c)

FIG.2.9. TYPICAL PLANES OF FAILURE.

To ensure that the ultimate strength predicted by above equations is to be safe, the region above the opening should fail by rotation, not shear, because the premature shearing failure always will not be on the safe side.

The proposed model of Kubik (Ref.33) supporting the Kong and Sharp's (Ref.34) idea of load path. It is applicable only when the opening intersects the line joining the loading and support reaction points.

2.4.3 Conclusion:

Elastic methods of analysis of reinforced concrete deep beams with openings do not provide useful information on the post cracking behaviour of the beam and on the ultimate strength. Due to complexity of the behaviour of deep beams the present design rules have been derived empirically. Experimental study of the behaviour of reinforced concrete deep beams is in progress. Many of the details and results of the tests have been published in technical journals and the new CIRIA design guide contain some design rules.

Sharp at the University of Nottingham and Kubik at the University of Cambridge carried out systematic study on the effect of the web openings on the behaviour of deep beams and data obtained by them is presented in previous section. The test results show that the behaviour of deep beams depend upon the reinforcement in the beam. It is not clear what governs the failure mode. Apart from the suggestion that web reinforcement/

should be used to protect the region above and below the web opening, no guidance has been given on the provision of the web reinforcement to resist the crack width. Nor is it clear from the structural idealization or from the ultimate strength equations how the reinforcement should be arranged for crack control.

Secondly, to produce the collapse of beam with web opening in which the web opening interrupt the flow of the stress, both the upper and lower load path must collapse. But the collapse of one load path will lead to wide cracks and large deflections. No specific account has been taken for such failures.

2.5 OUTLINES OF DESIGN METHODS FOR SOLID DEEP BEAMS

2.5.1 American Building Code ACI:

In 1971, the American building code ACI, for the first time included recommendations for solid deep beams. The design procedure according to ACI building code can be illustrated as follows:

(A) Flexural Design:

Beams shall be designed as deep flexural members with span to overall depth ratios less than 2.5 for continuous spans, or 1.25 for simple spans. The code does not contain any recommendation for flexural design except that no linearity of strain distribution and lateral buckling must be considered. In the commentary and notes to codes, (Ref.1 and 35) the designer is referred to other documents such as the Portland Cement Association bulletin.

(B) Shear Design:

Special provisions apply to both simple and continuous beams loaded at the top or compression face with a span/depth ratio ($\frac{l_n}{d}$) less than 5. The critical section for shear measured from the face of the support shall be taken as:

$0.15 l_n$ for uniformly loaded beam

$0.5a$ for beams with concentrated load

where a is shear span.

First the nominal shear stress v_u is calculated from the given design shear force V_u .

$$v_u = \frac{V_u}{\phi b d} \quad (2.14)$$

where ϕ is the capacity reduction factor (taken as 0.85), b is width of beam and d is effective depth.

The designer should ensure that the dimensions b and d are large enough for v_u not to be exceeded by the following limits

$$v_u \leq 8 \sqrt{f'_c} \quad \text{when } \frac{l_n}{d} < 2$$
$$v_u \leq \frac{2}{3} \left(10 + \frac{l_n}{d}\right) \sqrt{f'_c} \quad \text{when } 2 \leq \frac{l_n}{d} \leq 5$$

where f'_c is the concrete cylinder compressive strength.

Next the nominal shear stress v_c carried by concrete is calculated as

$$(a) \quad v_c = 2 \sqrt{f'_c} \quad (2.15a)$$

$$(b) \quad v_c = \left[3.5 - 2.5 \frac{M_u}{V_u d} \right] \times \left[1.9 \sqrt{f'_c} + 2500 \rho_w \frac{V_u d}{M_u} \right] \quad (2.15b)$$

where $(3.5 - 2.5 \frac{M_u}{V_u d}) \geq 2.5$ and $v_c \geq 6\sqrt{f'_c}$

M_u is design bending moment at critical section, f'_c is the specified concrete cylinder compressive strength, ρ is the ratio of main steel A_s to the area bxd of the concrete section.

Irrespective of the values of v_u and v_c so calculated an orthogonal mesh of web reinforcement is mandatory, the area of the vertical web steel should not be less than 0.15% of the horizontal concrete section b.L, and that of the horizontal web steel not less than 0.25% of the vertical concrete section b.d. Where v_u exceeds v_c the web reinforcement satisfy the requirements of the following equation:

$$v_s = \frac{v_u}{\phi} - v_c = \left[\frac{A_{sv}}{s_v} \left(\frac{1 + \frac{\ell_n}{d}}{12} \right) + \frac{A_{sh}}{s_h} \left(\frac{11 - \frac{\ell_n}{d}}{12} \right) \right] f_y d \quad (2.16)$$

where A_{sv} is the area of vertical web steel within a spacing s_v

A_{sh} is the area of horizontal web steel within a spacing s_h

f_y is specified yield strength of the steel.

2.5.2 EUROPEAN CONCRETE COMMITTEE (CEB.FIP)

When the span/depth ratio of simply supported beams is less than 2, or less than 2.5 for any span of continuous beam, it is regarded as deep beam according to European Concrete Committee. The design procedures can be illustrated as follows:

(A) Flexural reinforcement:

The quantity of tensile reinforcement A_s be determined from the following expression:

$$A_s = \frac{T}{f_y / \gamma_m Z} \quad (2.17)$$

where T is the sum of moments due to live and dead loads (calculated as for shallow beams), γ_m is the partial factor of safety for materials ($\gamma_m = 1.15$ for steel) and lever arm Z being taken as.

$$Z = 0.2 (L + 2D) \quad \text{for } 1 \leq \frac{L}{D} \leq 2$$

$$Z = 0.6L \quad \text{for } \frac{L}{D} < 1$$

The flexural reinforcement so calculated should be uniformly distributed over a vertical distance equal to $(0.25D - 0.05L)$ where $D \leq L$.

(B) Shear force for a certain section with beam width b , depth D and span L may be determined from the lesser of $v > 0.1 b D f'_c / \gamma_m$ or $0.1 b L f'_c / \gamma_m$. In which ($\gamma_m = 1.5$ for concrete partial safety factor) and f'_c is the characteristic cylinder strength of concrete.

(C) Web Reinforcement:

When the load is applied along the top edge of a beam, the web reinforcement be provided in the form of small diameter bars placed in both directions (horizontal bars and vertical stirrups). Near the support, however, additional bars should be provided.

When the load is suspended from near the bottom edge of a beam, the whole of load must be transferred by means of vertical reinforcement into upper zone of the beam. This should be achieved by introducing additional stirrups in the above mentioned orthogonal mesh.

2.5.3 CONSTRUCTION INDUSTRY RESEARCH AND INFORMATION ASSOCIATION

CIRIA:

The CIRIA guide provides simple and also supplementary rules for designing reinforced concrete deep beams of span/depth ratio below 2 for single span beams or 2.5 for multispan beams.

The recommendations for the design of solid deep beams are as follows:

(A) Using the simple rules for bending the main tension steel required is calculated from the following expression:

$$A_s > \frac{M}{0.87 f_y Z} \quad (2.18)$$

where M is design moment at ultimate state.

Z is lever arm and for single span $Z = 0.2 l + 0.4 h_a$, l is effective span and h_a is effective height. If $\frac{l}{h_a} > 1.5$ it is required to confirm the strength of concrete in compression due to bending and the condition $M \leq 0.12 f_{cu} b h_a^2$ must be satisfied.

The reinforcement calculated above is not to be curtailed in the span and may be distributed above a depth of $0.2 h_a$. The bars must be anchored to develop 80% of the maximum ultimate force beyond the face of support and 20% of the maximum ultimate force/

at or beyond a point $0.2l$ from the face of support, or at or beyond the face of support, whichever is less.

(B) As regard shear, the simple rules specify two conditions for the shear capacity of the beams with unreinforced webs. These are

$$i) V < 2b h_a k_s v_c / x \quad (2.19a)$$

$$ii) V < b h_a v_u \quad (2.19b)$$

where h_a is the height, x is the effective clear shear span.

v_c is ultimate concrete shear stress taken from CP110 (Table 5 & 25) for normal and lightweight concrete.

v_u is maximum value for shear in section taken from CP110

(Table 6 & 26) respectively for two types of concrete.

$k_s = 1.0$ for $\frac{h_a}{b} < 4$, $= 0.6$ for $\frac{h_a}{b} > 4$.

Under the supplementary rules when $0.3 < \frac{x}{h_a} < 0.7$, the ultimate shear capacity is given by

$$iii) V < \lambda_1 b h_a (1 - 0.35 \frac{x}{h_a}) \sqrt{f_{cu}} + \lambda_2 \sum \frac{100 A_r y_r \sin^2 \theta_r}{h_a} \quad (2.20a)$$

where $\lambda_1 = 0.44$ for normal weight and 0.32 for lightweight concrete.

$\lambda_2 = 1.95 \text{ N/mm}^2$ for deformed bars and 0.82 N/mm^2 for plain round bars.

$$iv) V < 1.3 b h_a \sqrt{f_{cu}} \quad (2.20b)$$

The ultimate shear capacity for a top loaded beam, may be determined from the lesser of (i) or (ii) or from lesser of (iii) or (iv) whichever is larger.

The ultimate shear strength of the beam with orthogonal reinforcement may be determined with the help of tables and is derived from:

$$i) \quad V = \lambda_1 b h_a v_x + b h_a (\beta_1 v_{ms} + \beta_2 v_{wh} + \beta_3 v_{wv}) \quad (2.21a)$$

where v_x is a tabulated shear stress parameter.

β_1 , β_2 and β_3 are parameters for different types of bars (i.e. deformed bars, round bars and wire weld bars) and determined in the guide.

v_{ms} , v_{wh} and v_{wv} are shear stress parameters. Their values are given in a series of Tables (CIRIA guide Tables 6,7 and 8).

$$ii) \quad V < \lambda_1 v_{max} b h_a \quad (2.21b)$$

where v_{max} is maximum shear stress parameter takes from CIRIA Table 5.

For the design of web reinforcement the guide refers two types of web reinforcement. i) inclined web reinforcement and ii) orthogonal web reinforcement. Inclined web reinforcement should be designed with the aid of supplementary rules. The contribution of reinforcement (the main tensile reinforcement should be regarded as part of web reinforcement) should not be less than 0.2V. The orthogonal reinforcement comprises both horizontal/

and vertical bars. The minimum amount should not be less than the reinforcement for shrinkage and temperature effects required for a wall under clauses 3.11 and 5.5 of CP110, namely 0.25% for high yield steel and 0.3% for mild steel time the volume of concrete is to be provided both horizontally and vertically.

2.5.4 DESIGN RECOMMENDATION FOR THE DEEP BEAMS WITH OPENINGS

No codes of practice include recommendations for the design of deep beams with openings except the CIRIA guide.

The detailed literature study conducted by CIRIA (Ref. 4) during the completion of the guide failed to find sufficient test data on the effect of web openings on the behaviour of deep beams. The most systematic study of the behaviour of reinforced concrete deep beams with web openings has been undertaken by Sharp and Kubik (Ref. 31 and 32). Based upon the experimental results, truss models were proposed. Although such models could prove to be a powerful tool to designers, both for the visualization of the load transfer mechanism in deep beams with openings and for the prediction of their ultimate strength. Realistic rules can only come from realistic behaviour i.e. experiments on reinforced concrete at large scale. As a step towards providing such data, the present experimental programme was carried out.

CHAPTER THREE

DESIGN PHILOSOPHY

3.1 INTRODUCTION

The current trend in reinforced concrete design is towards ultimate load methods. Until recently the design of reinforced concrete structural members was based on the elastic theory. This method is simple to apply but it does have some inconsistencies. Because it is based on an elastic stress distribution, it is not really applicable to a semi-plastic material such as concrete, nor is it suitable when the deformations are not proportional to the load.

An alternative method, is the, "Load-factor method". This method does not apply factor of safety to the material stresses, does not directly take account of the variability of the materials, and also cannot be used to calculate the deflection or cracking at working loads. (Ref.37)

More recently proposals has been made for the development of the Limit state methods (Ultimate load method) of design which overcome many of the disadvantages of the previous two methods. A partial factor of safety is applied both to the loads and to the material strengths, and the magnitude of the factors may be varied so that they may be used either with the plastic conditions in the ultimate state or with the more elastic stress range at working loads.

For skeletal structures such as frames ultimate load/

methods have been fully developed following an upper bound approach where a system of plastic hinges are selected which will convert the structure into a mechanism. The validity of these methods has been demonstrated by extensive experimental studies, and the permissible amount of plasticity is limited in CP110 (Ref. 3). For continuum structures, particularly those where the principal stresses are in-plane, proposals have been made to base ultimate load methods on a lower bound approach. For a given ultimate load, a stress field in equilibrium with external loads is obtained by a linear elastic stress analysis, e.g. finite element analysis. Reinforcement is provided such that the combined resistance of steel and concrete at every point is equal to or greater than the applied stresses. If the equilibrium and yield criteria are satisfied exactly at every point then the entire structure will be converted to a mechanism at ultimate load.

In the following section the design philosophy of ultimate load approach is broadly explained.

3.2 OBJECT OF LIMIT STATE DESIGN

The object of structural design is to achieve acceptable possibilities that the limit state of a structure (defined as a particular state at which it ceases to fulfil the function for which it has been designed) will not be reached during the design life of the structure. A structure, or part of a structure, which may cease to be fit for use will constitute a limit state and design aim is to avoid such condition.

The two principal types of limit state are the ultimate limit state and the serviceability limit state.

1) Ultimate limit state: This requires that neither the whole structure nor any part of the structure should collapse. Collapse is associated with the inability of the structure to carry any additional load.

2) Serviceability limit state: This requires that the structure should not suffer from excessive deflection, cracking, vibration, etc. at working loads.

The usual design procedure is to decide which is the collapse limit state for a particular structure and base the design on this state. Checks must also be made that the other limit states are satisfied (Ref.38). This chapter describes how the limit state philosophy is adopted to the design of deep beams with openings.

3.3 LIMIT STATE DESIGN

The philosophy of limit state design was developed mainly by the Comite European du Beton (CEB) and the Federation International de la Precontrainte (FIP), and is gaining international acceptance. The CEB recommendations (Ref.39) give no detailed methods of analysis and merely state that the calculations should be done by scientific methods based upon experimental data.

The object of the method of analysis is to predict accurately the actual behaviour of reinforced concrete structures/

at all the stages from zero load to collapse ; hence, it must take into account the appropriate stress-strain relationship of reinforced concrete.

The general approach to calculations (to determine the magnitudes of forces and moments throughout a structure) is still the classical elastic theory. This is used directly for limit states of deflection and local damage, but can be modified to take account of plasticity of reinforced concrete when the ultimate limit state is considered (Ref.40).

At present, plastic methods of analysis are implied to be those based upon consideration of collapse mechanism or upon non-elastic distribution of stresses. Such analysis exists for certain types of structures, the yield line theory of slabs is of this type. The difficulty in applying them to reinforced concrete is that owing to cracking the stiffness of a member varies along its length and with the magnitude of loading applied to it. The correct approach would be to use the appropriate stiffness for each section at each loading stage. But this is not practically possible.

The reinforced concrete does not exhibit perfectly plastic response, a collapse failure may occur in the concrete before yielding has redistributed the stresses. Generally single stiffness for the whole of a span can be selected to give as accurate as possible a distribution of stresses in the structure and ensure that the critical sections yield practically simultaneously. It has been found that if a slight, evenly /

distributed reinforcement is placed throughout the concrete section it is capable of holding the cracked section together and the compression strength of the concrete is still obtainable.

A basic concept of plastic method is that it is not generally possible to calculate a unique value for the collapse load of a structure. It is stated that the collapse load lies between two values known as upper and lower bounds to the collapse load. For certain structures these bounds coincide and a unique collapse load is obtained. This is not the general case and for vast number of commonly occurring structures coincidental upper and lower bounds have not been determined.

The methods for determining these bounds on collapse load are based upon two theorems namely lower and upper bound theorems. These theorems have been found very helpful in the problems associated with ductile materials such as steel, but have also been helpful in the analysis and design of reinforced concrete slabs and beams and in the calculation of bearing capacity of concrete blocks. A statement of these theorem follows:

i) Lower bound theorem: If an equilibrium distribution of stresses can be found which balances the applied loads on the structure and is everywhere below yield or at yield, the structure will not collapse or will just be at the point of collapse under these loads.

ii) Upper bound theorem: The structure must collapse if there is any compatible patterns of plastic deformation for which the rate at which the external forces do work is equal to/

or exceeds the rate of internal energy dissipation.

An upper bound method is unsafe in that it provides a value of the collapse load which is either greater than or equal to the true collapse load. On the other side lower bound methods are safe in that they provide a value of collapse load which is either less than or equal to the true collapse loads. As mentioned previously if the equilibrium and yield criteria are satisfied exactly at every point then the structure will be converted to a mechanism at collapse load. For this to happen it is essential that the structure should have sufficient ductility so that redistribution of stress takes place as cracking occurs. The following section shows how these conditions can be fulfilled.

3.3.1 Equilibrium Criterion:

In a reinforced concrete structure, the distribution of forces within the structure is usually found by some form of elastic analysis. Although the distribution of stresses is affected by cracking, it is permissible to base reinforcement on the stress field obtained by elastic analysis for ultimate conditions, if yielding regions have sufficient ductility to redistribute stress to other parts of the structure.

The actual ultimate strength of a beam so designed should at least reach the ultimate load predicted by elastic analysis because strength of materials are underestimated i.e. strain hardening of steel and biaxial compressive strength of concrete is neglected (Ref.43).

3.3.2 Yield Criterion:

In reinforced concrete structures forces have to be resisted either by concrete alone or by the combination of concrete and steel. In addition to reinforcement requirements based on stress/strength considerations there are often practical constraints on the direction in which reinforcement may lie ; on the proportion of steel which may be provided, or on the way the reinforcement percentage may vary across the structure. An efficient design is achieved by minimizing the total amount of reinforcement required by the design criteria within the bounds of these practical constraints.

A number of design proposals have been developed for determining the optimum arrangement of reinforcement in a concrete structure subjected to certain loading. (Ref.44-47) For in-plane forces Nielson (Ref.44) has presented the yield criterion for a section having known orthogonal reinforcement which can carry tension. This approach has been extended by Clark (Ref.47) to cover the possibility that compression steel may be required.

In order to establish the design equations the following assumptions are made.

- 1) The reinforcement is assumed to be positioned symmetrically with respect to the middle surface of the section and to be in two orthogonal directions.

- 2) The reinforcement can carry only uniaxial stress in their original bar direction. This means kinking of the bars/

and the contribution by dowel action of the bars in resisting shear is neglected.

3) The bar spacing is assumed to be small in comparison with the overall structure dimensions so that the reinforcement can be considered in terms of area per unit length rather than as individual bars.

4) The concrete is assumed to have zero tensile strength, to exhibit a square yield criterion (shown in fig. 3.1) in plane stress and to be perfectly plastic when yielding.

5) The reinforcing bars are also assumed to exhibit perfect elastic/plastic behaviour and to yield at stress of f_s in tension and f'_s in compression.

6) Instability failures, bond failures are assumed to be prevented by proper detailing and choice of the section.

Theory:

The principal concrete stresses are taken to be σ_1 and σ_2 with the major principal stress σ_1 at an angle θ to the x-axis. σ_1 is always numerically greater than σ_2 . All stresses are taken to be tension positive. A typical element from a deep beam as well as sign convention for in-plan and shear stresses is shown in fig. 3.2.

It is assumed that the applied stresses are resisted by the combination of concrete and steel. The applied stresses and the stresses resisted by the concrete are shown in fig. (3.3a) and (3.3b) respectively.

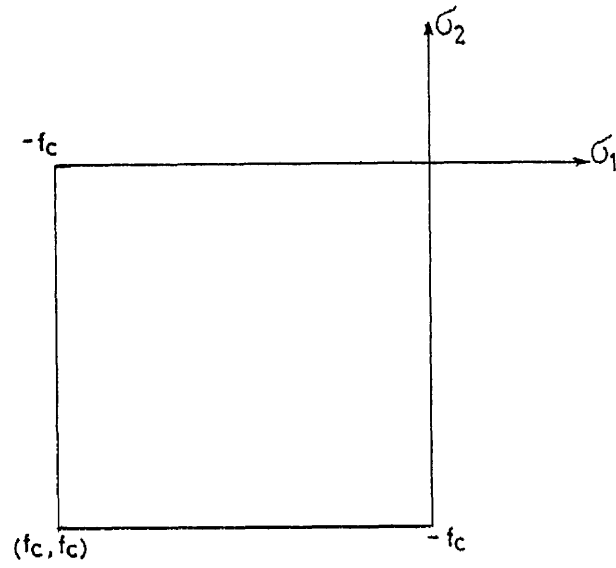


FIG.3.1. YIELD CRITERIA FOR CONCRETE IN PLANE STRESS..

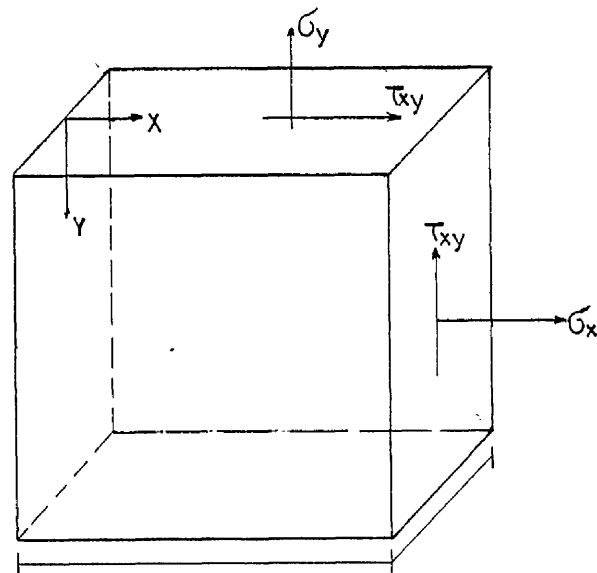


FIG.3.2. SIGN CONVENTION FOR IN-PLANE DIRECT AND SHEAR STRESSES.

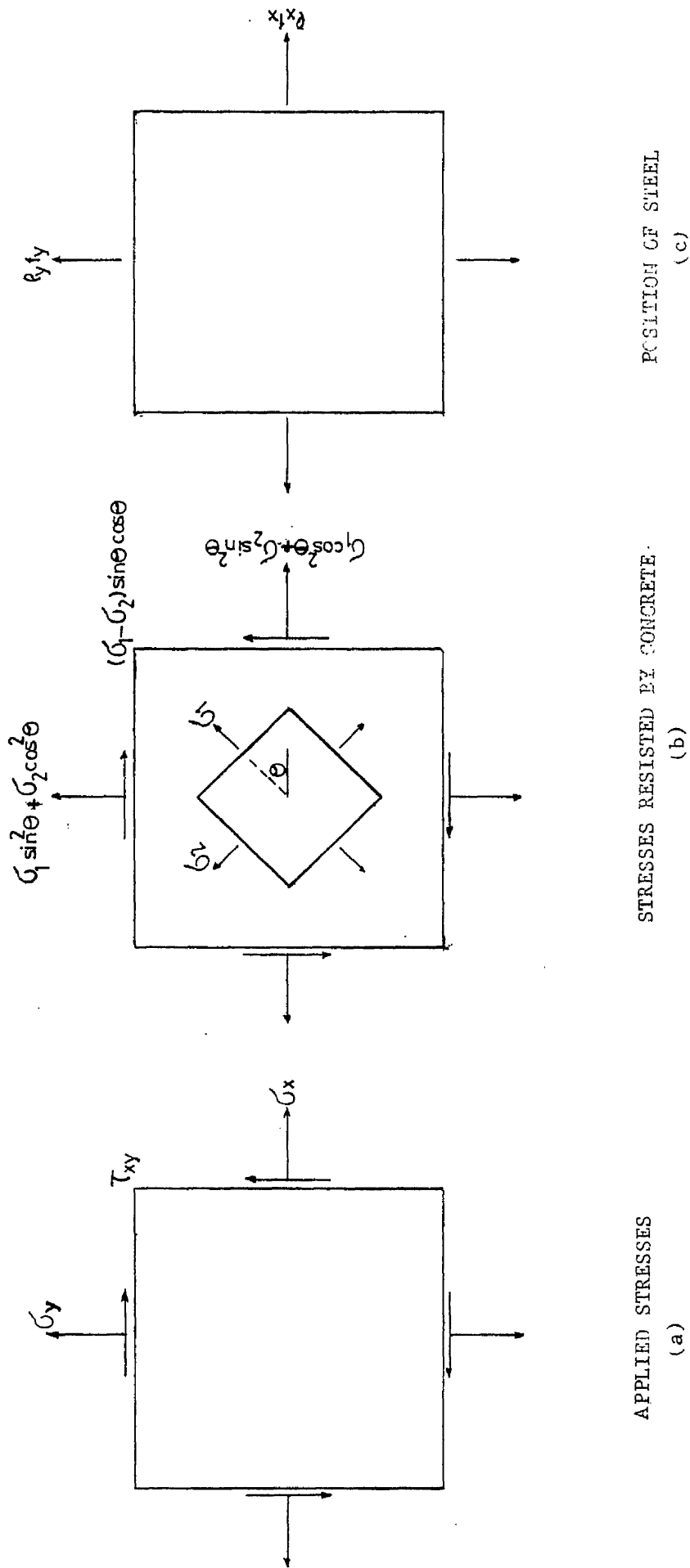


FIG. 3.8.

In fig. (3.3c), the reinforcement is to be positioned symmetrically with respect to the thickness and to be in orthogonal directions.

Let the area of reinforcement per unit length in the x and y direction be A_x and A_y respectively and their associated stresses \bar{f}_x and \bar{f}_y . On dividing by the thickness, the reinforcement ratio can be expressed as:

$$\rho_x = \frac{A_x}{t} \quad (3.1a)$$

$$\rho_y = \frac{A_y}{t} \quad (3.1b)$$

By equating the applied stresses to the internal stresses the following three equations of equilibrium may be written.

$$\sigma_x = \sigma_1 \cos^2 \theta + \sigma_2 \sin^2 \theta + \rho_x \bar{f}_x \quad (3.2a)$$

$$\sigma_y = \sigma_1 \sin^2 \theta + \sigma_2 \cos^2 \theta + \rho_y \bar{f}_y \quad (3.2b)$$

$$\tau_{xy} = (\sigma_1 - \sigma_2) \cos \theta \sin \theta \quad (3.2c)$$

The reinforcement in each direction can be tension reinforcement, compression reinforcement or there can be no reinforcement ; thus for a 2-D situation there are nine possible combinations to be considered, which are summarized in Table 3.1. It can be seen that a direct solution for reinforcement can be obtained except for Cases 1 and 4 where four unknowns are to be determined from three equations. The fourth unknown can be/

T A B L E 3.1
VARIOUS POSSIBLE COMBINATIONS OF REINFORCEMENT

Case	Reinforcement description	Known Values	Method of solution
1	Both tension.	$\bar{f}_x = \bar{f}_y = f_s, \sigma_1 = 0$	Minimization of $(\rho_x + \rho_y)$
2	X tension, No Y.	$\bar{f}_x = f_s, \rho_y = 0, \sigma_1 = 0$	Direct solution
3	No X, Y tension.	$\rho_x = 0, \bar{f}_y = f_s, \sigma_1 = 0$	Direct solution
4	Both compression.	$\bar{f}_x = \bar{f}_y = f'_s, \sigma_2 = f_c$	Minimization of $(\rho_x + \rho_y)$
5	X compression, No Y.	$\bar{f}_x = f'_s, \rho_y = 0, \sigma_2 = f_c$	Direct solution
6	No X, Y compression.	$\rho_x = 0, \bar{f}_y = f'_s, \sigma_2 = f_c$	Direct solution
7	X tension, Y compression.	$\bar{f}_x = f_s, \bar{f}_y = f'_s, \sigma_1 = 0, \sigma_2 = f_c$	Direct solution
8	X compression, Y tension.	$\bar{f}_x = f'_s, \bar{f}_y = f_s, \sigma_1 = 0, \sigma_2 = f_c$	Direct solution
9	No Reinforcement.	$\rho_x = \rho_y = 0$	Direct solution

determined from the additional equation obtained by considering the minimum total amount of reinforcement as follows:

$$\frac{\partial(\rho_x + \rho_y)}{\partial(\tan \theta)} = 0 \quad (3.3)$$

When tension reinforcement is to be provided, σ_1 is given as zero because the concrete must be cracked and when compression reinforcement is provided $\sigma_2 = f_c$, so as to make optimum use of concrete.

By means of equations (3.2), (3.3) and Table (3.1.) the solutions for the reinforcement ratios, principal concrete stresses and θ be obtained for each case and are summarized in Table 3.2.

The following symbols are introduced in Table 2.

$$\sigma_{xf} = \sigma_x + f_c$$

$$\sigma_{yf} = \sigma_y + f_c$$

$$\beta = \frac{\sqrt{\alpha^2 - 1}}{\alpha} \quad \text{where } \alpha = \frac{f_c}{2|\tau_{xy}|}$$

Having established the equations relevant to each of the nine cases, it is now necessary to establish a means of determining which set of equations should be used for particular stress trial. This can be achieved by considering the relationship among nine cases and the limitation of principal concrete stresses. In this way, the case boundary equations/

T A B L E 3.2
DESIGN EQUATIONS FOR REINFORCEMENT

Case	ρ_x	ρ_y	ϕ_1	ϕ_2	$\tan \theta$
1	$\frac{1}{f_s}(\sigma_x + \tau_{xy})$	$\frac{1}{f_s}(\sigma_y + \tau_{xy})$	zero	$-2 \tau_{xy} $	$-\frac{\tau_{xy}}{ \tau_{xy} }$
2	$\frac{1}{f_s}(\sigma_x - \frac{\tau_{xy}^2}{\sigma_y})$	zero	zero	$\sigma_y + \frac{\tau_{xy}^2}{\sigma_y}$	$\frac{\tau_{xy}}{-\sigma_y}$
3	zero	$\frac{1}{f_s}(\sigma_y + \frac{\tau_{xy}^2}{\sigma_x})$	zero	$\sigma_x + \frac{\tau_{xy}^2}{\sigma_x}$	$\frac{\sigma_x}{-\tau_{xy}}$
4	$\frac{1}{f_s}(\tau_{xy} - \sigma_x - f_c)$	$\frac{1}{f_s}(\tau_{xy} - \sigma_y - f_c)$	$f_c + 2 \tau_{xy} $	f_c	$-\frac{\tau_{xy}}{ \tau_{xy} }$
5	$\frac{1}{f_s}(\frac{\tau_{xy}^2}{\sigma_{yf}} - \sigma_{xf})$	zero	$\sigma_y + \frac{\tau_{xy}^2}{\sigma_{yf}}$	f_c	$\frac{\sigma_{yf}}{\tau_{xy}}$
6	zero	$\frac{1}{f_s}(\frac{\tau_{xy}^2}{\sigma_{xf}} - \sigma_{yf})$	$\sigma_x + \frac{\tau_{xy}^2}{\sigma_{xf}}$	f_c	$\frac{\sigma_{xf}}{\tau_{xy}}$
7	$\frac{1}{f_s}[\sigma_x - \frac{f_c}{2}(1-\beta)]$	$\frac{1}{f_s}[\sigma_y - \frac{f_c}{2}(1+\beta)]$	zero	f_c	$-\frac{1}{\alpha(1-\beta)}$
8	$\frac{1}{f_s}[\sigma_x - \frac{f_c}{2}(1+\beta)]$	$\frac{1}{f_s}[\sigma_y - \frac{f_c}{2}(1+\beta)]$	zero	f_c	$-\frac{1}{\alpha(1+\beta)}$
9	zero	zero	$\frac{\sigma_x + \sigma_y + \sqrt{(\sigma_x - \sigma_y)^2 + 4\tau_{xy}^2}}{2}$	$\frac{\sigma_x + \sigma_y - \sqrt{(\sigma_x - \sigma_y)^2 + 4\tau_{xy}^2}}{2}$	$\frac{\sigma_x - \sigma_y - \sqrt{(\sigma_x - \sigma_y)^2 + 4\tau_{xy}^2}}{2\tau_{xy}}$

are established and are shown in Table 3.3. Typical graph for boundary equation is illustrated in fig. 3.4. In addition to prevent the shear failure of unreinforced concrete it is required that

$$f_c \leq - 2 \left| \tau_{xy} \right| \quad (3.4)$$

3.3.3 Mechanism Criterion:

The inability of structure to carry any more load indicates that it become a mechanism. Due to formation of hinges or yield zones, e.g. inclined cracks the structure could become a mechanism. The inclined crack forming in the corner above and below the opening, propagates towards the loading and support reaction points respectively. These can be solitary cracks and suggests that the hinging regions are very localized. Consequently strain in the reinforcement crossing these cracks is likely to be high. The structure will convert into a mechanism when hinge region reaches its yield capacity.

3.4 SERVICEABILITY LIMIT STATE

According to CP110 (Ref.3), the two most important serviceability limit state requirements are:

i) Deflection: the final deflection including the effect of temperature, creep and shrinkage should not exceed either of the following limit:

a) Span/250.

b) Span/350 or 20 mm, which ever is the lesser, after the/

T A B L E 3.3
BOUNDARY CURVES

Curve	Equation
1	$\frac{\sigma_x}{ \tau_{xy} } = +\infty$
2	$\frac{\sigma_x}{ \tau_{xy} } = \frac{1}{2} \left(\frac{f_c}{ \tau_{xy} } + \sqrt{\left(\frac{f_c}{ \tau_{xy} }\right)^2 - 4} \right)$
3	$\frac{\sigma_x}{ \tau_{xy} } = -1$
4	$\frac{\sigma_x}{ \tau_{xy} } = \frac{f_c}{ \tau_{xy} } + 1$
5	$\frac{\sigma_x}{ \tau_{xy} } = \frac{1}{2} \left(\frac{f_c}{ \tau_{xy} } - \sqrt{\left(\frac{f_c}{ \tau_{xy} }\right)^2 - 4} \right)$
6	$\frac{\sigma_x}{ \tau_{xy} } = -\infty$
7	$\frac{\sigma_y}{ \tau_{xy} } = \frac{1}{2} \left(\frac{f_c}{ \tau_{xy} } - \sqrt{\left(\frac{f_c}{ \tau_{xy} }\right)^2 - 4} \right)$
8	$\frac{\sigma_y}{ \tau_{xy} } = -1$
9	$\frac{\sigma_x f}{ \tau_{xy} } = \frac{\sigma_y f}{ \tau_{xy} } = 1$
10	$\frac{\sigma_x}{ \tau_{xy} } = \frac{\sigma_y}{ \tau_{xy} } = 1$
11	$\frac{\sigma_y}{ \tau_{xy} } = \frac{f_c}{ \tau_{xy} } + 1$
12	$\frac{\sigma_y}{ \tau_{xy} } = \frac{1}{2} \left(\frac{f_c}{ \tau_{xy} } + \sqrt{\left(\frac{f_c}{ \tau_{xy} }\right)^2 - 4} \right)$

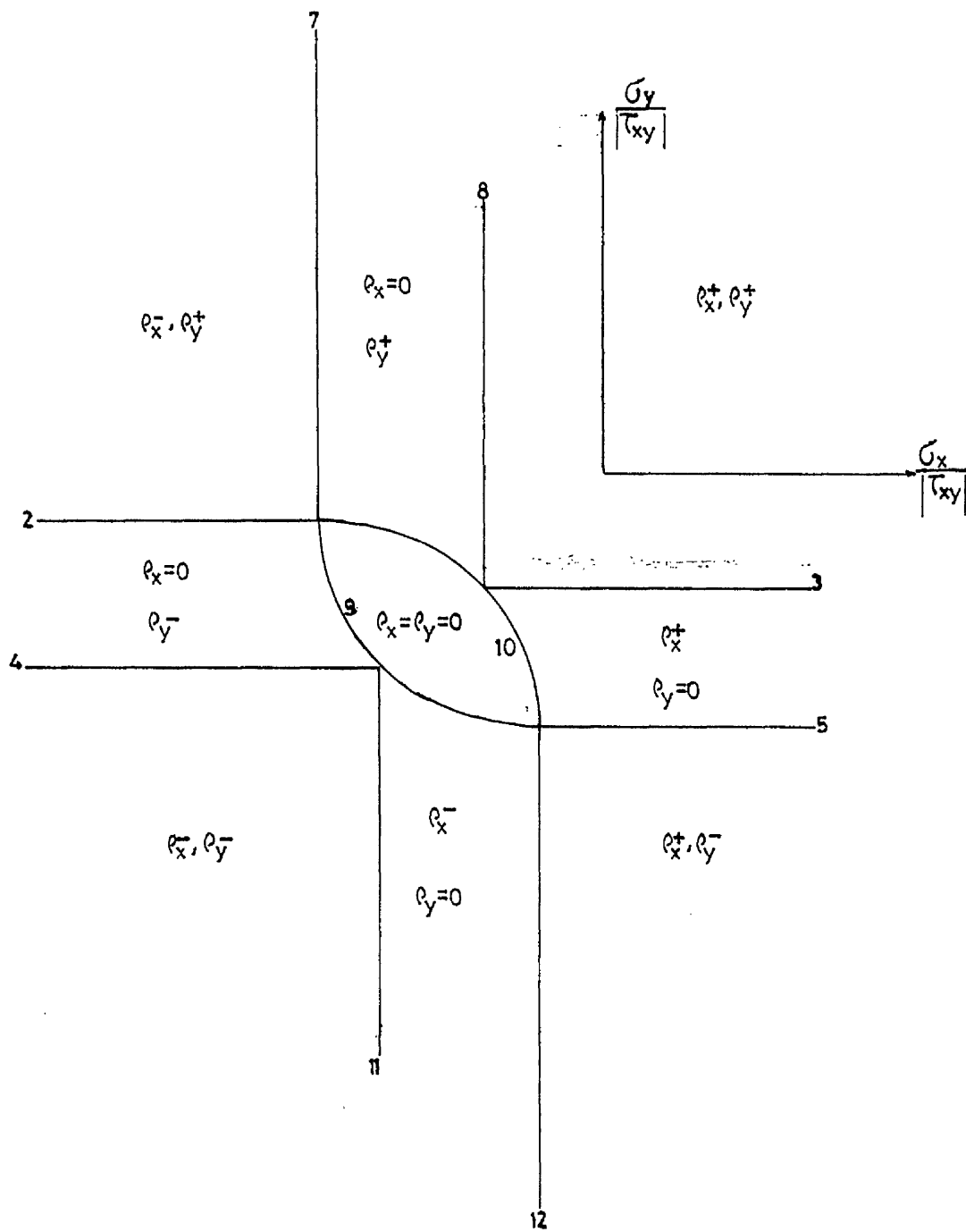


FIG. 3.4. BOUNDARY EQUATION GRAPH.

construction of the partitions or the application of finishes.

ii) Cracking widths: In concrete structures, the surface crack width should not, in general, exceed 0.3 mm.

In present study, the serviceability limit state is reached if either the deflection exceeds the limit of span/350 or cracking width exceeds the limit of 0.3 mm.

3.5 PRACTICAL CONSTRAINTS

The design procedure described in section 3.3 to reinforce each element of the structure against the forces acting on it is of limited application because there is practical constraint on the proportion of the steel which may be provided. It can be seen that the theoretical calculated reinforcement can not be rigorously applied because the reinforcement ratios varies throughout the structure. In this section, how this difficulty is overcome will be discussed. Also, local details, for instance, anchorage length, bearing capacity, etc., have to be considered and will also be discussed. The design process will be illustrated, where necessary by reference to the design of test beam B4- 0.95/0.22/2. (See section 4.2.2 of Chapter 4 for beam marking).

3.5.1 The application of the finite element programme:

An existing finite element programme was used in the present study.

The elastic stress distribution for all the beams had/

obtained from an analysis by reference (48). The finite element mesh of linear strain element is shown in fig.3.5.

3.6 DESIGN CONSIDERATION FOR REINFORCED CONCRETE DEEP BEAM WITH WEB OPENING.

3.6.1 Design for Reinforcement

The proposed design method has been programmed for the computer. A flow chart is shown in 3.6.

The required reinforcement ratios for the beam B4- 0.95/0.22/2 are shown in Table 3.5. It can be seen from the table 3.5 that the reinforcement ratio varied from element to element. Under the opening of the beam the horizontal ratios were maximum near the support and decrease towards the mid-span, while above the opening horizontal ratios were maximum at mid-span.

The use of orthogonal reinforcement for deep beams is emphasised by most of codes. As the shear-span to depth ratio of the beam decreases, the effectiveness of web reinforcement perpendicular to the longitudinal axis is reduced. At the same time, distributed reinforcement parallel to the longitudinal axis will increase the shear capacity. Some schools of thoughts suggested that horizontal bars within the web of beam should have beneficial effect on crack control particularly in deeper beams.

In practice reinforcement ratio will not vary exactly/

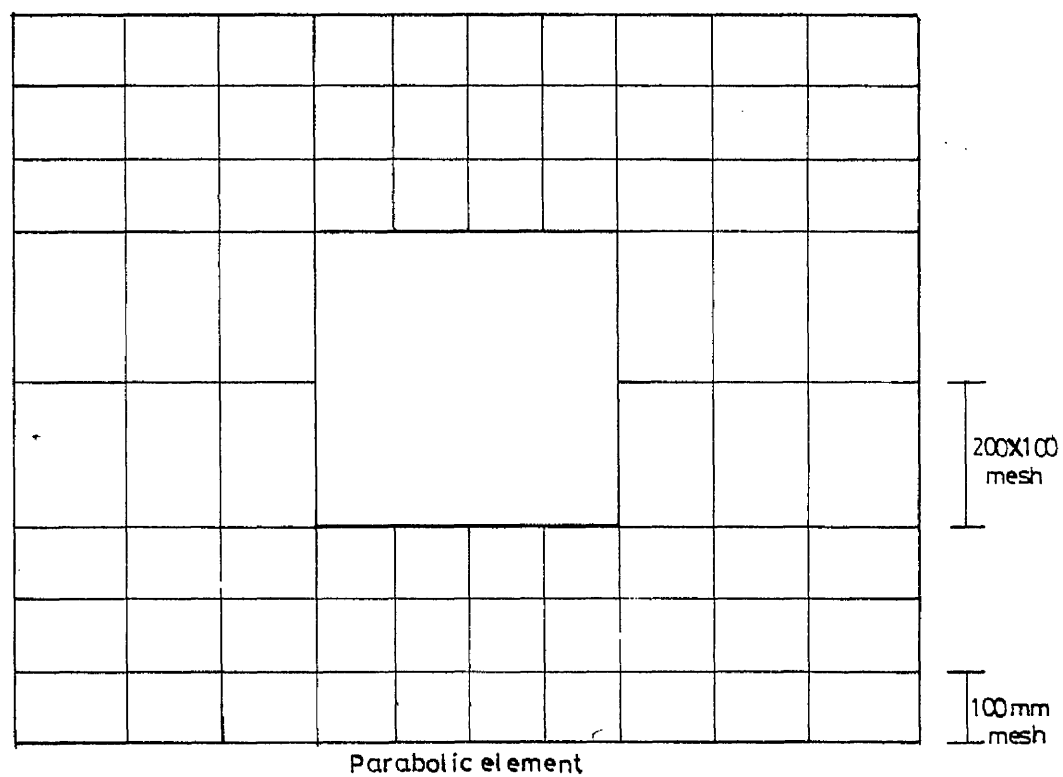
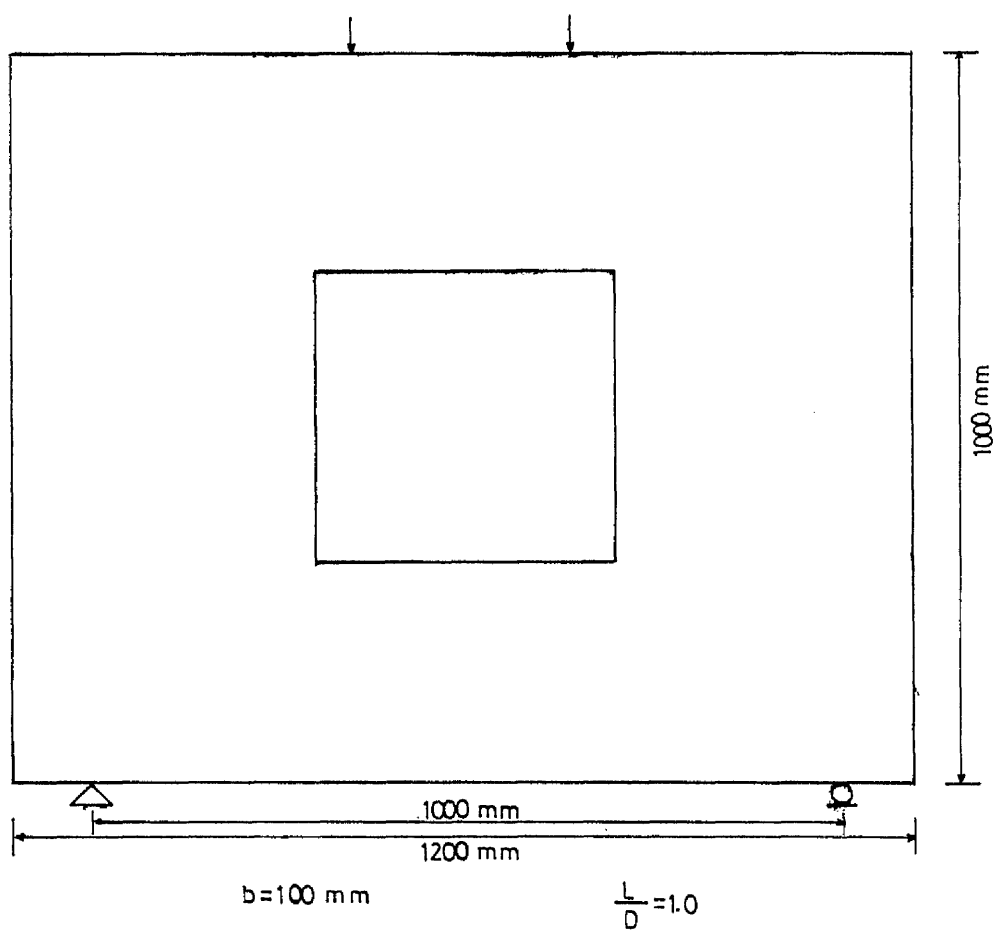


FIG.3.5. FINITE ELEMENT MESH.

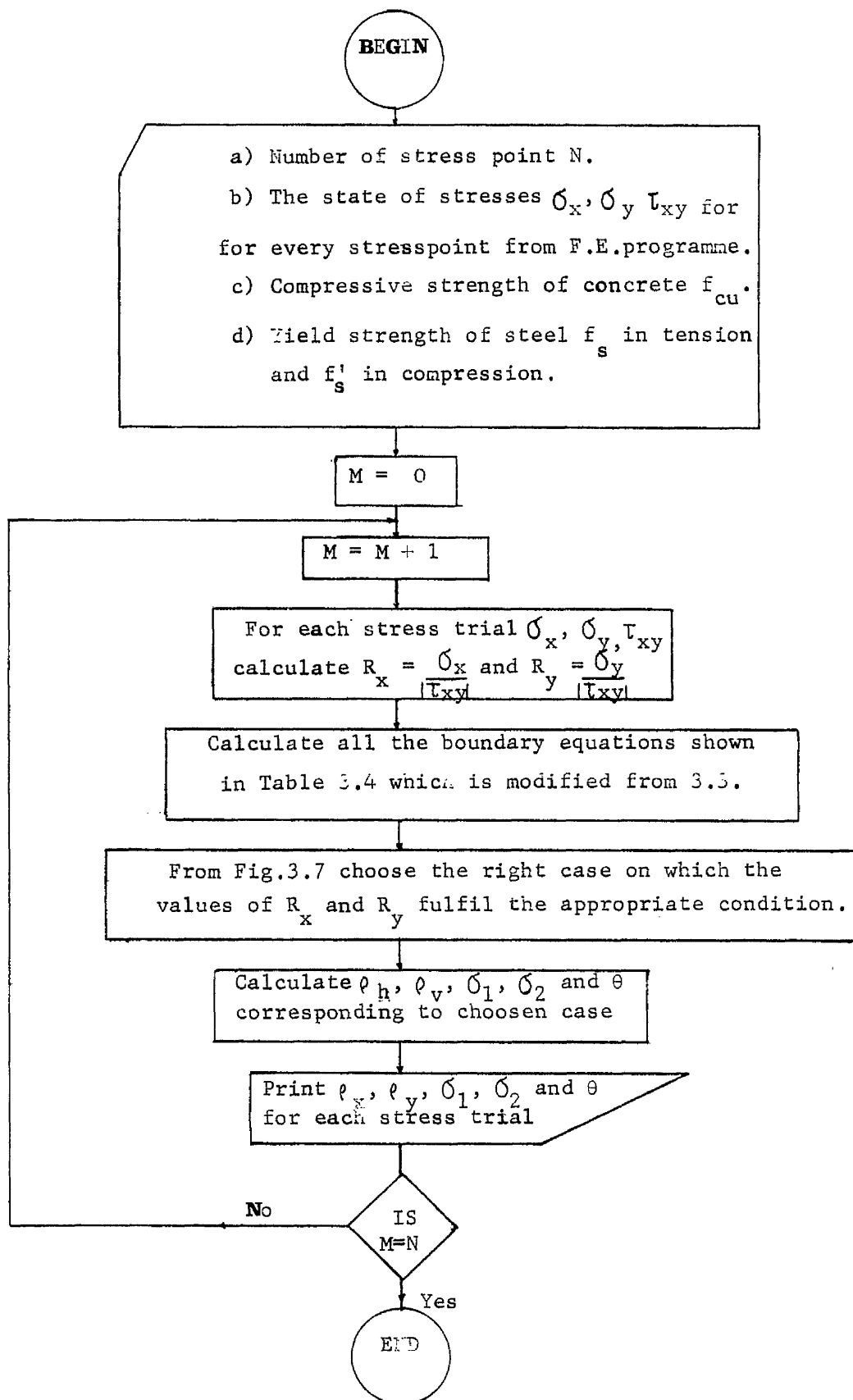


FIG.3.6.FLOW CHART

T A B L E 3.4

MODIFIED BOUNDARY EQUATIONS CORRESPONDING TO TABLE (3.3)

Curve	Equation
1	$E_1 = \frac{\sigma_x}{ \tau_{xy} } = +\infty$
2	$E_2 = \frac{\sigma_x}{ \tau_{xy} } = \frac{1}{2} \left(\frac{f_c}{ \tau_{xy} } + \sqrt{\left(\frac{f_c}{ \tau_{xy} }\right)^2 - 4} \right)$
3	$E_3 = \frac{\sigma_x}{ \tau_{xy} } = -1$
4	$E_4 = \frac{\sigma_x}{ \tau_{xy} } = \frac{f_c}{ \tau_{xy} } + 1$
5	$E_5 = \frac{\sigma_x}{ \tau_{xy} } = \frac{1}{2} \left(\frac{f_c}{ \tau_{xy} } - \sqrt{\left(\frac{f_c}{ \tau_{xy} }\right)^2 - 4} \right)$
6	$E_6 = \frac{\sigma_x}{ \tau_{xy} } = -\infty$
7	$E_7 = \frac{\sigma_y}{ \tau_{xy} } = \frac{1}{2} \left(\frac{f_c}{ \tau_{xy} } - \sqrt{\left(\frac{f_c}{ \tau_{xy} }\right)^2 - 4} \right)$
8	$E_8 = \frac{\sigma_y}{ \tau_{xy} } = -1$
9	$E_{9x} = \frac{ \tau_{xy} }{\sigma_{yf}} + \frac{f_c}{ \tau_{xy} } \text{ and } E_{9y} = \frac{ \tau_{xy} }{\sigma_{xf}} + \frac{f_c}{ \tau_{xy} }$
10	$E_{10x} = \frac{ \tau_{xy} }{\sigma_y} \text{ and } E_{10y} = \frac{ \tau_{xy} }{\sigma_x}$
11	$E_{11} = \frac{\sigma_y}{ \tau_{xy} } = \frac{f_c}{ \tau_{xy} } + 1$
12	$E_{12} = \frac{\sigma_y}{ \tau_{xy} } = \frac{1}{2} \left(\frac{f_c}{ \tau_{xy} } + \sqrt{\left(\frac{f_c}{ \tau_{xy} }\right)^2 - 4} \right)$

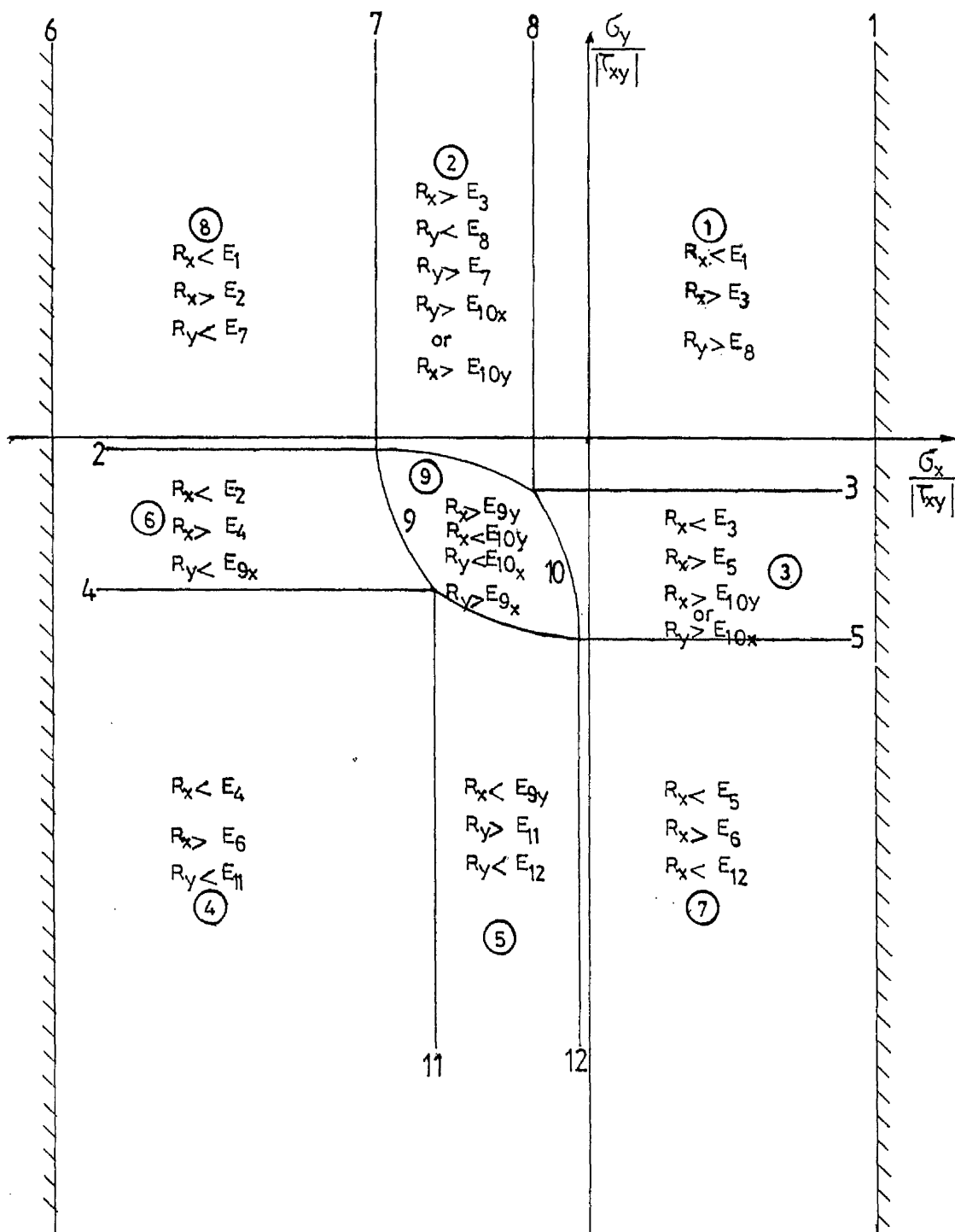


FIG.3.7. CONDITIONS FOR CHOSEN CASES OF BOUNDARY CURVES.

as required by the theoretical approach. Since the beams tested were quite small, there was little possibility of varying steel area to match the theoretical steel requirements. Only two possibilities were open.

a) Placing the steel bar according to the average of steel ratio at each level.

b) Choose the maximum steel ratio at each level and place the required bar through this level.

Comparison between the two methods, indicated that method (a) is economical but gives an unsafe design. On the other hand method (b) is rather uneconomical but it gives a safe design.

The design adopted for beam B4-0.95/0.22/2 is shown in fig. 3.8.

3.6.2 Bearing Capacity:

In clause 5.2.4.4 of the code CP110 (Ref.3), it states that the bearing capacity should not normally exceed $0.4 f_{cu}$ under the ultimate load. However, it may increase to $0.8 f_{cu}$, provided the stress zone is adequately confined.

A short column design is employed to ensure no premature failure due to bearing. According to clause 3.5.3 CP110, the following equation was used for column design.

$$N = 0.4 f_{cu} A_c + 0.67 A_{sc} f_y \quad (3.5)$$

where N is the applied load.

f_{cu} is the characteristic strength of the concrete.

A_c is the area of concrete. (It is assumed equal to bearing area).

A_{sc} is the required area of compressive reinforcement in bearing area.

f_y is the characteristic strength of the compression reinforcement.

The area of reinforcement A_{sc} should start from the bearing plate and extend such that forces may be transmitted from the bearing area into the inner concrete zone. The required length can be calculated by the full anchorage length $l_a = 0.18 f_y \phi / f_{ba}$ where f_{ba} is ultimate anchorage bond stress and ϕ is a diameter of bar. Links should also be supplied to avoid buckling failure.

Beside the direct bearing, the main factor which also cause bearing failure is Poisson's effect. The Poisson's effect results in a lateral force of one-sixth the magnitude of the vertical force in the vicinity of the loading zone. In real structures sufficient concrete cover and reinforcement should be provided also. In the present tests because of congestion of the reinforcement, the expansive forces is resisted by the external plates. (see fig. 4.5).

B4-0.95/0.22/2

NOTE: The upper figure in each region represents the horizontal steel ratio (ρ_x) required in percentage and the lower figure in each region represents the vertical steel ratio (ρ_y) required in percentage in that region. Where figures are not shown are zero.

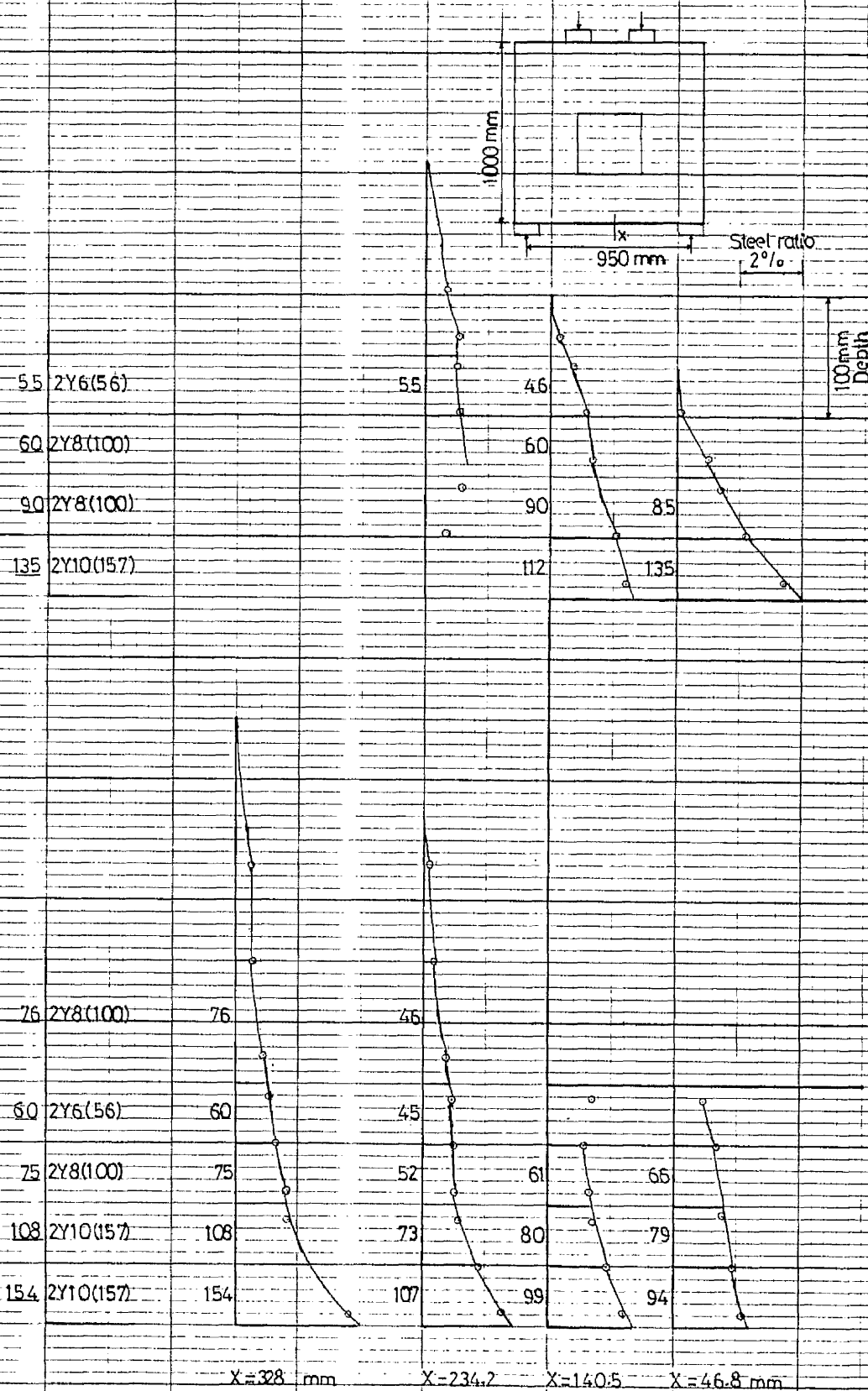


FIG.3.8. DESIGN FOR REINFORCEMENT FOR BEAM B4/0.95/0.22/2.

NOTE: FIGURES UNDERLINED REPRESENT THE STEEL AREA REQUIRED(mm²) IN THAT AREA. FIGURES IN BRACKETS REPRESENT THE ACTUAL STEEL AREA SUPPLIED IN THAT AREA.

3.6.3 Bond and Anchorage:

Anchorage bond stresses and the effective dimensions of hooks and bends should comply with clauses 3.11.6.2 and 3.11.6.7 and 8, respectively, of CP110 (Ref.3).

In deep reinforced concrete beams, the full tensile force must be developed in anchorage at the support, because of the arch-action behaviour which is thought to occur at ultimate loads. The main tensile reinforcement which may reach its yield stress near the face of support due to diagonal crack should be securely anchored. It is suggested that full positive anchorage should be provided beyond the face of support and bars should not be bent up within $\frac{1}{8}$ to $\frac{1}{5}$ of the depth of the beam between the centre of supports.

Due to the tied-arch action, the stresses will become approximately constant along the main tensile bar hence the local bond stresses do not need to be checked.

CHAPTER FOUR

TEST PROGRAMME

4.1 INTRODUCTION

The object of the test programme conducted was to study the strength and behaviour characteristics of reinforced concrete deep beams with openings subjected to in-plane loads.

A total of seven beams with and without openings were tested, subjected either to single central point loading or to an off-centre two point loading. The study of the beams is carried out in terms of

- i) Load - deflection, relationship.
- ii) Strain distribution at various sections.
- iii) Crack pattern and crack propagation.
- iv) Failure characteristics.

4.2. TEST PROGRAMME

4.2.1 Test Specimens

The test specimens consisted of seven (7) deep beams with rectangular web opening, each having an overall depth of 1000 mm (39.37 in), thickness of 100 mm (3.94 in) and span length of 950 mm (37.4 in) and 1000 mm (39.37 in) giving span to depth ($\frac{L}{D}$) ratios of 0.95 and 1.0 respectively. Two clear shear span distances were used giving clear shear-span to depth ($\frac{x}{D}$) ratios of 0.22 and 0.2 respectively except for centrally loaded beam, where the clear shear-span to depth ratio was 0.32.

The opening used in the beams was at two different locations, identified by numbers 1 and 2, details of the size and locations are explained in fig. 4.1.

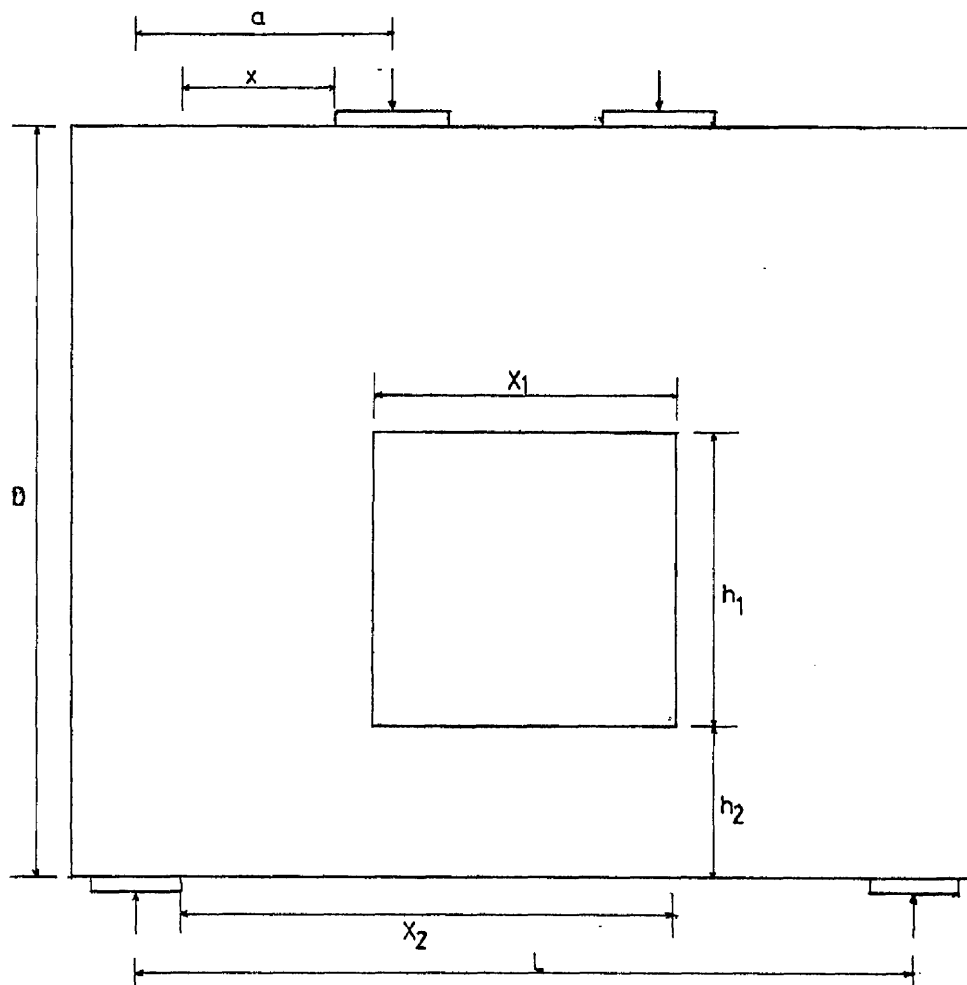
Four beams were simply supported on an effective span of 950 mm (37.4 in). Three of these had a two-point loading system while one was loaded at the centre. The length of the bearing plates was 100 mm at the support in all cases, 100 mm at the load points for the two-point loading and 200 mm for the central loading.

The rest of the beams were simply supported on an effective span of 1000 mm. The length of the bearing plates at the support and at the loading points was 120 and 160 mm respectively. Two beams with the same reinforcement mesh but different concrete mixes were fabricated to investigate the effect of the concrete strength.

Details of the span and shear span of each of the beam, arrangement of reinforcement and properties of test specimens are given in Table (4.1) and fig. (4.2).

4.2.2 Beam Notation:

A letter B before the hyphen indicates beam number ; the span to depth ($\frac{L}{D}$) ratio is given after the hyphen, followed by the clear shear-span to depth ($\frac{x}{D}$) ratio and web opening reference number. For example B1- 0.95/0.32/1 refers to a beam number one, with span to depth ratio of 0.95, having clear shear-span to depth ratio of 0.32 and a web opening type 1.



Opening Type	Size		Position	
	x_1	h_1	x_2	h_2
1	400	400	625/640	300
2	400	400	625/640	200
2A	500	400	690	200

FIG.4.1. DETAILS OF SIZE AND POSITION OF THE OPENINGS.

T A B L E 4.1
DETAILS OF THE DIMENSIONS AND PROPERTIES OF THE BEAMS

Beam Mark	Span-depth L/D	Shear span depth a/D	Clearshear span-depth x/D	Overall depth Dmm	Width bmm	f_{cu}^2 N/mm ²	f'_c N/mm ²	f_t N/mm ²	E_c kN/mm ²	ρ_s %
B1-0.95/0.32/1	0.95	0.47	0.32	1000	100	35.38	27.6	2.74	17.64	1.15
B2-0.95/0.22/0	0.95	0.32	0.22	1000	100	49.52	38.6	3.61	24.64	1.25
B3-0.95/0.22/1	0.95	0.32	0.22	1000	100	38.20	29.8	2.85	22.92	1.11
B4-0.95/0.22/2	0.95	0.32	0.22	1000	100	38.0	29.6	2.85	22.30	1.38
B5-1.0/0.2/2A	1.0	0.35	0.20	1000	100	54.1	42.2	4.16	25.97	2.03
B6-1.0/0.2/1	1.0	0.35	0.20	1000	100	46.4	36.2	3.34	24.16	1.11
B7-1.0/0.2/2	1.0	0.35	0.20	1000	100	58.0	45.2	4.93	26.40	1.38

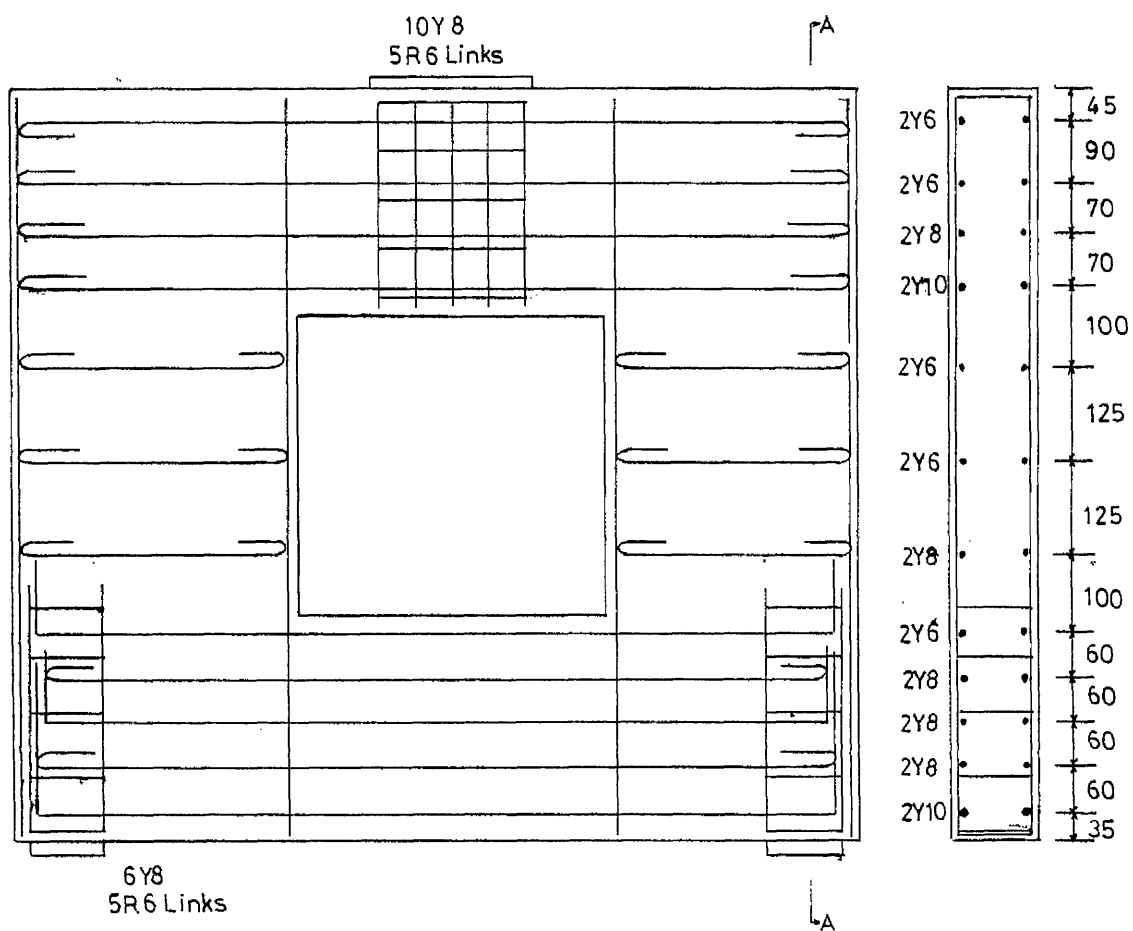


FIG.4.2a. ARRANGEMENT OF REINFORCEMENT FOR BEAM B1. SECTION A-A.

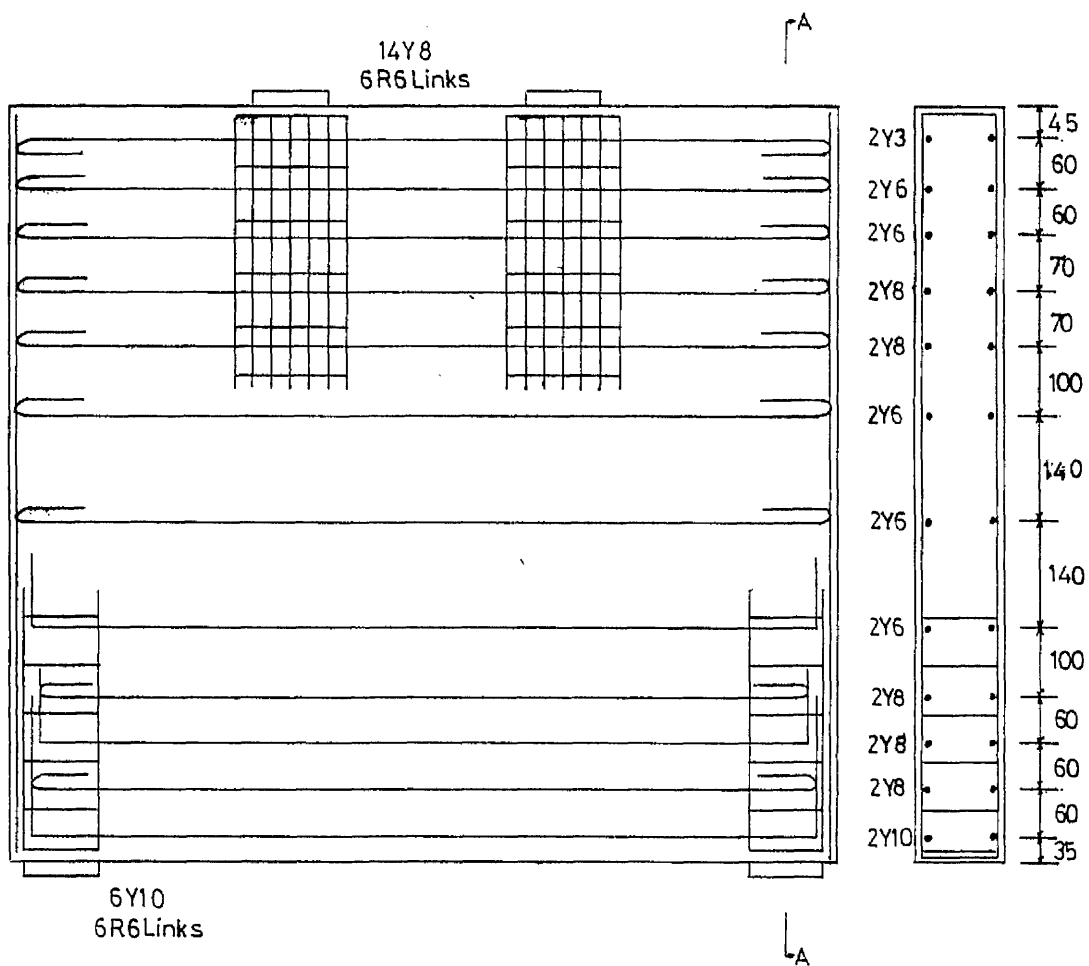


FIG. 4.2b.. ARRANGEMENT OF REINFORCEMENT FOR BEAM B2. SECTION A-A.

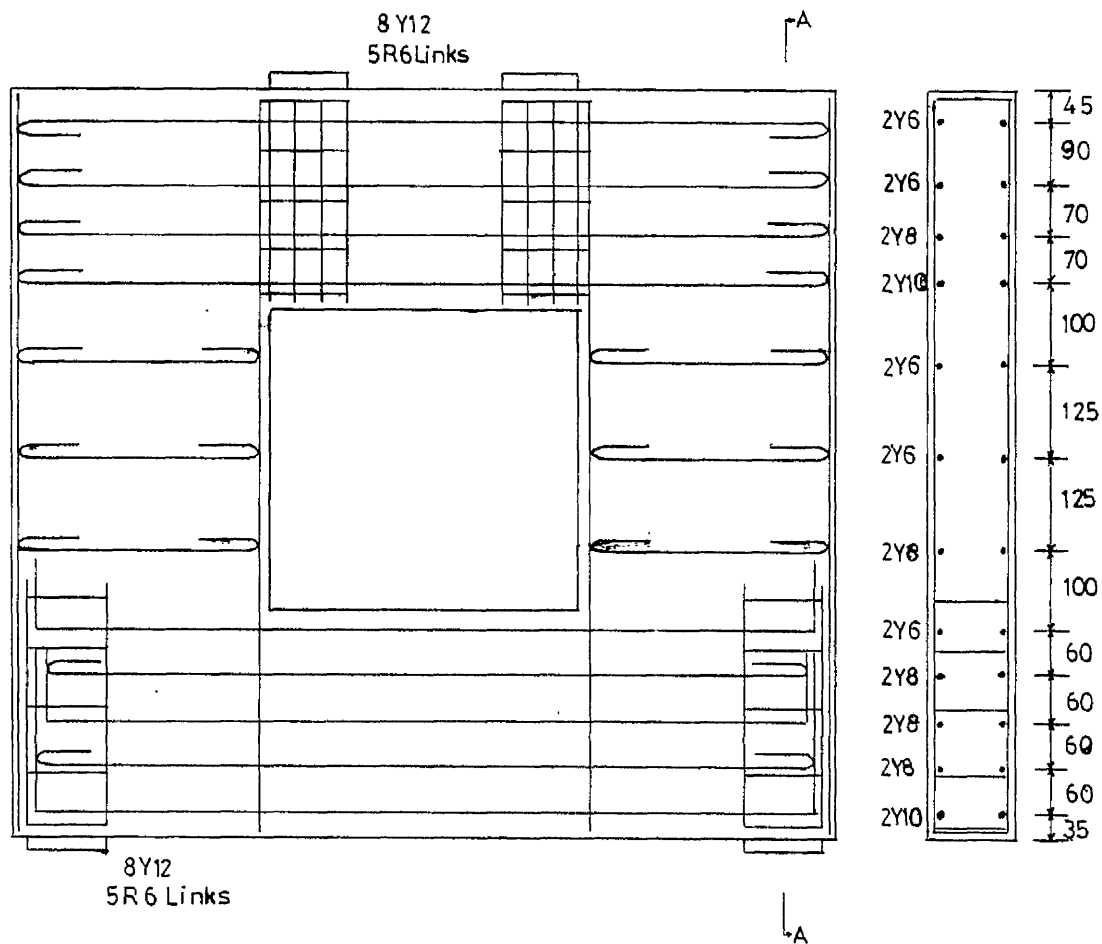


FIG. 4.2c. ARRANGEMENT OF REINFORCEMENT FOR BEAM B3. SECTION A-A.

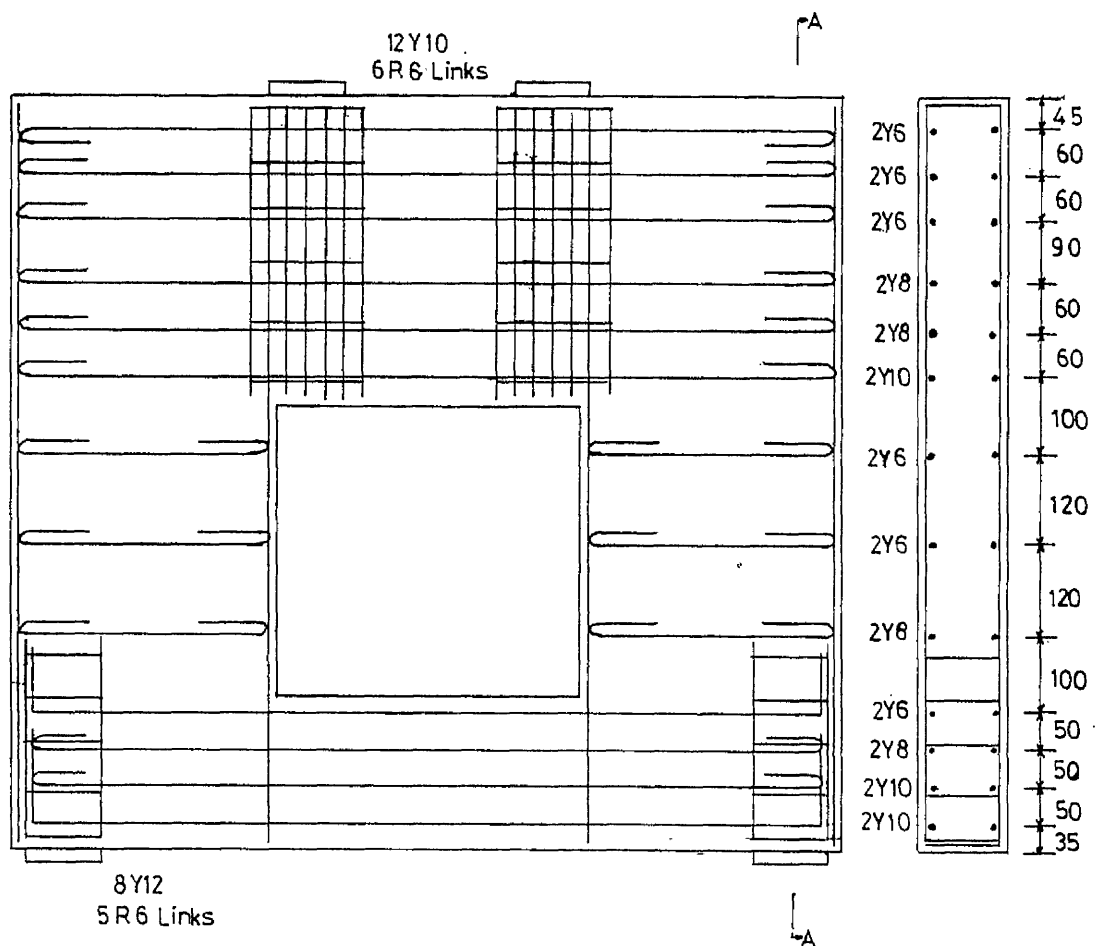


FIG.4.2d. ARRANGEMENT OF REINFORCEMENT FOR BEAM B4. SECTION A-A.

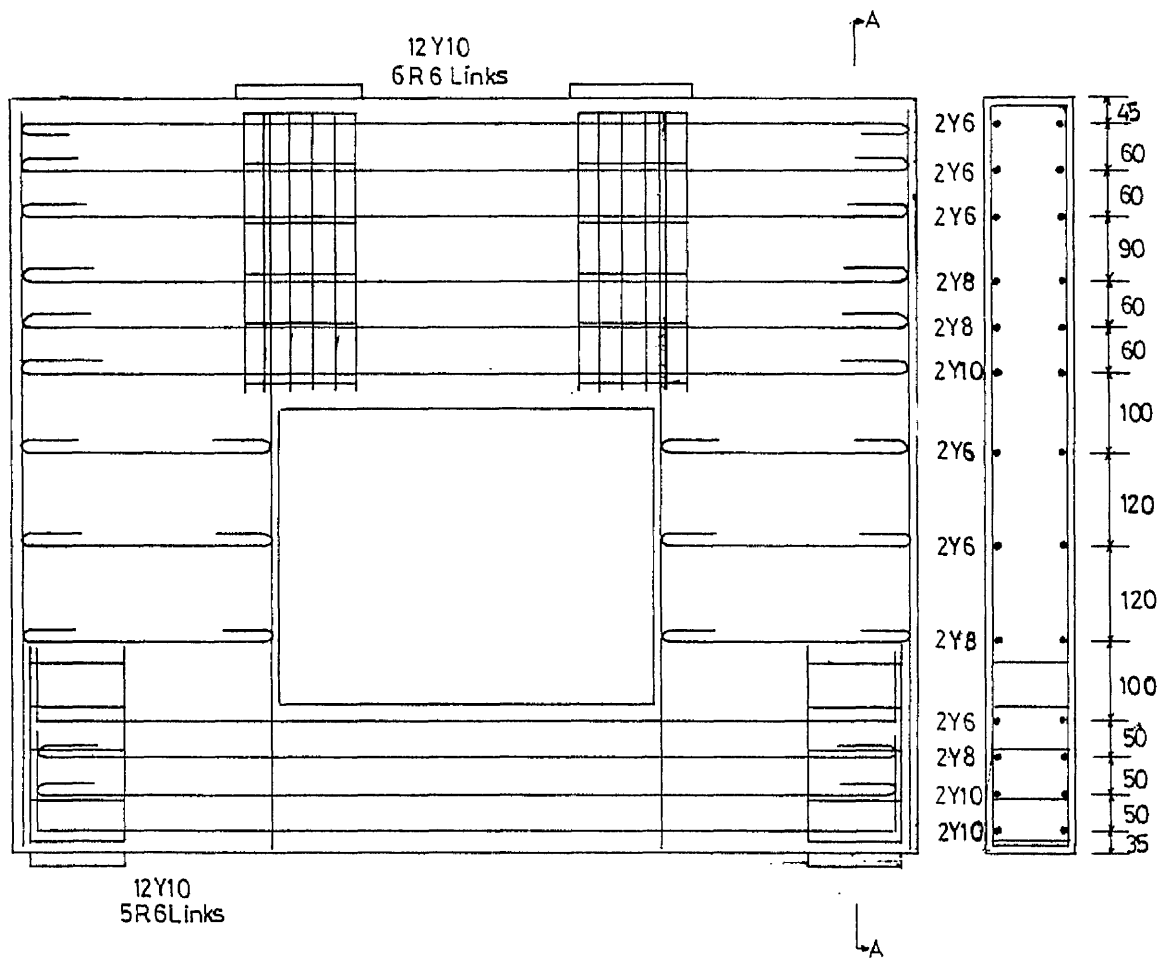


FIG.4.2e. ARRANGEMENT OF REINFORCEMENT FOR BEAM B5. SECTION A-A.

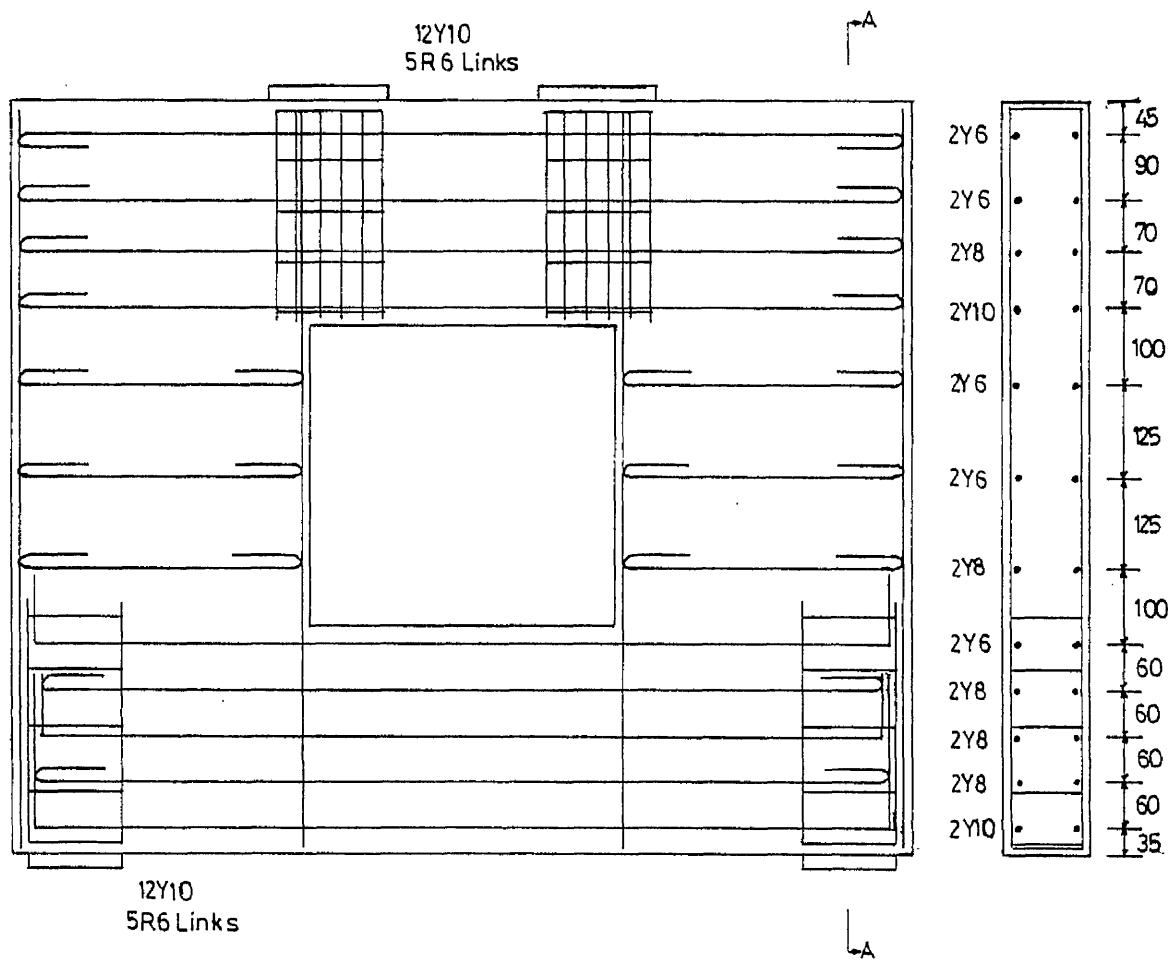


FIG.4.2f. ARRANGEMENT OF REINFORCEMENT FOR BEAM B6. SECTION A-A.

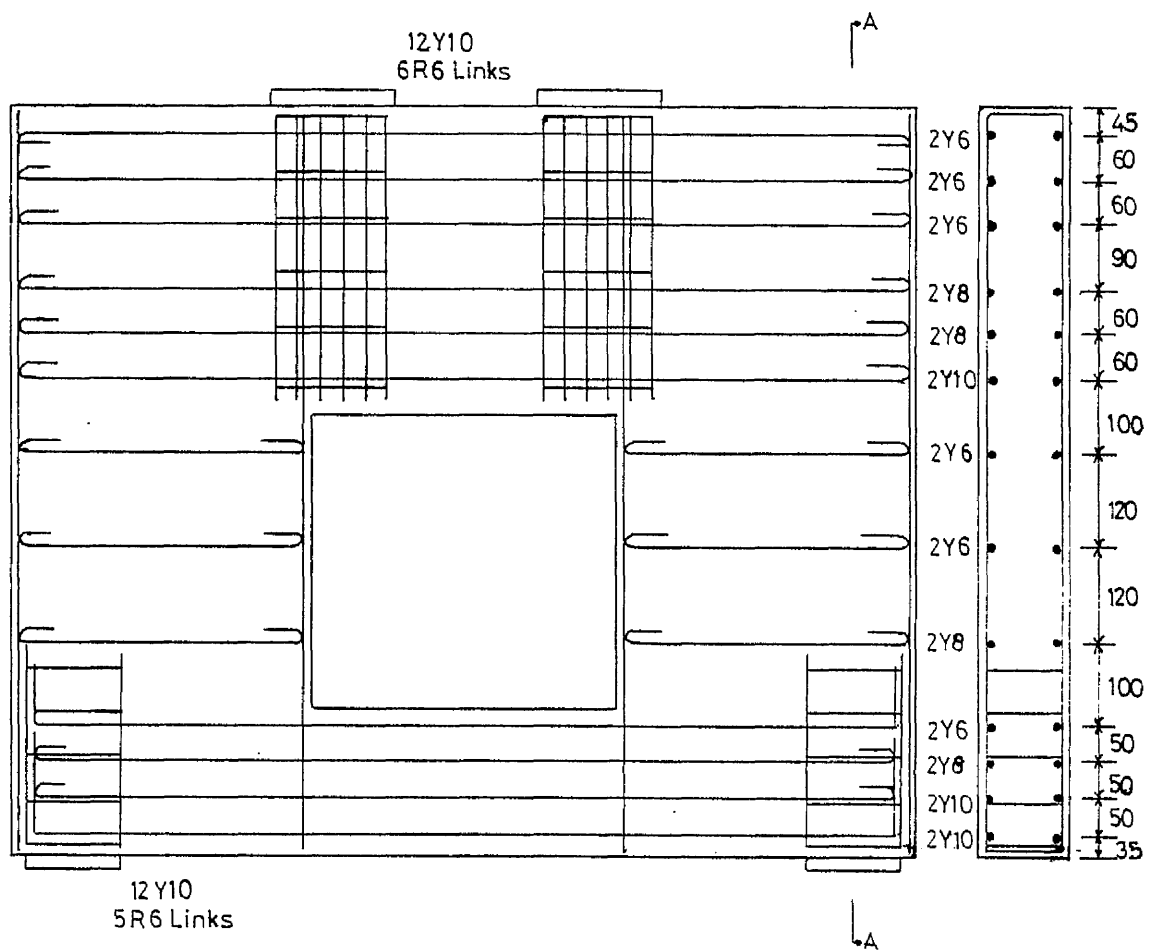


FIG.4.2g. ARRANGEMENT OF REINFORCEMENT FOR BEAM B7. SECTION A-A.

4.3 MATERIALS

4.3.1 Concrete:

Cement: Ordinary portland cement was used in all beams.

Aggregate: Hyndford sand and 10 mm uncrushed gravel were used for all concrete mixes. The grading of the sand was in Zone 2 (Ref.50).

Weighted quantities of cement, sand, 10 mm aggregate and water were mixed thoroughly in a 3 cu.ft capacity cum-flow pan mixer to prepare the concrete mix. For each mix slump and compacting factor were determined. Also for determining the strength properties of hardened concrete at the time of beam testing standard cubes and cylinders were cast and cured and were tested on the day of testing the beam. The concrete mix proportions used for beams along with some of properties are given in Table 4.2.

The compressive strength of concrete was taken as an average of 4- 100 mm cubes, while the cylindrical tensile strength was taken as an average value of 2- 300 x 150 mm diameter cylinders. Two cylinders were used to determine the modulus of elasticity and cylinder compressive strength. Details of the properties of the beams can be found in Table 4.1. The typical stress-strain curve of the concrete obtained from the cylinder test is shown in fig.4.3.

4.3.2 Reinforcement

Tar bars made by British Steel Corporation were used in all beams. These were the cold worked ribbed reinforcing bars complying with the requirements of CP 110 (Ref.3) for the type of/

T A B L E 4.2
CONCRETE MIX PROPORTIONS USED FOR THE BEAMS

Beam Mark	Mix Ratio	Cement Content kg	Sand kg	Coarse Aggregate kg	W/C Ratio	Slump mm	Compacting Factor
B1-0.95/0.32/1	1:1.4:2.85	20.92	29.26	59.62	0.49	33	0.82
B2-0.95/0.22/0	1:1.56:3.24	19.15	29.90	62.0	0.47	19	0.79
B3-0.95/0.22/1	1:1.56:3.24	19.15	29.90	62.0	0.47	18	0.78
B4-0.95/0.22/2	1:1.56:3.24	19.15	29.90	62.0	0.47	18	0.81
B5-1.0/0.2/2A	1:1.44:3.0	20.36	29.52	61.0	0.44	20	0.80
B6-1.0/0.2/1	1:1.44:3.0	20.36	29.52	61.0	0.44	21	0.83
B7-1.0/0.2/2	1:1.44:3.0	20.36	29.52	61.0	0.44	20	0.83

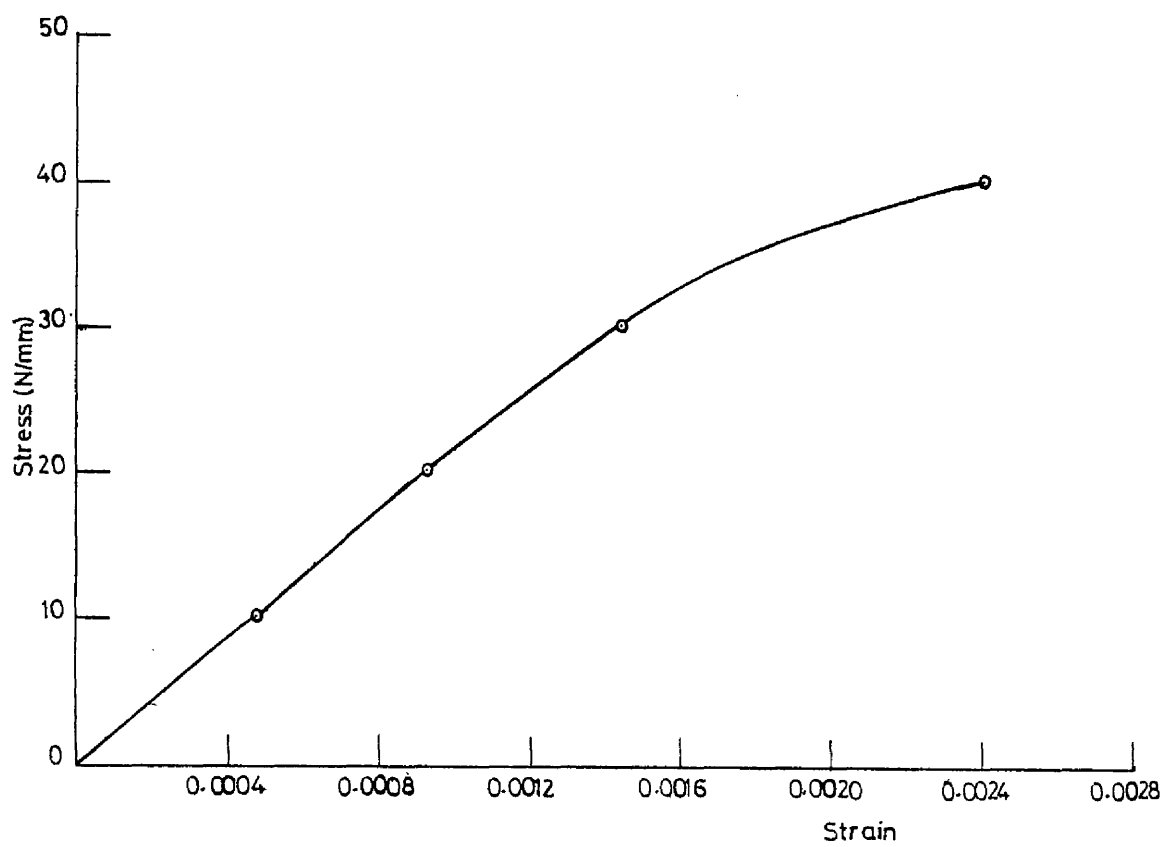


FIG.4.3. UNIAXIAL STRESS STRAIN CURVE FOR PLAIN CONCRETE.

deformed bars. Since each test involved a considerable amount of reinforcement of different bar sizes, strength properties of the reinforcement were determined by conducting tensile tests (Ref.51) on bar specimens. Tests were carried out in accordance with the recommendations of the "Panel for standard practices in Testing" DOE-TRRL working group on long term research into steel box-girder bridges. Typical stress-strain curves for different reinforcing bars are shown in fig.4.4. The average values represent the actual strength and the properties of various sizes of steel bars are given in Table 4.3.

Because of the absence of vertical stirrups in the original design, extra vertical loops at both ends and at the sides of the opening were added to locate all the steel bars in position.

4.3.3. Fabrication and Curing

The beams were cast in oiled wooden moulds. The concrete was placed in the mould with shovels and was compacted by the vibrating table. Four 300 x 150 mm diameter cylinders and eight 100 mm cubes were cast in steel moulds as control specimens for each beam, and were also compacted by a vibrating table. The cylinders were used to determine the splitting tensile strength of the concrete while the cubes were used to determine the compressive strength.

The control specimens were removed from the moulds a day after the casting, they were then submerged in water in a curing tank. The beams were covered in the mould for at least four days with a damp sacking cover. After four days the beams were/

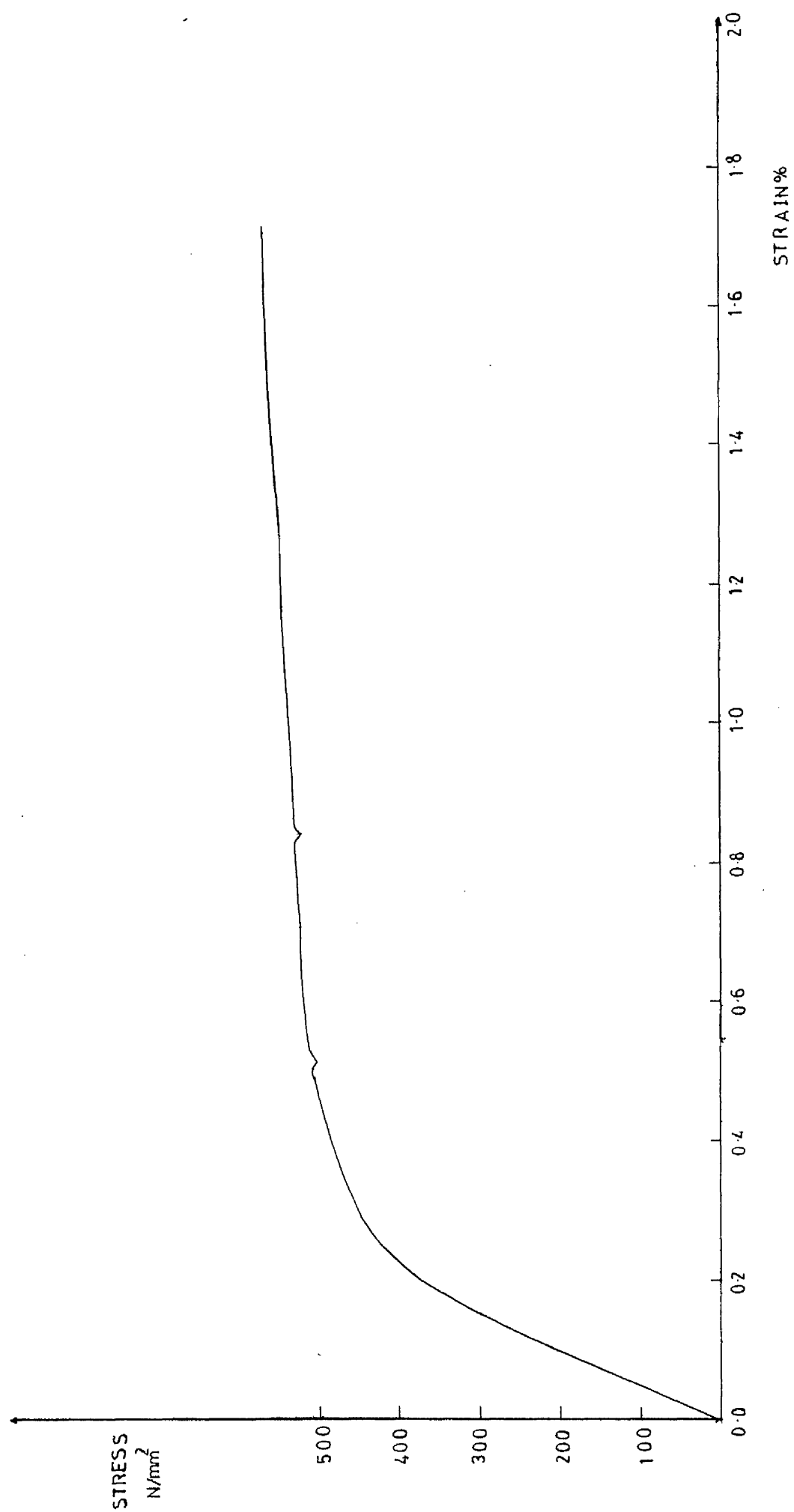


FIG.4.4. TYPICAL STRESS-STRAIN RELATIONSHIP FOR VARIOUS SIZES OF BARS ($D = 6 \text{ mm}$).

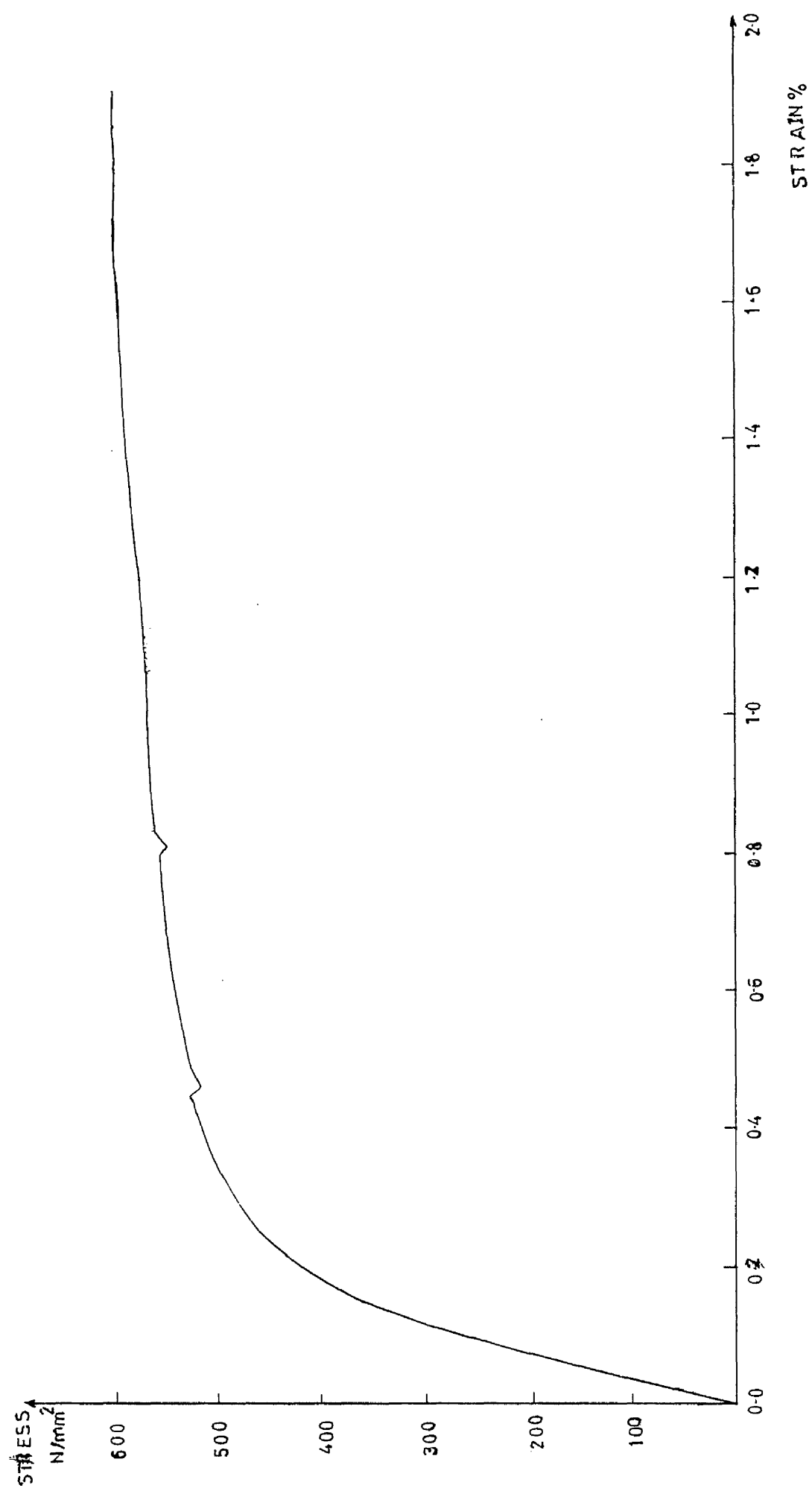


FIG. 4.4. -CONTINUED-(D = 8 mm).

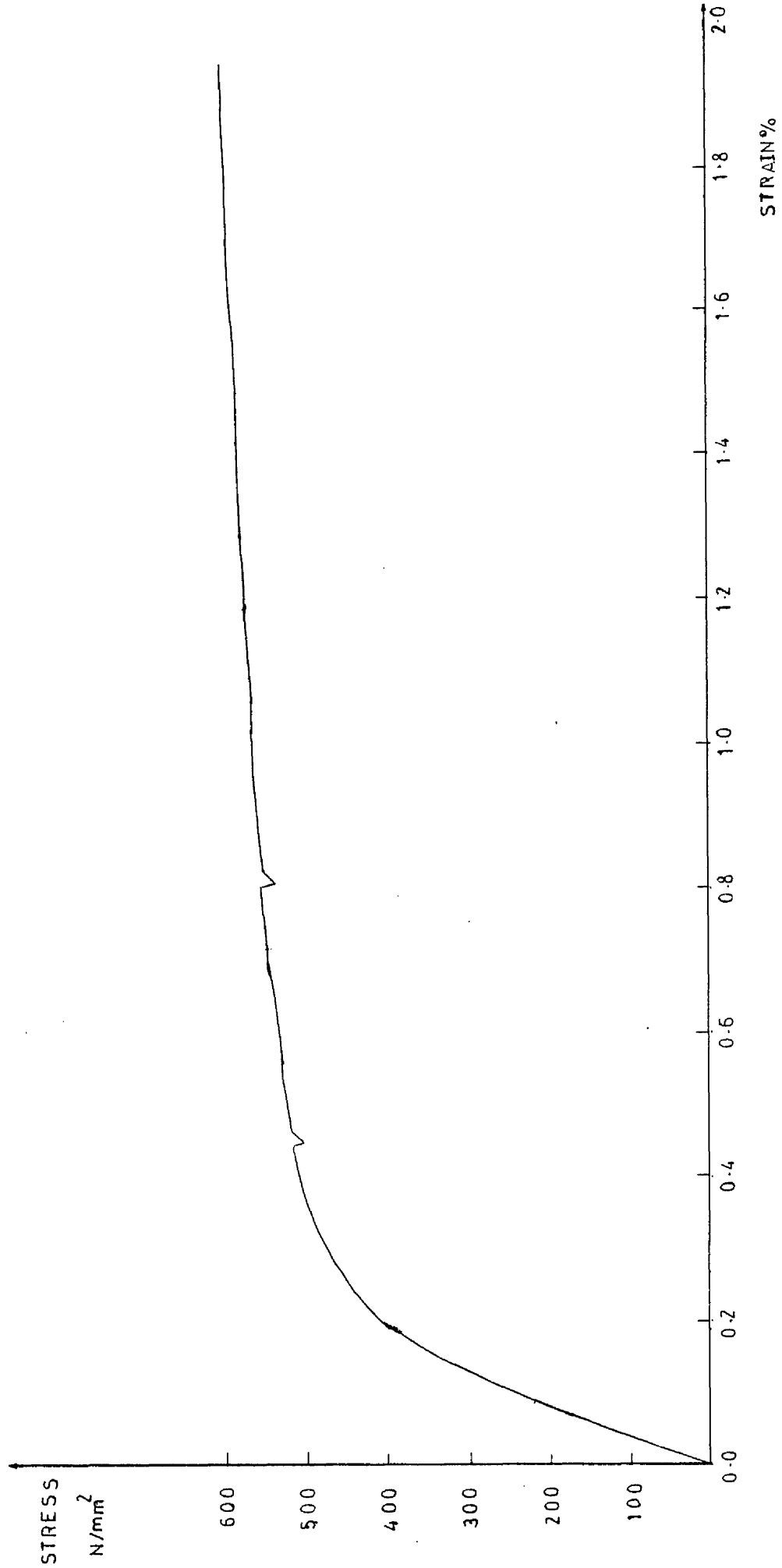


FIG. 4.4. -CONTINUED-(D = 10 mm).

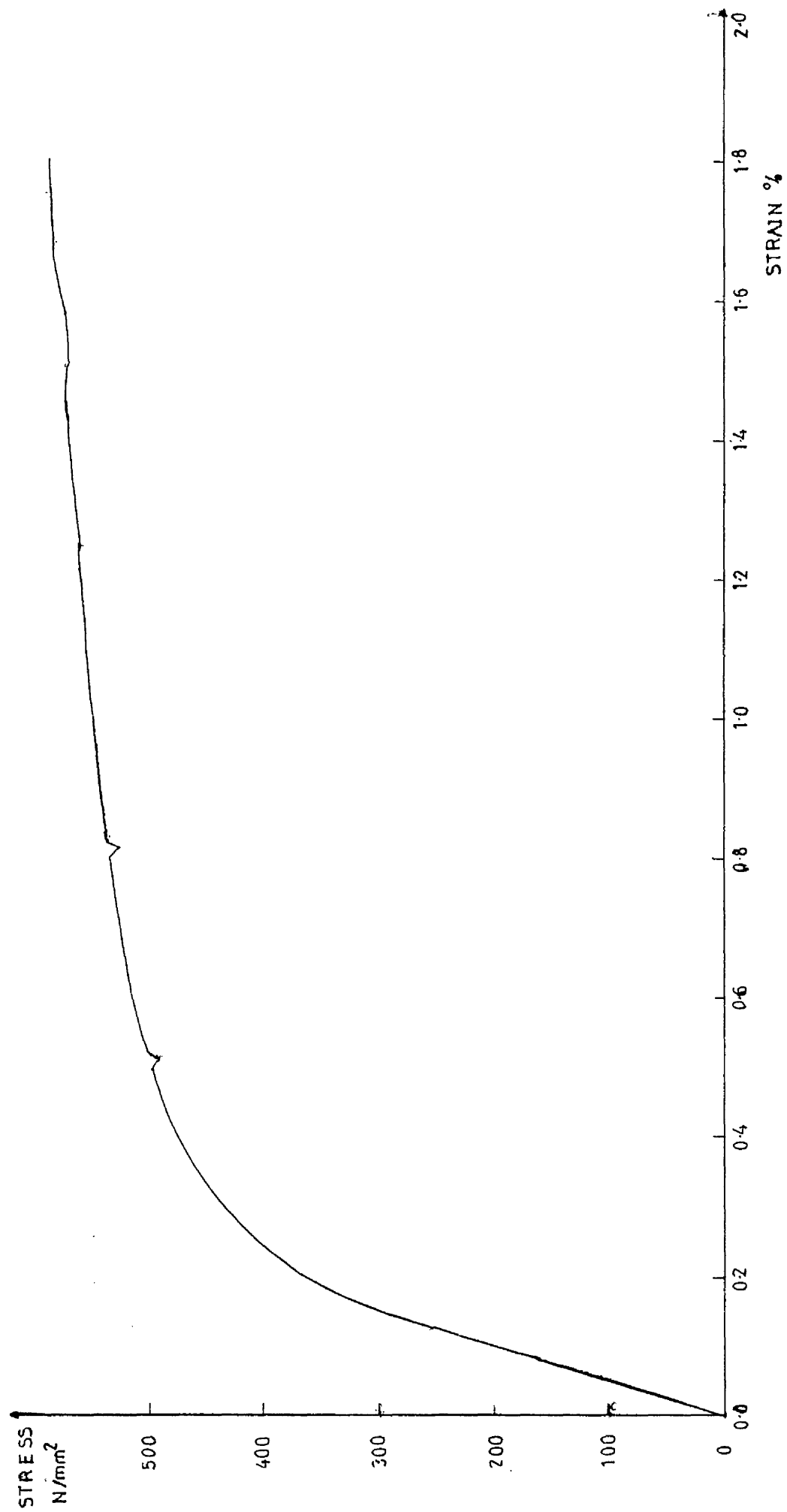


FIG.4.4. -CONTINUED-(D = 12 mm).

T A B L E 4.3
PROPERTIES OF REINFORCEMENT

Nominal Bar Diameter mm	Young's Modulus kN/mm^2	0.2% Proof Stress f_y N/mm^2	Strain at 0.2% Proof Stress ϵ_y	Ultimate Stress N/mm^2
6	251.5	503.0	0.45	566.0
8	252.0	531.0	0.41	542.0
10	252.0	504.0	0.42	679.0
12	246.4	492.8	0.46	585.5

demoulded and then left in the laboratory until they were tested about 12-15 days after casting.

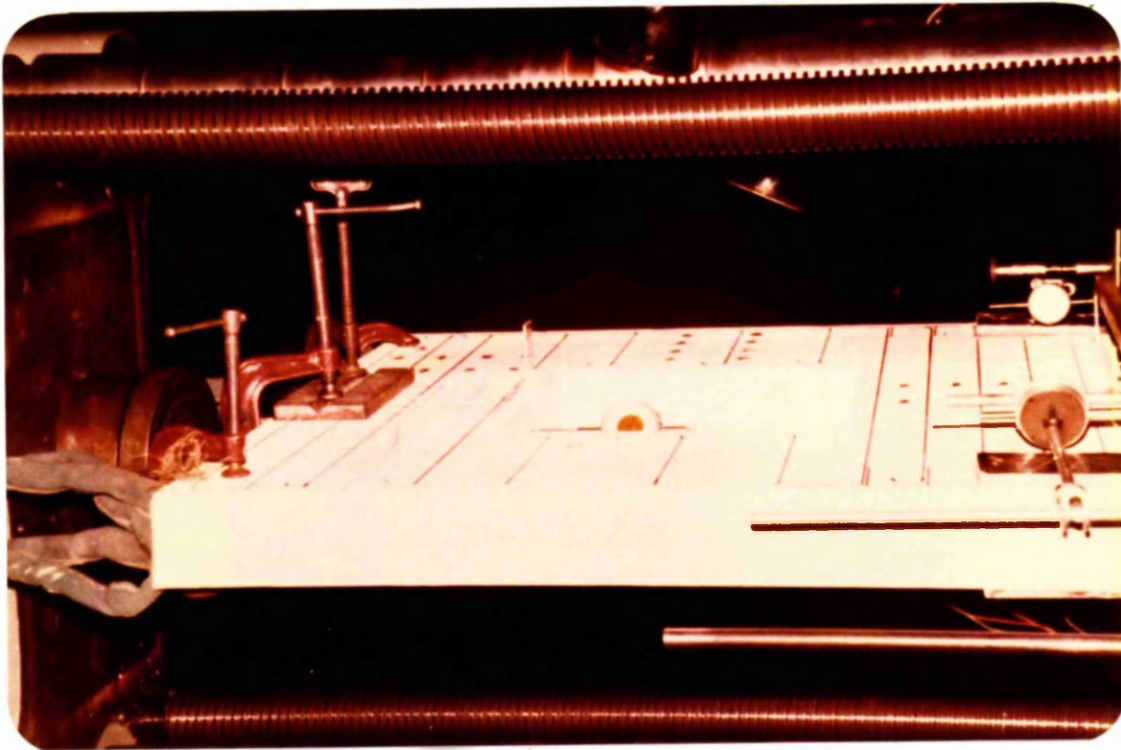
4.4 TEST PROCEDURE

The loads were applied symmetrically to the top surface of the beams through 100 mm square x 30 mm deep and 160 x 100 x 100 mm deep steel bearing blocks, which were bedded to the concrete with approximately 3 mm of quick-setting plaster. The support reactions were applied to the beam soffit through 100 x 100 x 40 mm deep and 120 x 100 x 100 mm deep steel bearing blocks bedded in the same way to the concrete with about 3 mm of quick setting plaster.

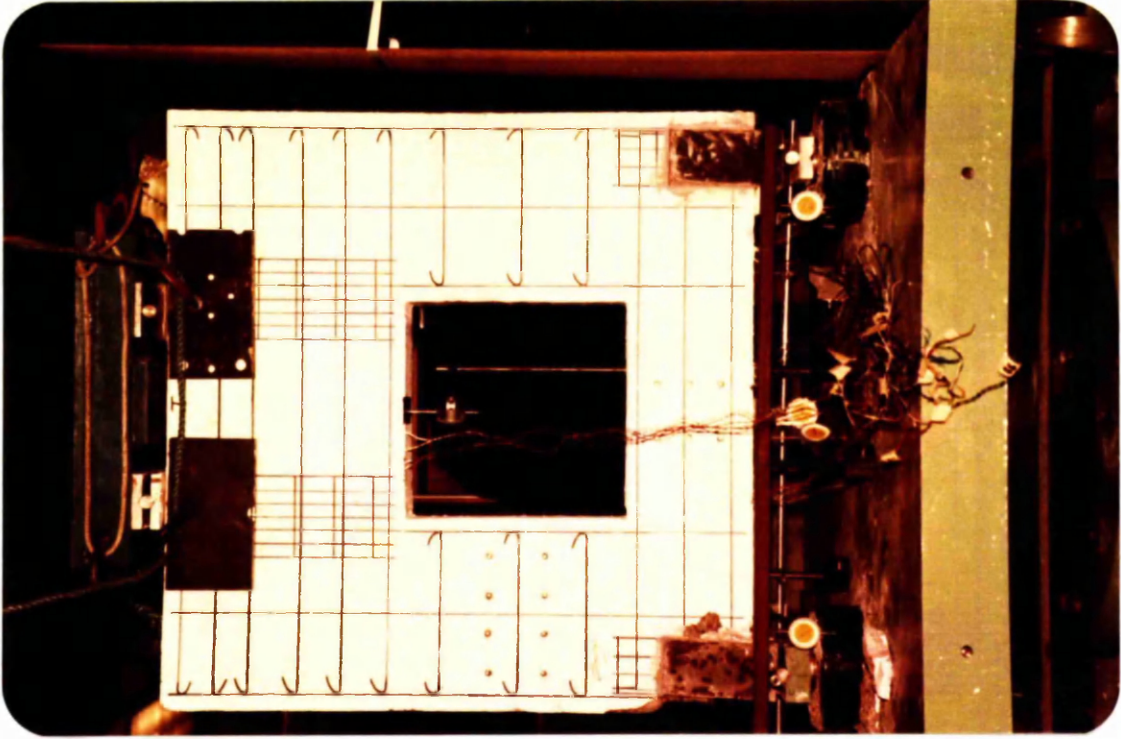
Under concentrated loads and at supports of the beam, the limiting bearing stress may be exceeded, provided the stressed zone is adequately confined. Apart from the direct bearing Poisson's effect may cause bearing failure. In order to prevent the lateral movement of concrete steel plates were clamped on the top surface of the beam. Reinforcement cages were also used at the loading and supporting points to reduce the local crushing failure in the concrete at these points.

4.4.1 Test Apparatus

Olsen screw type universal testing machine (Ref.52) was used for the centrally loaded beam. The rest of the beams were loaded in Losenhausen universal testing machine (Ref.53). The load was symmetrically applied to the bearing plate on the top surface of the beam through cylindrical rollers. The beams were pin-supported on one end and roller supported on the other end, allowing free translation of the beam in the direction of the span and free/



ON OLSEN UNIVERSAL TESTING MACHINE



ON LAUSENHAUSEN UNIVERSAL TESTING MACHINE

FIG.4.5. TYPICAL TEST ARRANGEMENT

rotation in the plane of the beam.

4.4.2 Test Method

A few days before testing, each beam was white-washed to facilitate crack observation. Load was applied to the beam in 50 kN (5 Tons) increments up to failure without unloading. The duration of each loading stage was usually 15 minutes. At each loading stage the extent and location of the cracks were marked on the beam, deflections were measured with dial gauges and concrete surface strains were measured with 100 mm demec gauge. For each test, photographs were taken of the crack pattern and failure type after the testing was over.

4.5. INSTRUMENTATION:

The strain in the steel bars was measured using electrical resistance strain gauges. The gauges were located diametrically opposite to each other at the top and bottom of the bar at quarter and half span positions below the opening and also at half span above the opening.

Demec mechanical gauges were used to measure the concrete surface strains at selected sections. The concrete surface where "Demec" gauge points were to be fixed was cleaned of the dust and grease. Stainless steel gauge points were to be then fixed by means of araldite. The correct location of gauge points fixed by using standard setting bar provided for the purpose.

Load cells were employed to check the reactions at the supports. Unfortunately the capacity of the load cell was not/

enough to measure the reaction up to failure. However, in the range of design ultimate load the readings showed that the two reactions did not differ by more than 3.5%.

The deflections of the beam were measured at mid span and the support points using dial gauges with sensitivity of 0.01 mm/division. The average settlement was measured directly at the middle of the bar which was supported at the centre of the supports. As one of the aims of the tests was to examine the behaviour of beams up to failure, the readings of the dial gauges were continuously taken till the final stages of loading. Central deflection was obtained by subtracting the average support settlement from the mid span deflection.

CHAPTER FIVE

TEST RESULTS

5.1 PRESENTATION OF TEST DATA AND RESULTS

5.1.1 Crack Patterns and modes of failures

The crack patterns of the beams at failure are shown in fig. 5.1. The number marked at the end of the corresponding crack shows the extent of the crack at that load increment. Each unit represents a load of 50 kN on the beam. The formation of the cracks occurs in two stages as follows:

Stage No.1.

A number of flexural cracks appeared in the region of maximum tensile strain in the part of the beam above and below the opening. Under the opening one of the flexural cracks was located at or near the mid-span of the beam and was quite often found to be a through crack on both sides of the beam while the others were located at or near the lower corners of the opening (see fig. 5.1) also shows the extension of the corner cracks which were the first to appear. These cracks were widest close to, or at the soffit of the beam. Above the opening the cracks propagated slowly, close at the edge of the opening. On further increase in load, one or two cracks appeared at or very near the inside edge of the support bearing block from or just above the beam soffit. These cracks were inclined towards the central line of the beam.

Stage No.2.

At 55% and 75% of the measured ultimate load for beams with span to depth ($\frac{L}{D}$) ratios equal to 0.95 and 1.0 respectively, diagonal cracks appeared within the shear span. The cracks originated from the inside edge of support bearing block, confirming the arch action behaviour of the deep beams. At formation the inclined crack appeared to extend from a point close to the level of bottom reinforcement over the lower third of the beam. Extension of the cracks occurred mainly at the upper end as the load increased. In general the inclined cracks propagated along a line joining the inside edge of the bearing block at the support to the outside edge of the bearing block at the loading point. At this stage, a series of short inclined cracks also developed in the top chord under both loading points. Above the opening, in beam B1 which was centrally loaded, a horizontal crack appeared at the outside vertical edge of the beam and extended in the direction of the beam span. This was also observed in beam B6. At higher loads further inclined cracks formed in the shear span of most of the beams. In beams (B2-0.95/0.22/0, B5-1.0/0.2/2A, B6-1.0/0.2/1 and B7-1.0/0.2/2) additional cracks formed parallel to the previous ones, and were widest close to the mid-length, reducing to zero width at both ends as the load approaching to the ultimate load. Finally four out of seven beams failed in shear failure mode above the opening, two failed in bearing failure mode at loading point and the remaining one failed in splitting - spalling failure at support point.

FAILURE MODES:

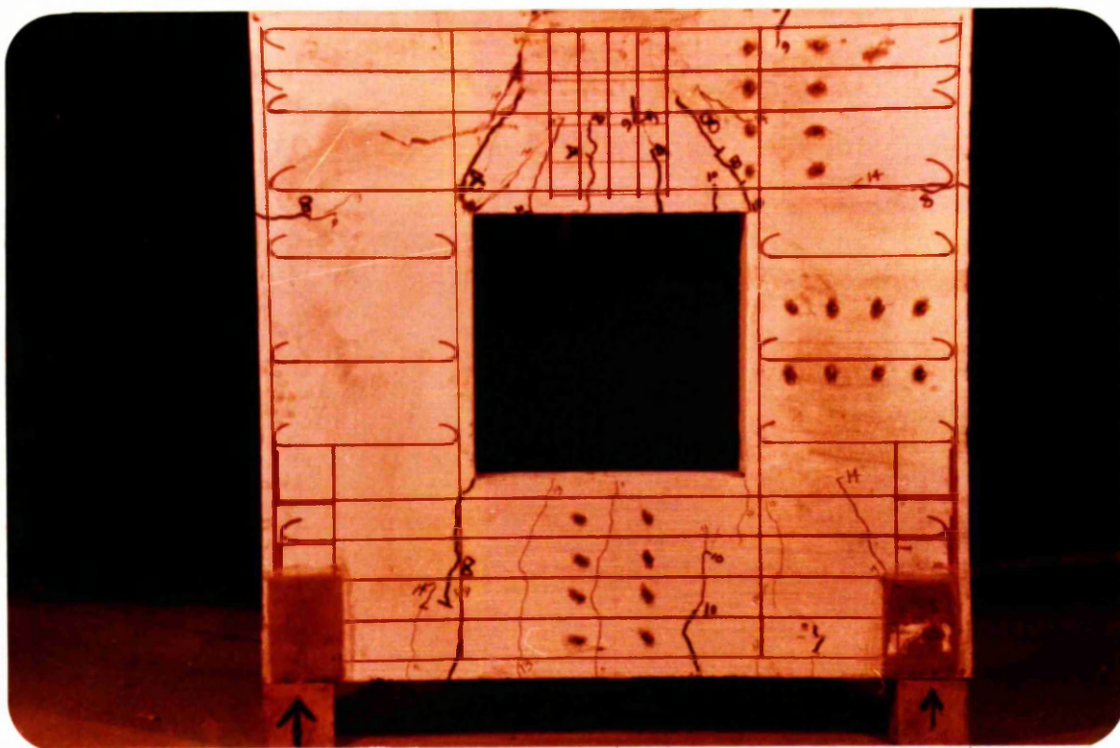
Shearing Failure: Four out of seven beams failed in this mode. While the existing cracks were growing a new inclined crack suddenly appeared at one side of the beam along a line joining the inside edge of the support point and outside edge of the loading point. The failure plane, incorporated one or more of the inclined splitting cracks in the shear span above the opening. The concrete failed in shear rather than by spalling.

Bearing Failure: This failure occurred locally around the steel bearing block at the loading point. Two of the seven beams failed in this mode. Following the appearance of the concrete splitting cracks, the beam eventually failed when a portion of concrete beneath the load bearing block crushed or when considerable destruction and spalling of concrete occurred.

Splitting Failure: Only one beam failed in this mode. The splitting was due to the high compression force in support region and the lack of confinement of concrete beyond the region where the reinforcement was terminated. The failure was followed by the spalling of concrete cover around the support which led to sudden reduction in the load carrying capacity of the beam.

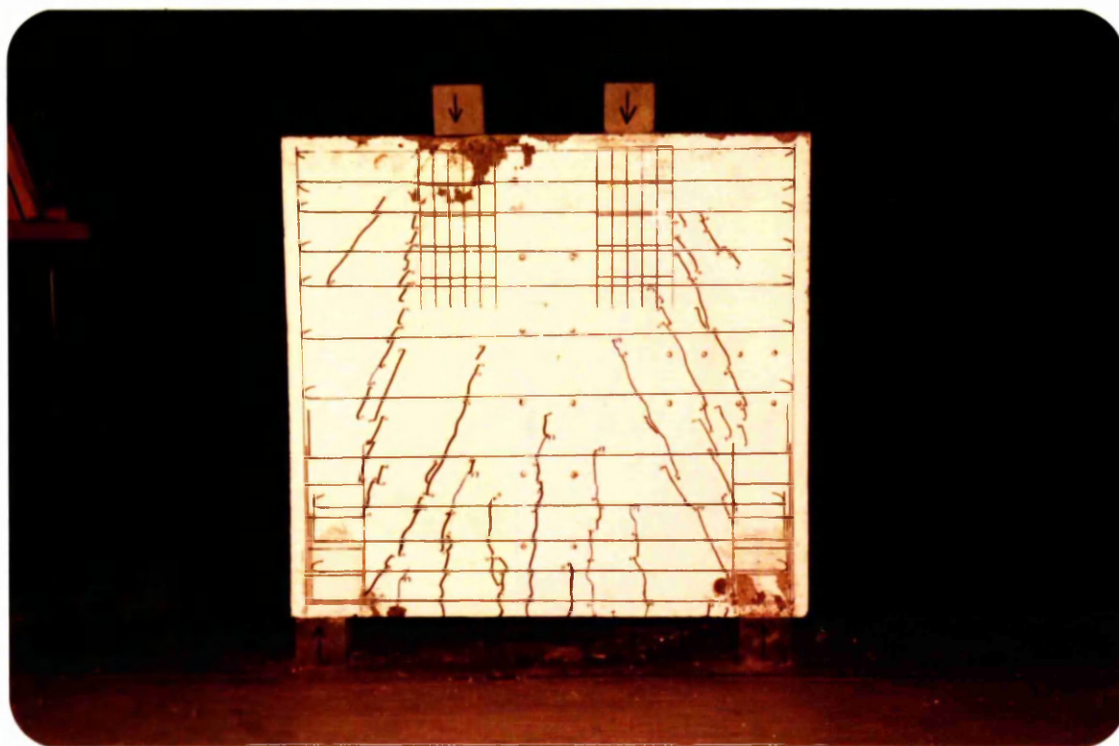
5.1.2 Crack Width

The maximum width of the measured crack is plotted in fig. 5.2 as a function of applied load. The maximum crack /

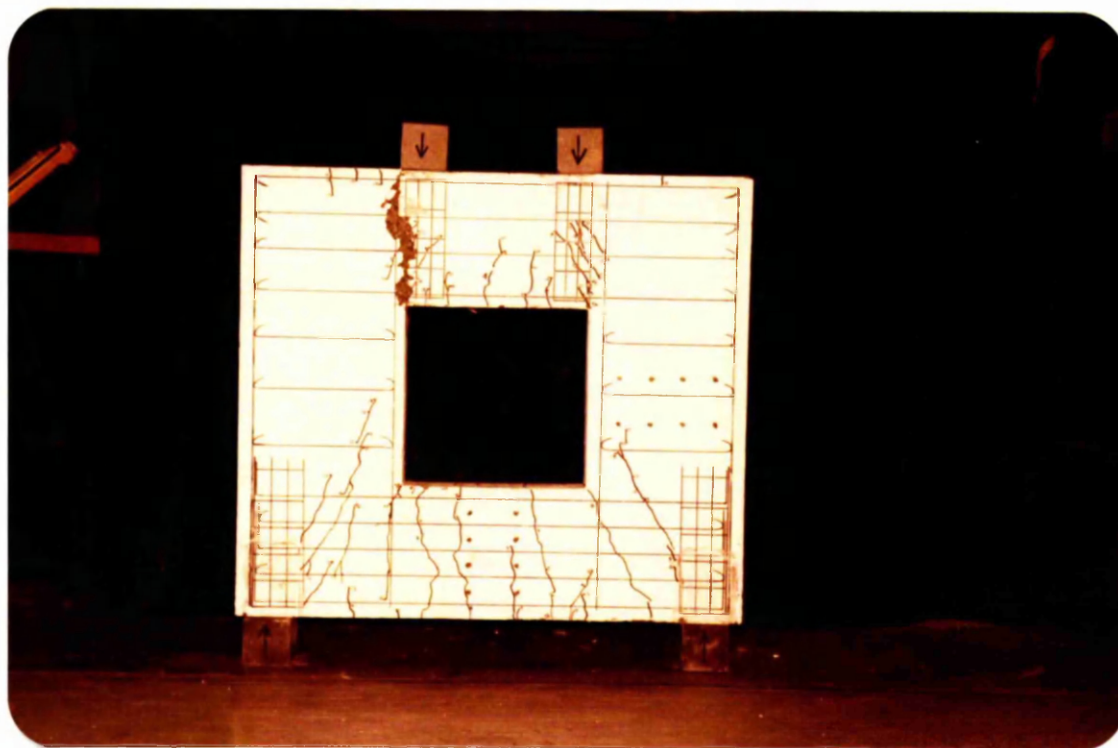


(a) BEAM B1. SHEAR FAILURE

FIG. 5.1. PHOTOGRAPHS AFTER FAILURE OF BEAMS.

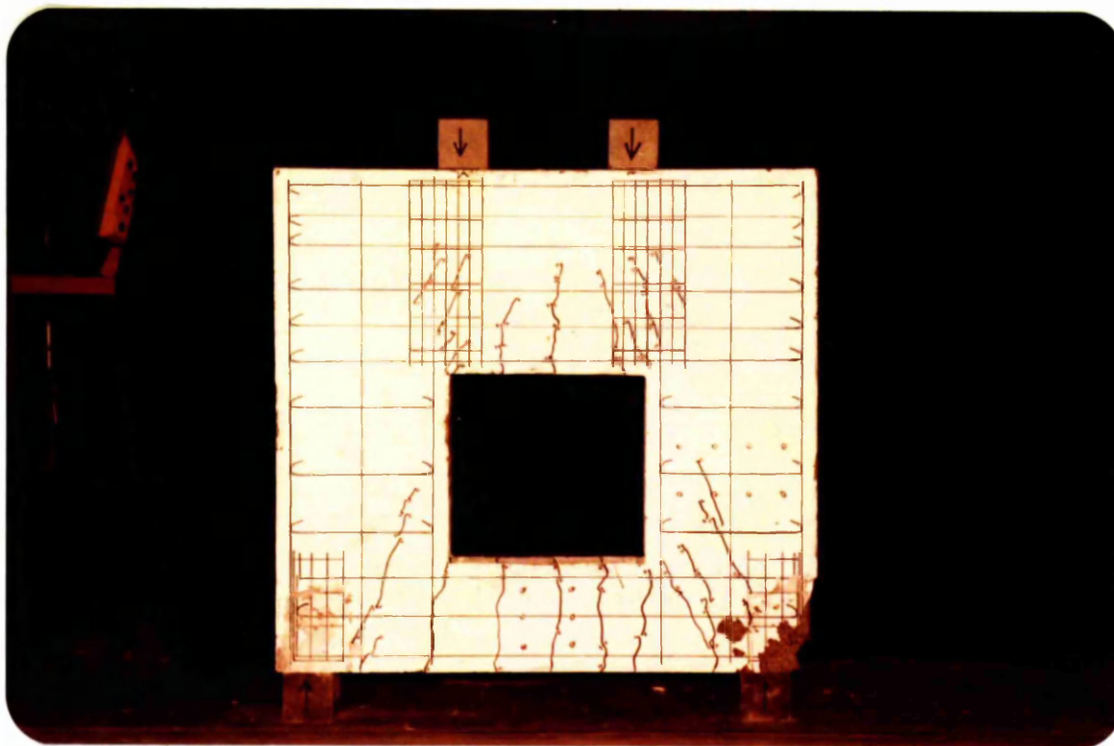


(b) BEAM B2. BEARING FAILURE

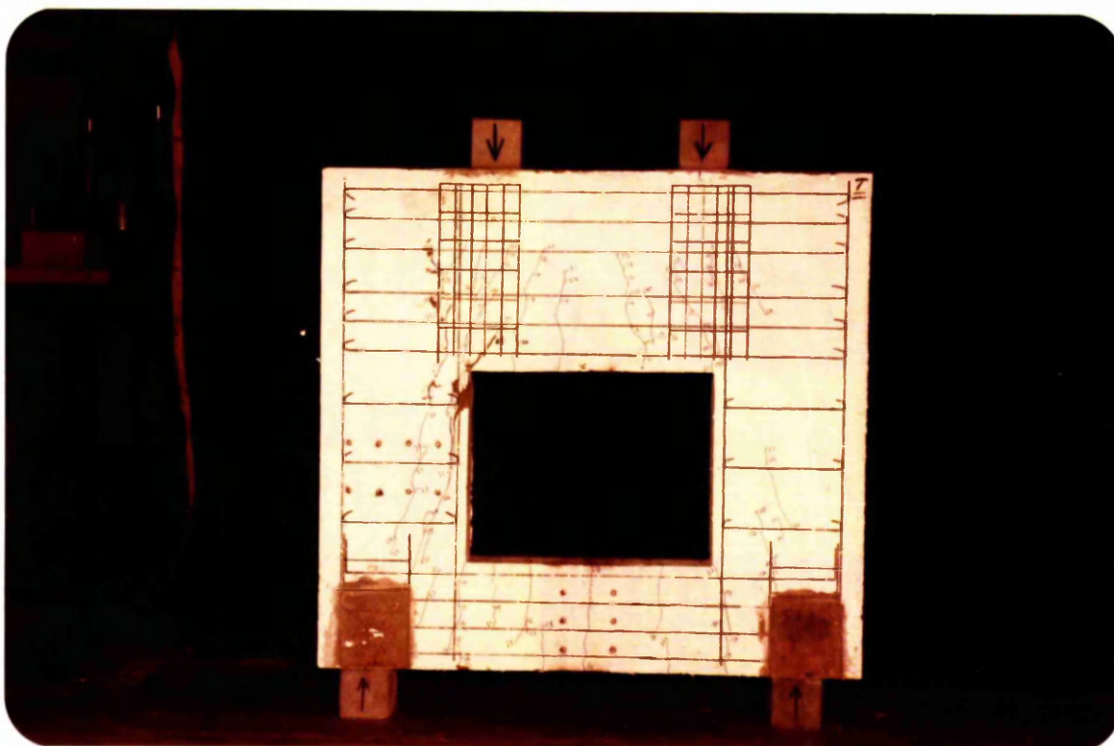


(c) BEAM B3. BEARING FAILURE

FIG.5.1.- CONTINUE -

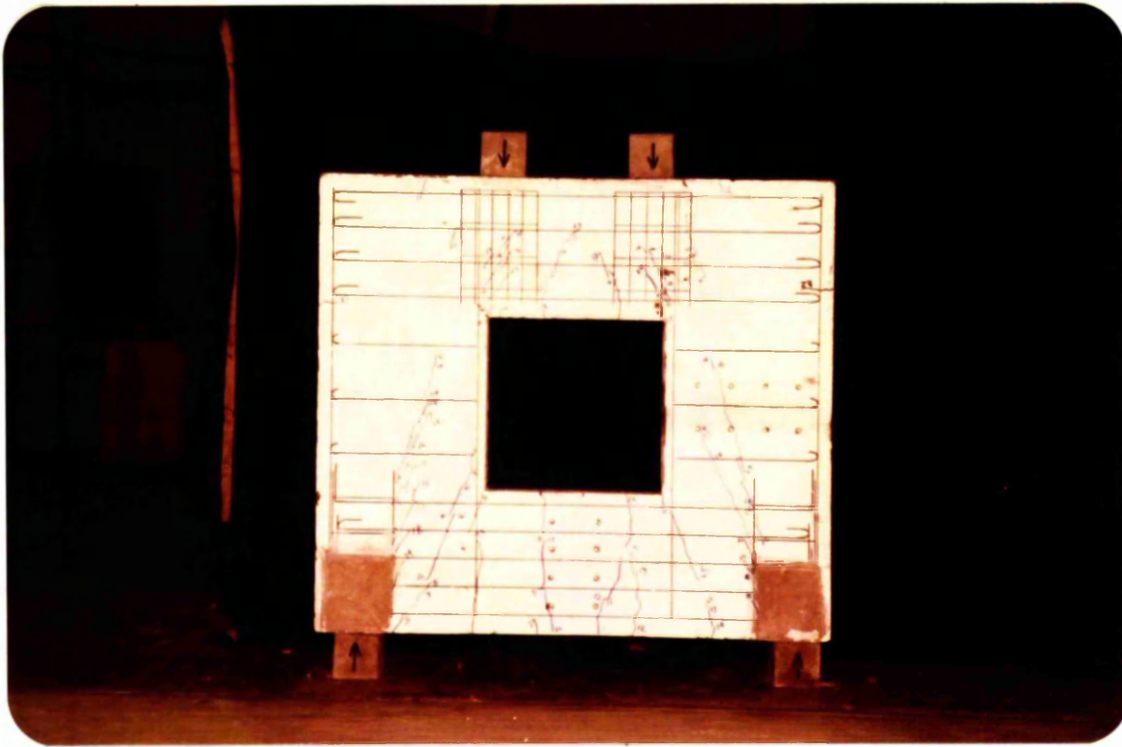


(d) BEAM B4. SPLITTING SPALLING FAILURE

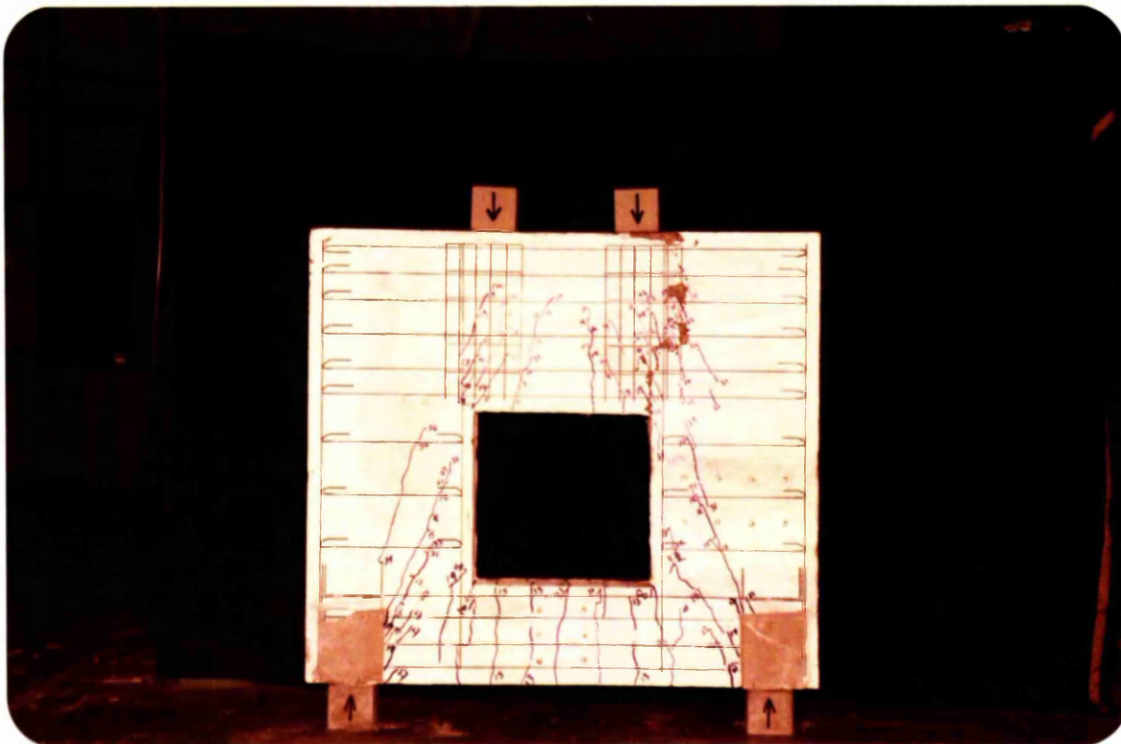


(e) BEAM B5. SHEAR FAILURE

FIG.5.1. - CONTINUE -



(f) BEAM B6. SHEAR FAILURE

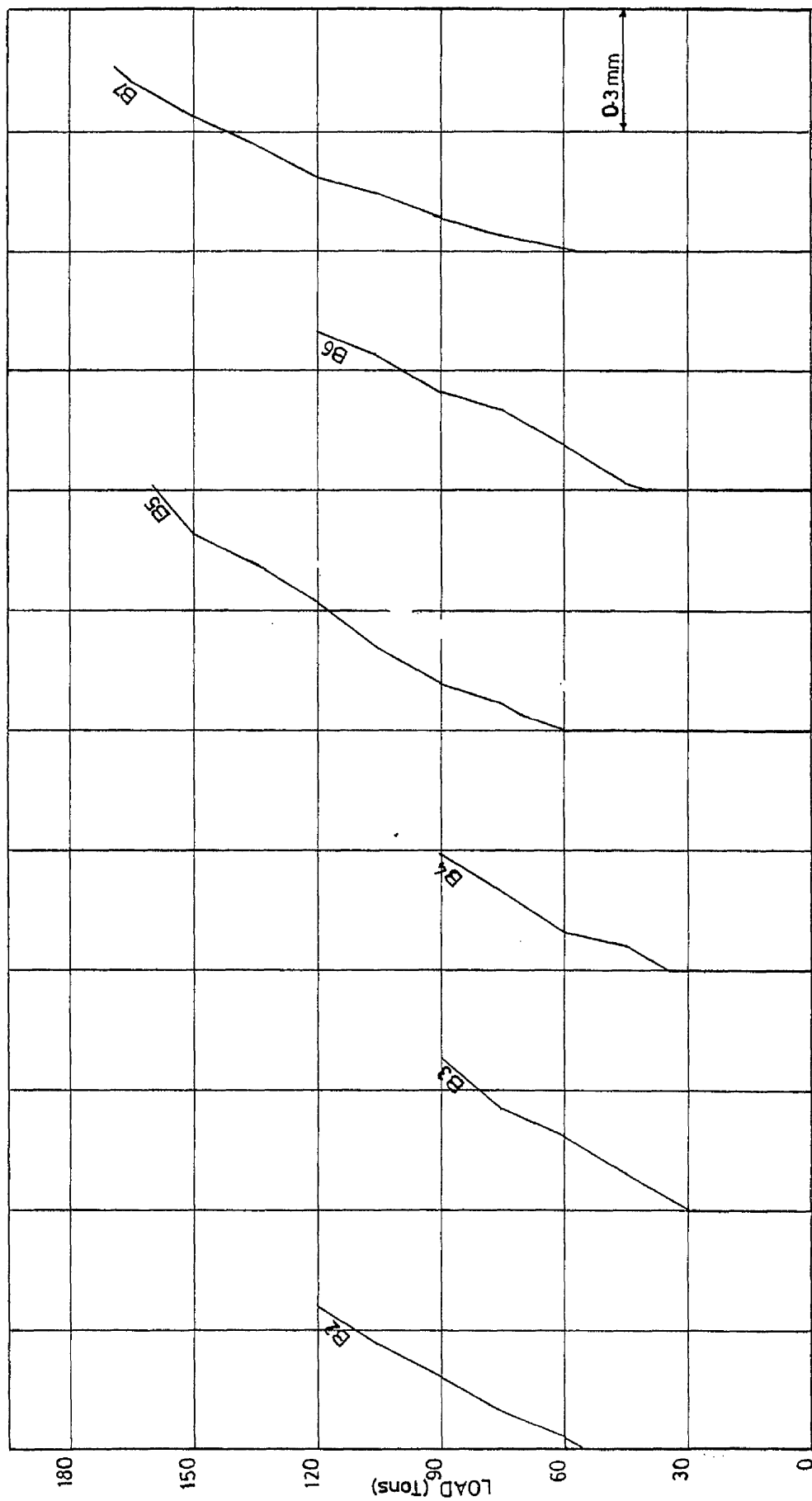


(g) BEAM B7. SHEAR FAILURE

widths were taken as the greater of (except beam B1-0.95/0.32/1) the widest cracks originating from beam soffit below the opening or a diagonal crack originating from inside edge of support bearing block. It was found that, after 70% of the measured ultimate load the diagonal crack started to widen more quickly than the bottom flexural cracks. The only exception were beams B3-0.95/0.22/1 and B4-0.95/0.22/2 where the diagonal crack widened at comparatively slower rate than the flexural crack. The flexural crack in these cases was wider than the diagonal crack at the failure.

A study of crack width curves shows that the maximum crack width increased with the extent to which the web opening intercepted the load path. Beam B5-1.0/0.2/2A was a typical example where the increase in horizontal dimension of the opening caused an increased interruption of the line of action between load point and resulted in larger crack size.

Figure 5.2 has been drawn using a gird of 0.3 mm for the crack width, this being a commonly accepted serviceability limit state CP 110 (Ref. 3). The loads at which the 0.3 mm crack width was exceeded are shown in Table 5.1 where they also compared with the measured ultimate loads. It will be noted that the service cracking loads were less than 88% of the measured ultimate load. However, the average value of 0.81 was obtained.



BEAMS B5-B7 $\frac{L}{D} = 1.0$

BEAMS B2-B4 $\frac{L}{D} = 0.95$

FIG. 5.2. MAXIMUM CRACK WIDTH CURVES.

TABLE (5.1) COMPARISON OF SERVICE-CRACKING LOADS AND MEASURED
ULTIMATE LOADS.

Beam Notation	Service Cracking		Measured Ultimate		$\frac{W_{sc}}{W_u}$
	Load	W_{sc} kN	Load	W_u kN	
B1-0.95/0.32/1	-		-		-
B2-0.95/0.22/0	1100		1250		0.88
B3-0.95/0.22/1	800		950		0.84
B4-0.95/0.22/2	*		1000		-
B5-1.0/0.2/2A	1180		1600		0.73
B6-1.0/0.2/1	970		1250		0.78
B7-1.0/0.2/2	1400		1700		0.82

* Crack-width did not reach 0.3 mm.

5.1.3 Load-Deflection

The behaviour of the beams as measured by the deflection of the soffit at the mid-span is plotted in fig. 5.3 against the total applied load. The deflections were larger in beams having span to depth ($\frac{L}{D}$) ratio equal to 1.0 (B5-1.0/0.2/2A, B6-1.0/0.2/1 and B7-1.0/0.2/2) than those beams having ($\frac{L}{D}$) ratio equal to 0.95 (B2-0.95/0.22/0, B3-0.95/0.22/1 and B4-0.95/0.22/2). As more diagonal cracks appear in the shear span so the beam deflections increase. The deflections were less in beams where the opening was near the beam soffit than in beams where the opening was at mid-depth.

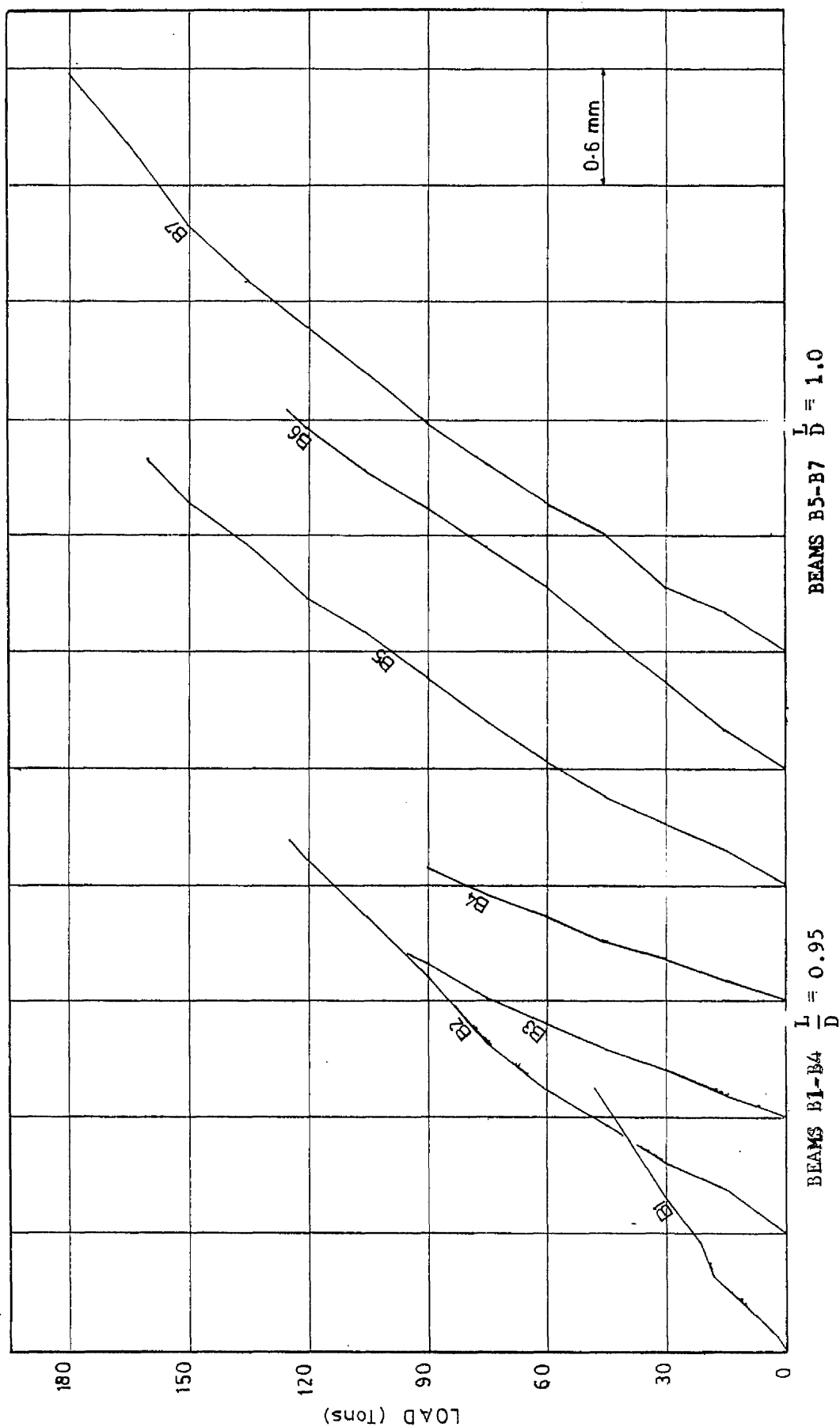


FIG.5.3. LOAD - DEFLECTION CURVES.

In general the deflections were small in all the beams being of the order 1.0 mm only at 60% of the measured ultimate load. The CP 110 (1972) deflection limit of span/350 was not attained except in beam B7-1.0/0.2/2. Thus, serviceability with respect to deflection would not appear to be a problem.

5.1.4 Concrete Surface Strain

The horizontal strain distribution at section 1-1 and vertical strain distribution at section 2-2 (Figures Appendix 1) are plotted in Appendix 1. External plates were clamped under the loading points to confine the concrete laterally and strains were not measured there except for only beam B1-0.95/0.32/1 which was loaded centrally.

The distribution of horizontal strains at section 1-1 indicate the change in the behaviour from that of a beam to that of tied arch as cracking develops. Prior to cracking, the strains were associated with an elastic stress distribution. As the cracks formed and progressed below the opening the concrete strains at mid-span (section 1-1) increased rapidly. Comparatively large strains occurred in beams B4-0.95/0.22/2, B5-1.0/0.2/2A and B7-1.0/0.2/2 where the centroid of the opening was 400 mm from the beam soffit than in beams B1-0.95/0.32/1, B3-0.95/0.22/1 and B6-1.0/0.2/1 where the centroid of the opening was at the mid-depth of the beam.

Vertical strain distribution at section 2-2 showed that initially higher strains were developed near the edge of the opening. With the formation of inclined cracks in the web/

of the beam the vertical strains increased at half clear shear span and strain near the edge of the beam remained small. The exception was beam B4-0.95/0.22/2 which failed by spalling of the concrete at the support. It is believed that the increase in strains at half clear shear span is associated with the widening of the diagonal cracks.

5.1.5. STEEL STRAIN:

The steel strains measured along the bottom row of horizontal reinforcement above and below the opening at various loads are shown in Appendix 2. In all the beams steel yielded below the opening except in beams B1-0.95/0.32/1. Steel yield also occurred above the opening except in beam B4-0.95/0.22/2.

A study of steel strains shows that the arching behaviour developed with the formation of inclined cracks. Higher strains were observed in beams B4-0.95/0.22/2, B5-1.0/0.2/2A, B6-1.0/0.2/1 and B7-1.0/0.2/2 not at mid-span but in the region of shear span (see Appendix 2). This is because the tied arch action in deep beams causes a high tensile force in the shear span. Also high compressive forces in the region of supports, because of a Poisson's effect result in an increased horizontal tension in the region of the shear span near the support.

Figures in Appendix 2b shows that the steel strain above the opening increased linearly. A comparison between the design ultimate load (W_d) and the first yield load above (W_{fya}) and below (W_{fyb}) the opening is shown in Table 5.2. The first yield load represents the load at which the yield strain (.002) was/

observed in both bottom row of horizontal reinforcement above and below the opening. The values of W_{fya}/W_d and W_{fyb}/W_d are shown in Table 5.2. The average values of W_{fya}/W_d and W_{fyb}/W_d are greater than 1.0. This is reasonable because of the amount of reinforcement was greater than that required for the design ultimate load corresponding to elastic analysis.

5.1.6. Ultimate loads:

The measured ultimate loads of all the beams are presented in Table 5.2. An examination of the measured ultimate loads clearly reveals that the effect of an opening on the ultimate strength depend upon the extent to which it interrupted the "load path" joining the bearing blocks at the loading and support reaction points. Serious strength reduction occurred in beams B3-0.95/0.22/1 and B4-0.95/0.22/2 as compared to beam B2-0.95/0.22/0 which had no opening. Typical crack pattern of solid deep beams was not obtained when an opening was present (see photograph of fig.5.1.), hence significant reduction in the ultimate strengths were recorded.

Figure 4.2f in Chapter 4 shows that the beam B6-1.0/0.2/1 which has an opening at mid-depth has lower measured ultimate load (1250 kN) than beam B5-1.0/0.2/2A which has an opening near the beam soffit (see Table 5.2). A possible explanation is that, the upper path in beam B6-1.0/0.2/1 was less effective than in beam B5-1.0/0.2/2A, hence the ultimate load was lower.

A comparison between design ultimate load (W_d) and/

T A B L E 5.2
DESIGN LOAD, YIELD LOAD AND MEASURED ULTIMATE LOAD

Beam Notation	Design Load W_d kN	Yield Load		Yield Load		Measured Ultimate	
		above the opening kN	$\frac{W_{ya}}{W_d}$	below the opening kN	$\frac{W_{yb}}{W_d}$	kN	Load $\frac{W_u}{W_d}$
B1-0.95/0.32/1	750	499	0.66	*	-	533	0.71
B2-0.95/0.22/0	1000			1050	1.05	1250	1.25
B3-0.95/0.22/1	"	*	-	900	0.9	950	0.95
B4-0.95/0.22/2	"	*	-	800	0.8	1000	1.00
B5-1.0/0.2/2A	"	1340	1.34	1400	1.40	1600	1.60
B6-1.0/0.2/1	"	980	0.98	1100	1.10	1250	1.25
B7-1.0/0.2/2	"	1360	1.36	1300	1.30	1700	1.70

* Steel did not yield.

measured ultimate load W_u is shown in Table (5.2). Apart from beam B1-0.95/0.32/1 the average value for $\frac{W_u}{W_d}$ of 1.29 was obtained. The highest values of $\frac{W_u}{W_d}$ occurred in two beams where the opening is near the beam soffit and concrete strength is high i.e. 1.6 for beam B5-1.0/0.2/2A and 1.7 for beam B7-1.0/0.2/2.

5.2 FACTORS AFFECTING THE BEHAVIOUR OF DEEP BEAM WITH OPENING

1) CONCRETE STRENGTH:

Although other parameters as well as concrete strength differed in different tests certain test models were sufficiently similar for the conclusion to be drawn that concrete strength has a major effect on ultimate strength of a deep beam with an opening. This can be observed from Table 5.3. In beams B3 and B6 where the opening is at mid-depth, an increase of concrete strength of 8 N/mm^2 produced an increase of 31% in ultimate strength and in beams B4 and B7 where the opening is near the beam soffit, an increase of concrete strength of 20 N/mm^2 produced an increase of 41% in ultimate load.

TABEL (5.3) RELATIONSHIP BETWEEN THE MEASURED ULTIMATE LOAD

AND CONCRETE STRENGTH				
Beam Notation	Concrete Strength N/mm^2	Measured Ultimate load kN	Increase of concrete strength N/mm^2	Increase of ultimate load
B6	46	1250		
			46- 38 = 8	31%
B3	38	950		
B7	58	1700		
			58- 38 = 20	41%
B4	38	1000		

In deep beams with openings it would seem that the regions above and below the opening are very susceptible to diagonal cracking, and that if diagonal cracks occurred at an early load the ultimate load would be reduced. An increase of concrete compressive strength provides an increase of strength and which is likely to inhibit the formation of diagonal cracks at an early load stage and enhances the ultimate load of deep beams with web openings.

2) Total Steel Ratio:

An increase of total steel ratio increased the load capacity of the beams and tended to change the mode of failure. This may be observed from the results in Table 5.4. Beam B3-0.95/0.22/1 with a low steel ratio, had a low strength, and failed in bearing failure. On the other hand beams B5-1.0/0.2/2A and B7-1.0/0.2/2 with a high steel ratio, had a high strength, and failed in shear failure. Comparison of beams B5-1.0/0.2/2A and B7-1.0/0.2/2 shows that lower steel ratio produced higher ultimate loads because the ultimate strength of deep beam is more dependent upon the concrete strength than dependent on the steel ratio.

The steel ratio did not have much effect on the maximum crack widths at lower loads but it did have a beneficial effect on restricting the crack width at higher loads and thus delaying failure. This was evident in beams B4-0.95/0.22/2 and B7-1.0/0.2/2.

TABLE (5.4) RELATIONSHIP BETWEEN THE MEASURED ULTIMATE LOAD AND
THE STEEL RATIOS.

Beam Notation	Steel Ratio $\rho_s \%$	Measured Ultimate Load kN	Mode of Failure
B1-0.95/0.32/1	1.15	533	Shear-Failure
B2-0.95/0.22/0	1.25	1250	Bearing Failure
B3-0.95/0.22/1	1.11	950	Bearing Failure
B4-0.95/0.22/2	1.38	1000	Splitting- Spalling Failure
B5-1.0/0.2/2A	2.03	1600	Shear Failure
B6-1.0/0.2/1	1.11	1250	Shear Failure
B7-1.0/0.2/2	1.38	1700	Shear Failure

3) Location of Opening

The deflections were less, the ability of preventing the diagonal crack from becoming wide was better and the ultimate loads were higher in beams with opening near the beam soffit than in beams with opening at mid-depth. This is illustrated in figures 5.3, 5.2 and Table 5.2.

From the Load-deflection diagrams in fig. 5.3, it can be observed that deflections were less in beams with opening near the beam soffit than in beams with opening at mid-depth.

In figure 5.2, by comparing beams B3-0.95/0.22/1 and B4-0.95/0.22/2, B6-1.0/0.2/1 and B7-1.0/0.2/2, there is indication that the beams in which the location of opening was near beam/

soffit have pronounced effect on retaining the diagonal crack width than in beams in which the location of opening was at mid-depth.

A study of data presented in Table 5.2 shows that, regardless the type of failure, the ultimate loads were higher in beams having opening near beam soffit than in beams having opening at mid-depth.

5.3 ANALYSIS OF TEST RESULTS:

a) Serviceability Limit State:

Comparison of service loads, design ultimate loads (W_d) and measured ultimate loads (W_u) together with service cracking loads at which the maximum crack width exceeds 0.3 mm limit are shown in Table 5.5. The service load is dependant on the service cracking load rather than the service deflection load. In deep beams the service loads were controlled by crack widths since the deflections of deep beams are very small.

It can be observed that the service loads were nearly equal to design ultimate loads except in beams B4-0.95/0.22/2 and B1-0.95/0.32/1. In beam B4-0.95/0.22/2 the maximum crack width did not reach 0.3 mm and in beam B1-0.95/0.32/1 the crack width was not recorded. In all the beams apart from B1 and B4 the ratio of $\frac{W_s}{W_u}$ was similar to and an average of 0.81 was obtained.

A comparison between service load to design ultimate load W_s/W_d and the concrete cube strength f_{cu} is shown in fig. 5.4, which shows that the value of W_s/W_d lies between 0.8 and 1.4.

T A B L E 5.5
Measured Service Load, Design Load and Measure Ultimate Load

Beam Notation	Service-cracking		Measured Service		Design		Measured Ultimate	
	Load	W_{sc} kN	Load	W_s kN	Load	W_d kN	Load	W_u kN
B1-0.95/0.32/1	-	-	-	-	750	533	-	-
B2-0.95/0.22/0	1100	1100	1100	1100	1000	1250	1.10	0.88
B3-0.95/0.22/1	800	800	800	800	"	950	0.80	0.84
B4-0.95/0.22/2	*	*	-	-	"	1000	-	-
B5-1.0/0.2/2A	1180	1180	1180	1180	"	1600	1.18	0.73
B6-1.0/0.2/1	970	970	970	970	"	1250	0.97	0.78
B7-1.0/0.2/2	1400	1400	1400	1400	"	1700	1.40	0.82

* Maximum crack width did not reach 0.3 mm.

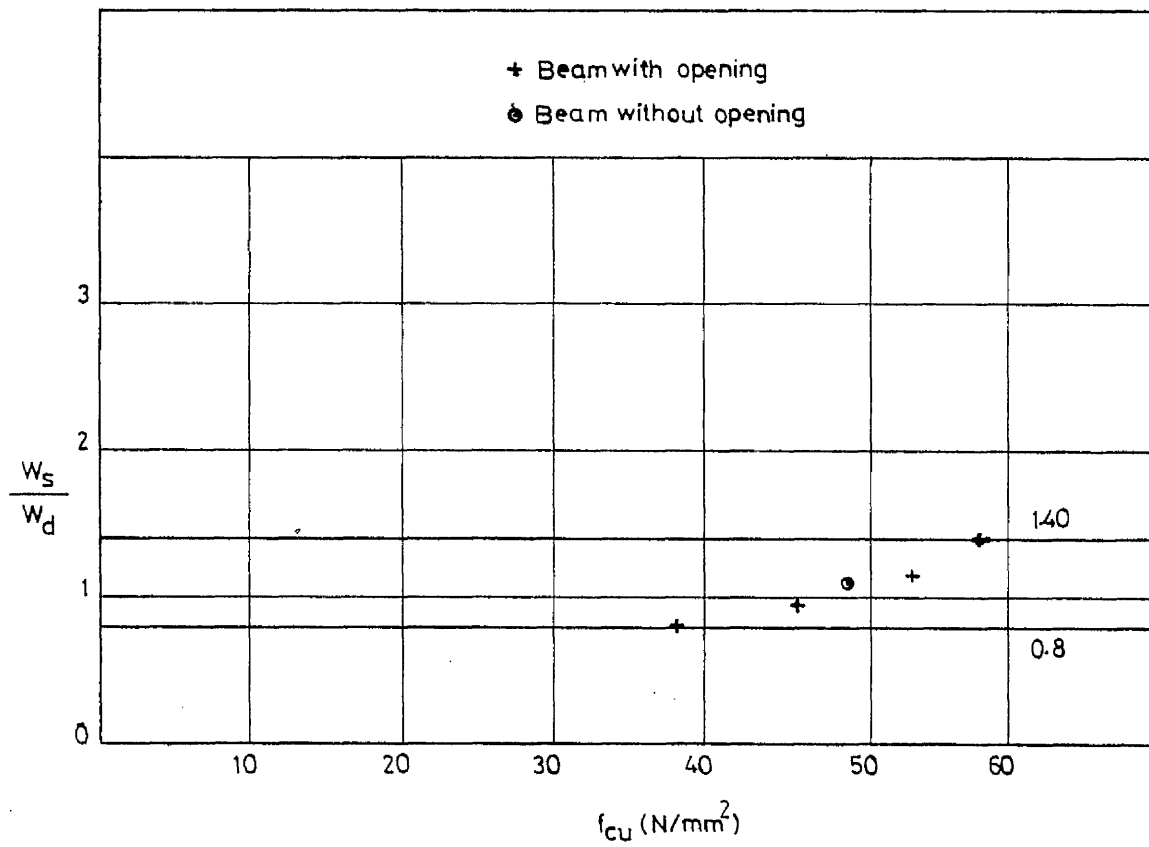


FIG.5.4. COMPARISON OF SERVICE LOAD AND DESIGN ULTIMATE LOAD.

Beams having opening near beam soffit tend to have higher value of W_s / W_d than beams having opening at mid-depth.

B) ULTIMATE LIMIT STATE

a) Flexural Strength:

In reinforced concrete deep beams, the stresses predicted by elastic analysis differ widely from the actual stresses after cracking. The moment arm increases with the development of cracking and will be greater than that predicted by elastic analysis. Therefore the stresses in the main tension steel will remain below those values predicted by elastic analysis.

In the present design, the flexural strength will always be greater than the design flexural strength because it based upon the result of elastic analysis (Ref.6).

b) Ultimate Shear Strength:

In all the beams tested, the applied load was transmitted from the loading point to the reaction point along the 'load path' as shown in fig. 5.5. When the force in the path reached a sufficiently high value, the critical diagonal crack had occurred in a manner similar to those beams without opening.

It appears that the force in the load path depend upon the location of the opening and it seems the load carrying capacity of the beam is affected by the opening location. It is clear that the measured ultimate loads were higher than the design ultimate loads. It may be due to the following reasons:

- i) the stresses are well redistributed after the cracking.
- ii) the reinforcement has a high reserve of strength after yielding.

An approximate estimate of ultimate strength of this series of test may be made by extending the ultimate shear formula suggested by Kong (Ref. 10).

$$Q_{ult} = c_1 f_t b \bar{k} h + c_2 \sum_{\text{all bars}} A \frac{y}{h} \sin^2 \alpha \quad (5.1)$$

where Q_{ult} is the ultimate shear strength ($Q_{ult} = \frac{w}{2}$)

c_1 is the empirical co-efficient equal to 1.4.

c_2 is the empirical co-efficient equal to 300 N/mm^2 .

f_t is the cylinder-splitting tensile strength of concrete.

b is the breadth (thickness) of beam.

\bar{k} is the co-efficient defining the position of opening.

$$(\bar{k} = \frac{x_1}{h_1}) \quad \text{fig. (5.5).}$$

h is the overall height of beam.

A is the area of an individual bar.

y is the depth at which typical web bar intersects the diagonal crack which is approximately the line joining the loading and reaction points.

α is an angle of intersection between a typical bar and the diagonal crack described in the definition of y above.

Figure 5.6 is a plot of predicted ultimate strength versus the measured ultimate strength.

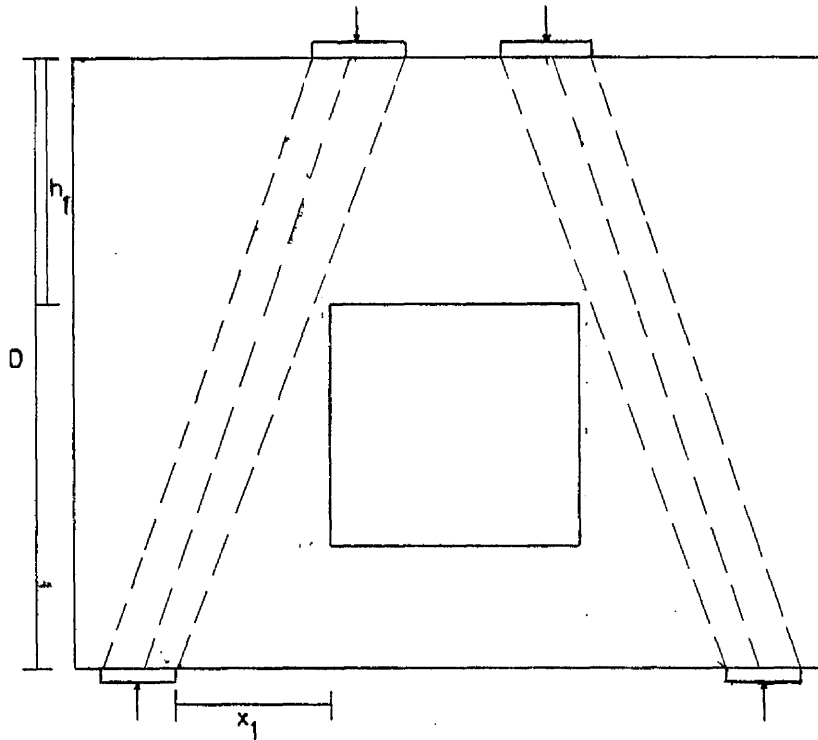


FIG.5.5. LOAD-TRANSMISSION PATHS.

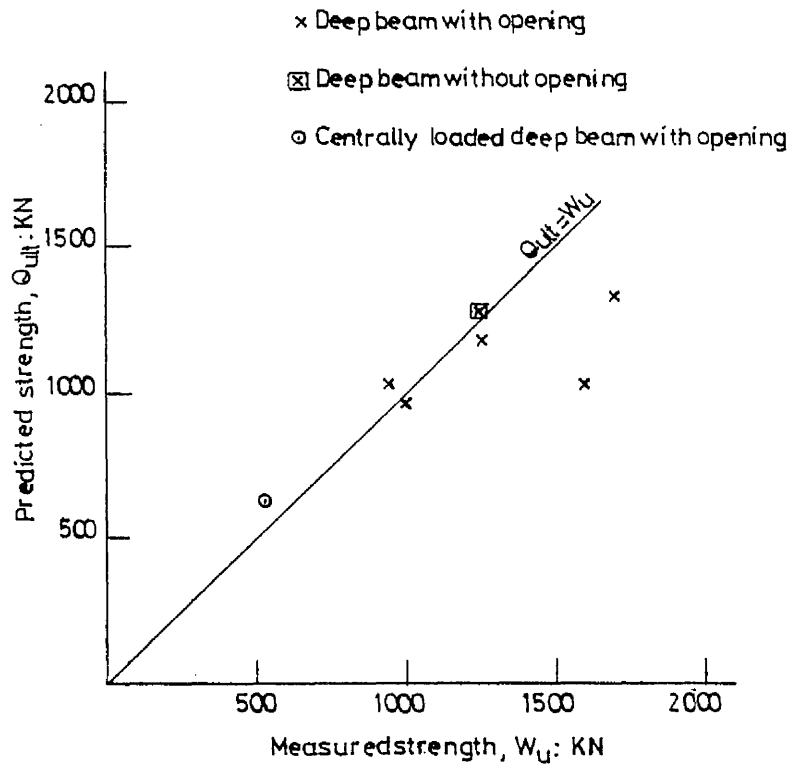


FIG.5.6. COMPARISON OF PREDICTED AND MEASURED STRENGTH.

In Table 5.6, the computed ultimate loads are compared with the measured loads. A satisfactory agreement between measured and computed loads is achieved. The possible reason for the low $\frac{W_c}{W_u}$ ratio for beams B5-1.0/0.2/2A is the width of the opening. It was pointed out earlier that the serious strength reduction occurred when the opening completely interrupted the load path.

TABLE (5.6) MEASURED AND COMPUTED ULTIMATE LOADS

Beam Notation	Measured Ultimate Load		Computed Ultimate Load		$\frac{W_c}{W_u}$
	kN	W_u	kN	W_c	
B1-0.95/0.32/1	533		618		1.16
B2-0.95/0.22/0	1250		1279		1.02
B3-0.95/0.22/1	950		1035		1.09
B4-0.95/0.22/2	1000		959		0.96
B5-1.0/0.2/2A	1600		1102		0.68
B6-1.0/0.2/1	1250		1167		0.93
B7-1.0/0.2/2	1700		1314		0.77

The average value of the ratio $\frac{W_c}{W_u}$ apart from beams B₁ and B₂ is 0.88, the standard derivation 0.145 and the co-efficient of variation 16.4 per cent.

Based upon the truss analogy which has been described in section 2.4 of chapter 1, Kong and Sharp (Ref.33) proposed equations for predicting the ultimate shear strength of beams with openings. The equations are repeated below with the notations/

as described earlier.

$$Q_{ult} = c_1 \left(1 - 0.35 \frac{x}{D}\right) f_t b \cdot D + c_2 \sum \frac{A_y}{D} \sin^2 \alpha \quad (5.2)$$

$$Q_{ult} = c_1 \left(1 - 0.35 \frac{k_1 x}{k_2 D}\right) f_t b \cdot k_2 D + c_2 \sum \frac{A_y}{D} \sin^2 \alpha \quad (5.3)$$

Equation (5.2) was originally proposed for the shear strength of beams without web opening/openings and can also be applied when the web opening does not interrupt the load path which exists between the loading and supporting points. The equation 5.3 applies when the opening interrupt the above mentioned load path.

The prediction of equation 5.2. is comparable with the measured ultimate strength of deep beam without opening of the present test. For the rest of beams, the measured ultimate strengths are not comparable with prediction of equation 5.3 because, firstly, the geometry and location of web opening is widely different from the tests of Kong and Sharp and secondly, the shear-span to depth ($\frac{x}{D}$) ratio is noticeably outside the range of 0.25-0.4 which they suggested for the application of proposed equation 5.3.

In deep beams with openings the collapse of one path will lead to wide cracks and large deflections (as observed in the present test). The load at collapse of one load path should be regarded as the ultimate load of the beam. The collapse of the remaining load path will not be necessary occurred at same load.

The strength of deep beam with centrally located web opening can be predicted by using the proposed equation (5.1). Though the strength predictions are conservative because they are/

T A B L E 5.7
DESIGN LOAD, MEASURED ULTIMATE LOAD AND THEORETICAL LOAD

Beam Notation	Design Load W_d kN	Measured Ultimate		Theoretical		Theoretical/Design		Theoretical/Measured	
		Load W_u kN	Load W_u kN	Load W_{th} kN	Load W_{th} kN	$\frac{W_u}{W_d}$	$\frac{W_{th}}{W_d}$	$\frac{W_{th}}{W_u}$	Load
B1-0.95/0.32/1	750	533		900		0.71	1.2	1.68	
B2-0.95/0.22/0	1000	1250		1600		1.25	1.6	1.28	
B3-0.95/0.22/1	"	950		1200		0.95	1.2	1.26	
B4-0.95/0.22/2	"	1000		1450		1.0	1.45	1.45	
B5-1.0/0.2/2A	"	1600		1600		1.6	1.6	1.0	
B6-1.0/0.2/1	"	1250		1550		1.25	1.55	1.24	
B7-1.0/0.2/2	"	1700		1900		1.70	1.9	1.12	

based on only a few test results. However, it is expected with further experimental work the prediction of beam strength will be improved.

To check the validity of the present design procedure to reinforce the beam, an analysis using a non-linear finite element analysis was carried out. (Ref.54). It is not the intention of this study to present detailed study of the deep beam behaviour using non-linear finite element approach but to demonstrate the ability of present design method.

Theoretical collapse loads obtained by non-linear finite element programme compare with design and measured ultimate loads are shown in Table 5.7. It can be seen that apart from beam B1-0.95/0.32/1 the ratio between theoretical (finite element method) and measured (experimental) ultimate $\frac{W_{th}}{W_u}$ ranges 1.12 to 1.60 and the average value is 1.32.

CHAPTER SIX

GENERAL CONCLUSIONS.

6.1 INTRODUCTION:

Deep beams with a single web opening under two concentrated top loads were tested in this investigation, however, the present design philosophy is also applicable to the uniform loading case. The tested beams were few in number and it is expected that with further experimental work prediction of beam behaviour will be improved. Based upon the experimental results formulae for service loads and ultimate loads are developed. Such formulae should be used until the range of geometry and testing details are extended by further test results.

6.2 CONCLUSIONS

Based upon the results of present tests and the findings of other investigators, the following conclusions were drawn.

1) For the design ultimate load, the total reinforcement ratio was found following the stress field obtained by linear elastic analysis. The most effective arrangement of web steel depends upon the ratio of clear shear span to depth. For beams having clear shear-span to depth ($\frac{x}{D}$) ratio in the range 0.2-0.32 the horizontal bars are more effective than vertical ones (absence of vertical bars). This agrees with the findings of Kong (Ref. 4).

2) Concrete strength is very important in deep beam behaviour. High concrete strength i.e. f_{cu} is greater than/

40 N/mm² provides a better control over cracking. This agrees with the suggestion of Lin. (Ref.27).

3) An increase in percentage of reinforcement does not have much effect on the crack patterns in the beams but it does have pronounced effect on the mode of failure and on the ultimate load.

4) The maximum crack width increases with the extent to which an opening interrupts the natural "load path" joining the loading and supporting reaction points. This is in agreement with the findings of Sharp. (Ref.31).

5) As the deflections in the deep beams are very small, hence the serviceability limit state quoted in the British Code CP110 is seriously overestimated by using deflection criterion. The important criterion in determining the serviceability limit state of deep beam is the maximum crack width.

6) When deep beams incorporate web openings the region above and below the opening must be protected against the diagonal cracking. Therefore proper detailing is an important requirement.

7) Because of the arch action, the full tensile force must be developed in anchorage at the support hence it is important to confine the concrete there. It is desirable to anchor horizontal reinforcement placed within $\frac{D}{8} - \frac{D}{5}$ from bottom soffit of the beam into the end bearing plates so as to avoid the unconfined concrete outside the reinforcement cage.

8) Proposed design equation:

The proposed equation 5.1 is intended to predict the actual collapse load. Because it is based on only a few test results, the strength which it predicts may be conservative. Certain amount of scatter is observed while comparing the predicted and actual strength. In order to modify the equation to make it appropriate for design, the experimental study of this type of the structure should be extended.

It is noted that the cylinder splitting tensile strength of concrete f_t , which is used in the equation is based on the characteristic cube strength, the concrete strength parameter adopted in design practice. The tensile strength of concrete usually ranges between 5-15% of the concrete crushing strength. The relationship between the concrete cube and cylinder splitting tensile strength is taken as $0.52 \sqrt{f_{cu}}$ as assumed by CIRIA guide. (Ref. 4).

The steel contribution as given by the second term of the equation should not be less than 20% of the design shear force as recommended by Kong and Sharp (Ref.10) and CIRIA also (Ref. 4).

Using the above equation, the design ultimate load can be calculated by choosing a suitable concrete cube strength and assuming 20% of the total shear strength contributed by the steel.

The reinforcement ratio throughout the structure can be found for the desired design ultimate load. Based upon the/

reinforcement ratios, the reinforcement cage will be designed by following the limitations on the spacing of reinforcement as recommended by CP110 and limitations described in section 3.5 of Chapter 3.

6.3. SUGGESTIONS FOR FURTHER WORK:

The conclusions drawn from the present study may be modified by further investigation. A few suggestions for further research are given below:

- 1) Experimental studies could be extended to include the other types of loading and various geometries of the web opening.
- 2) A few larger scale beams than those considered here should be tested to verify that scale effects do not influence the results of these tests.
- 3) The shear strength equation is based on the limited measurements and on the observed behaviour at failure should be refined by further investigation.
- 4) Test should be carried out on lightweight concrete deep beams with single web opening since it is expected that in future years lightweight concrete will be widely used.
- 5) A more elegant analytical study which takes non-linear behaviour and crack development into account should be made to predict the reserve of strength over that given by elastic analysis.

APPENDIX 1

CONCRETE SURFACE STRAIN DISTRIBUTION AT SECTIONS 1-1 and 2-2.

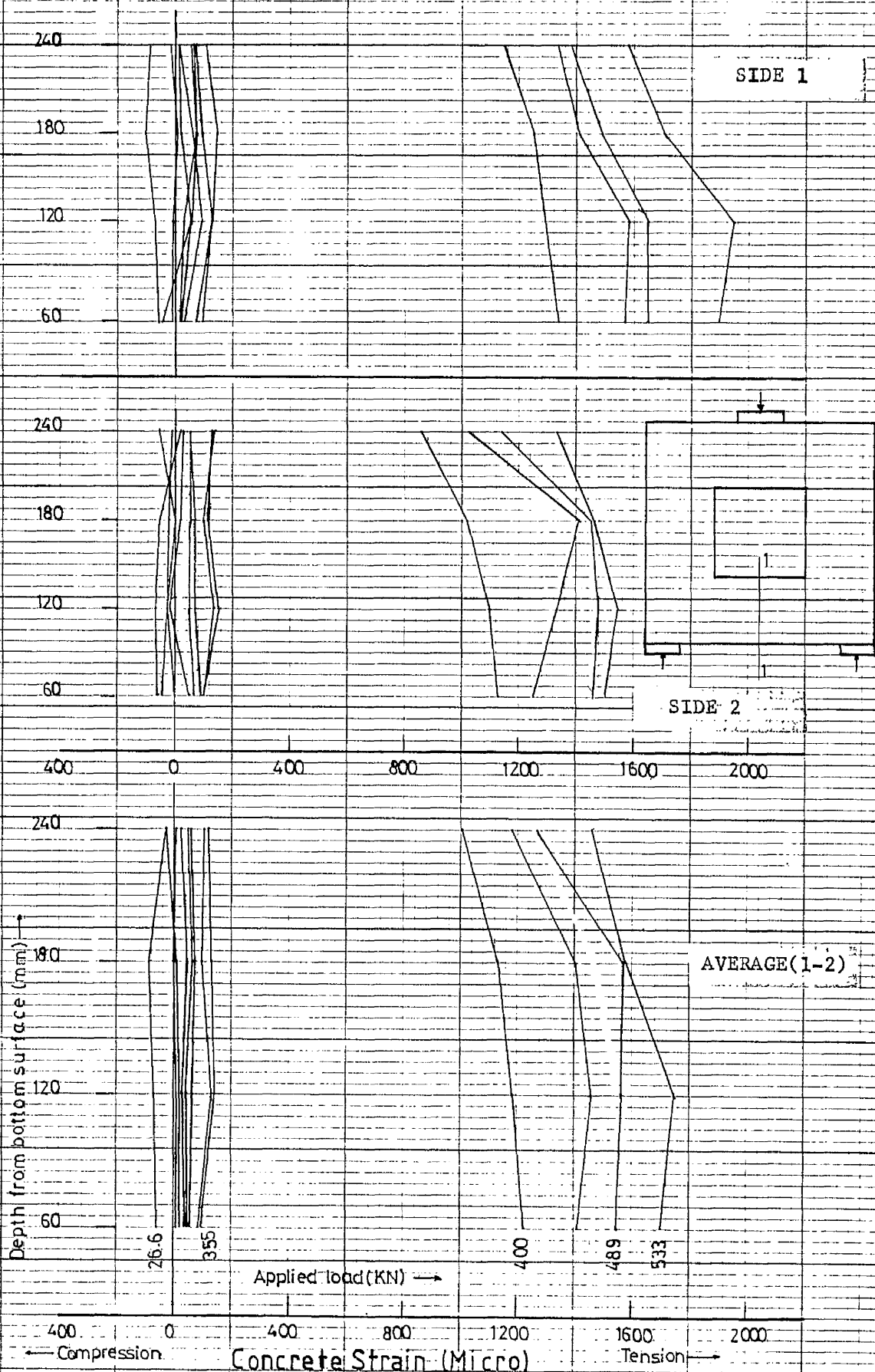


FIG. A1.1a. CONCRETE SURFACE STRAIN (HORIZONTAL) FOR SECTION 1-1 OF BEAM B1.

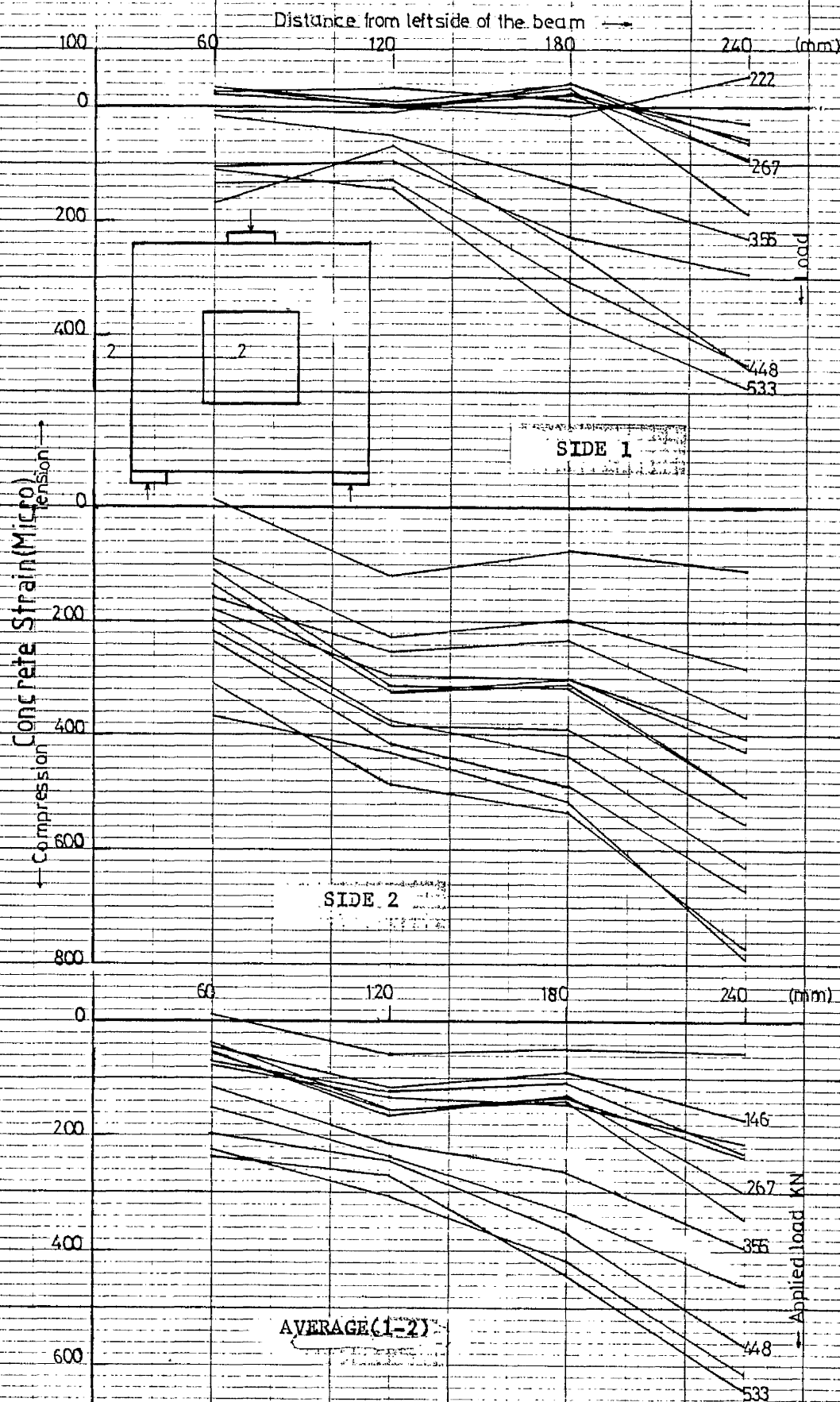


FIG.A1.1b.CONCRETE SURFACE STRAIN(VERTICAL)FOR SECTION 2-2 OF BEAM B-1

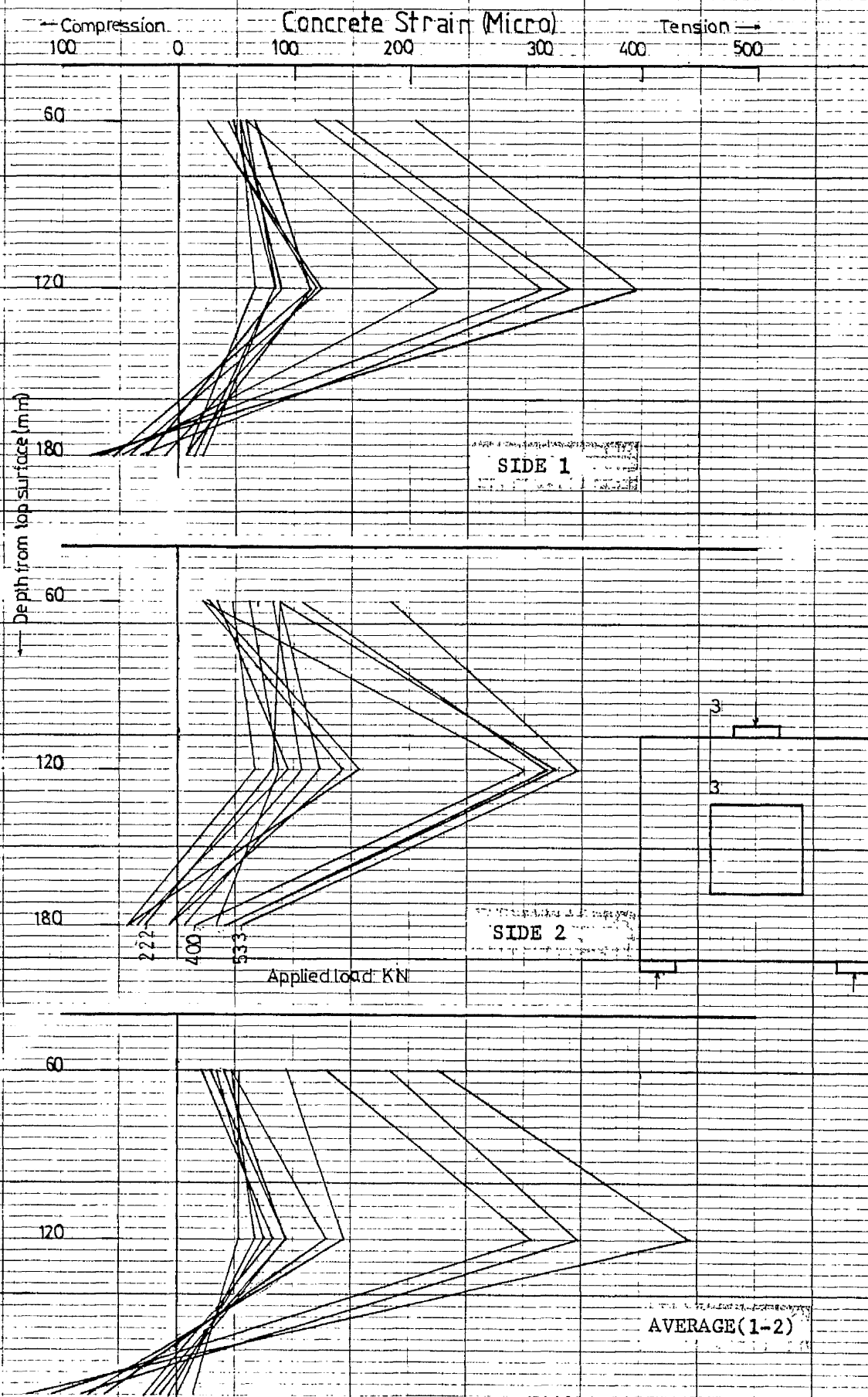


FIG. A1.1c. CONCRETE SURFACE STRAIN (HORIZONTAL) FOR SECTION 3-3 OF BEAM B1.

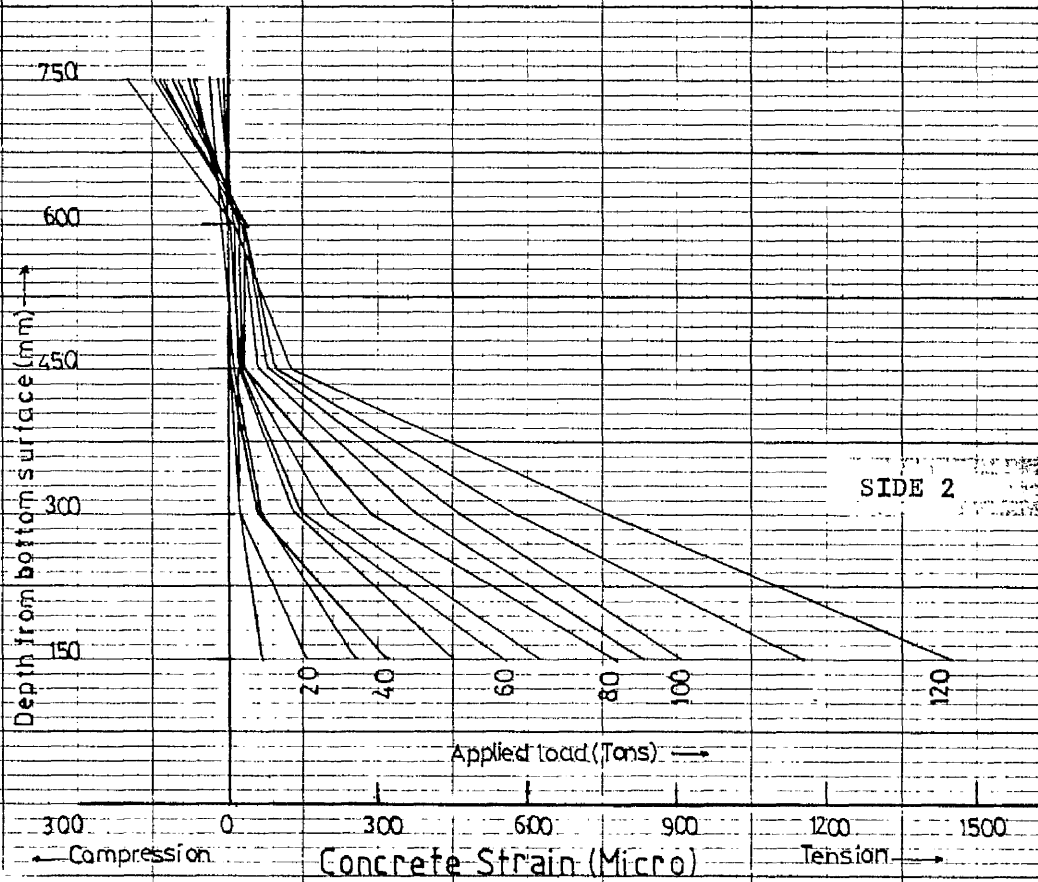
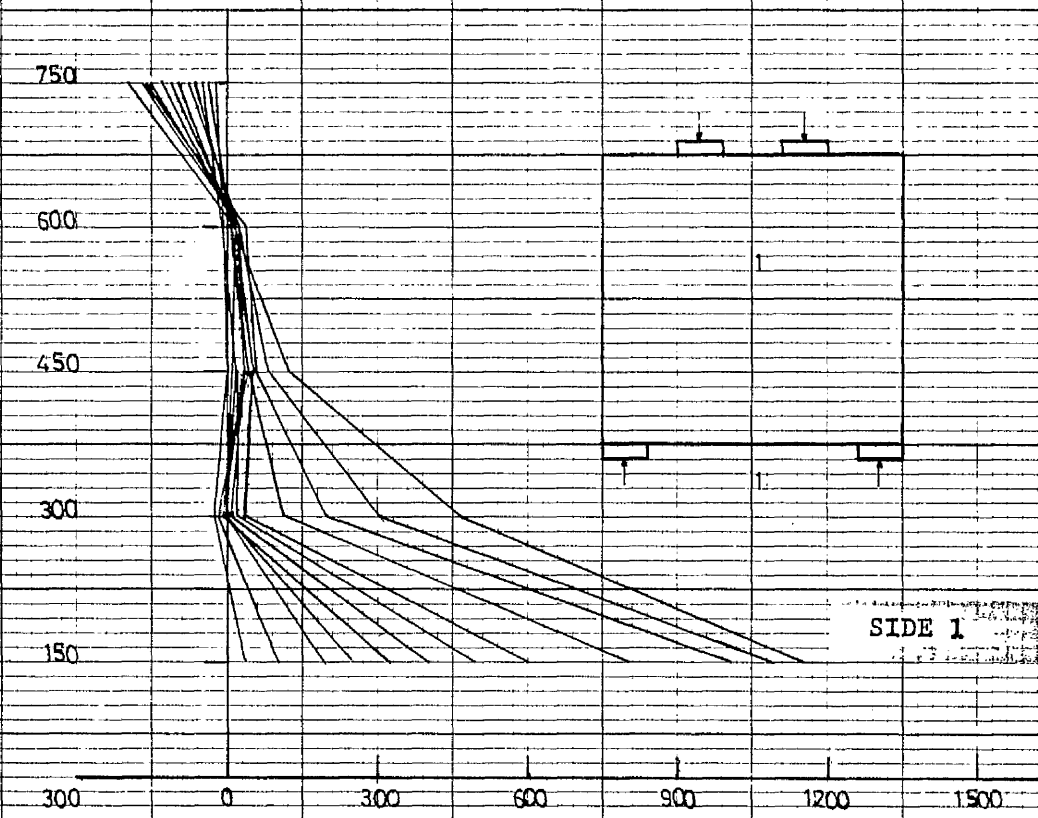


FIG.A1.2a. CONCRETE SURFACE STRAIN(HORIZONTAL)FOR SECTION 1-1 OF BEAM B2.

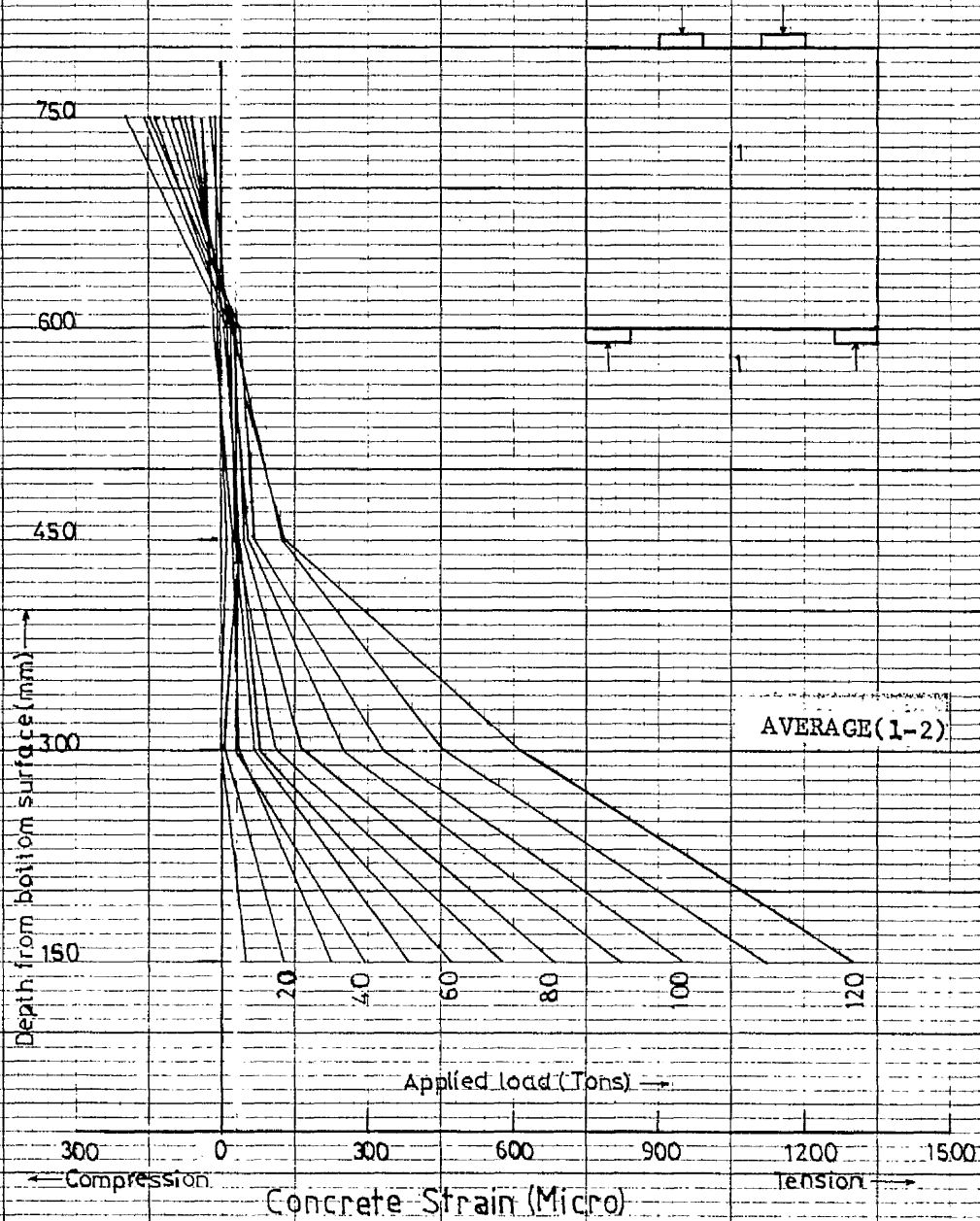


FIG. A.112a: CONCRETE SURFACE STRAIN (HORIZONTAL) FOR SECTION 1-1 OF BEAM

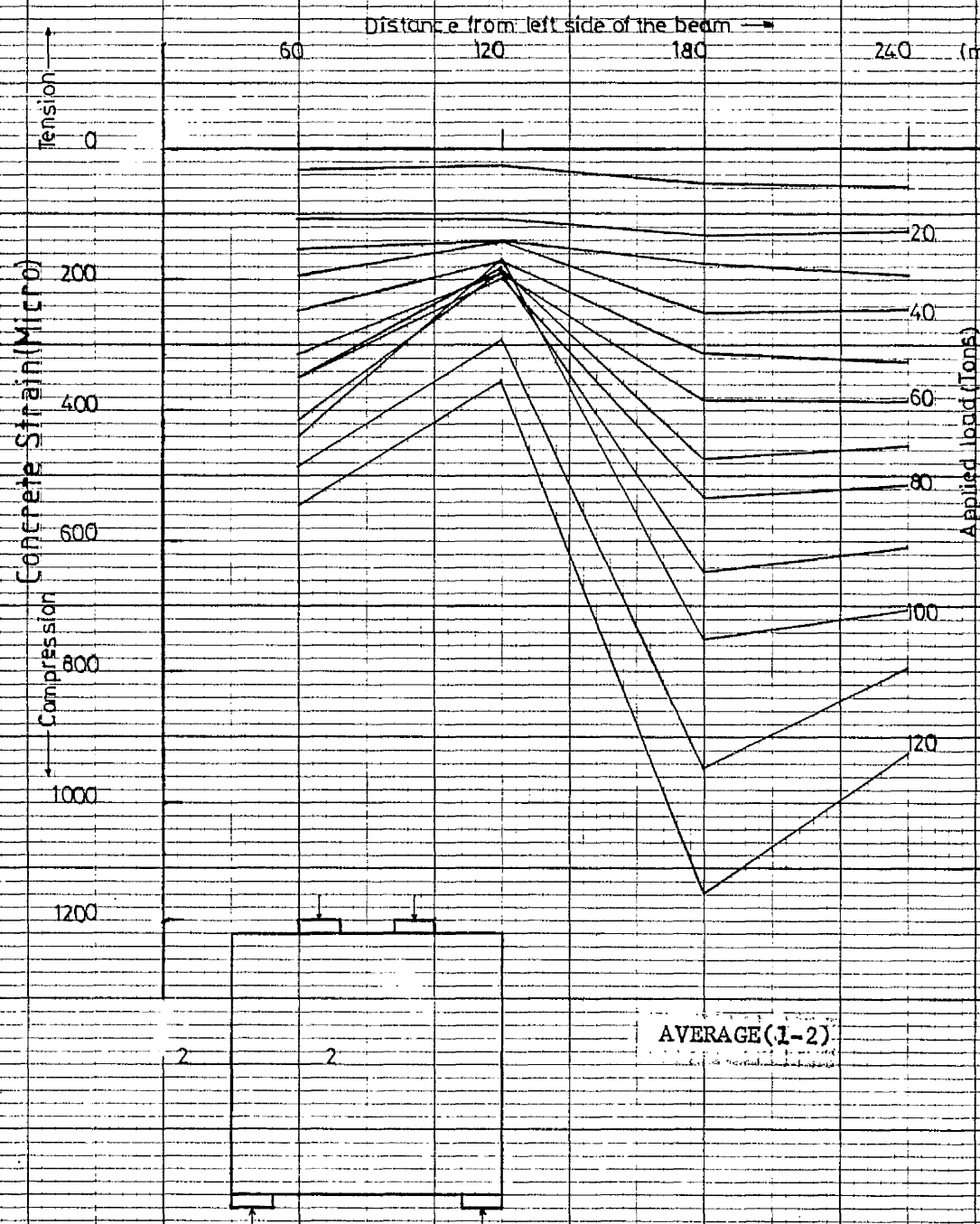


FIG. A1-2b. CONCRETE SURFACE STRAIN (VERTICAL) FOR SECTION 2-2 OF BEAM B2

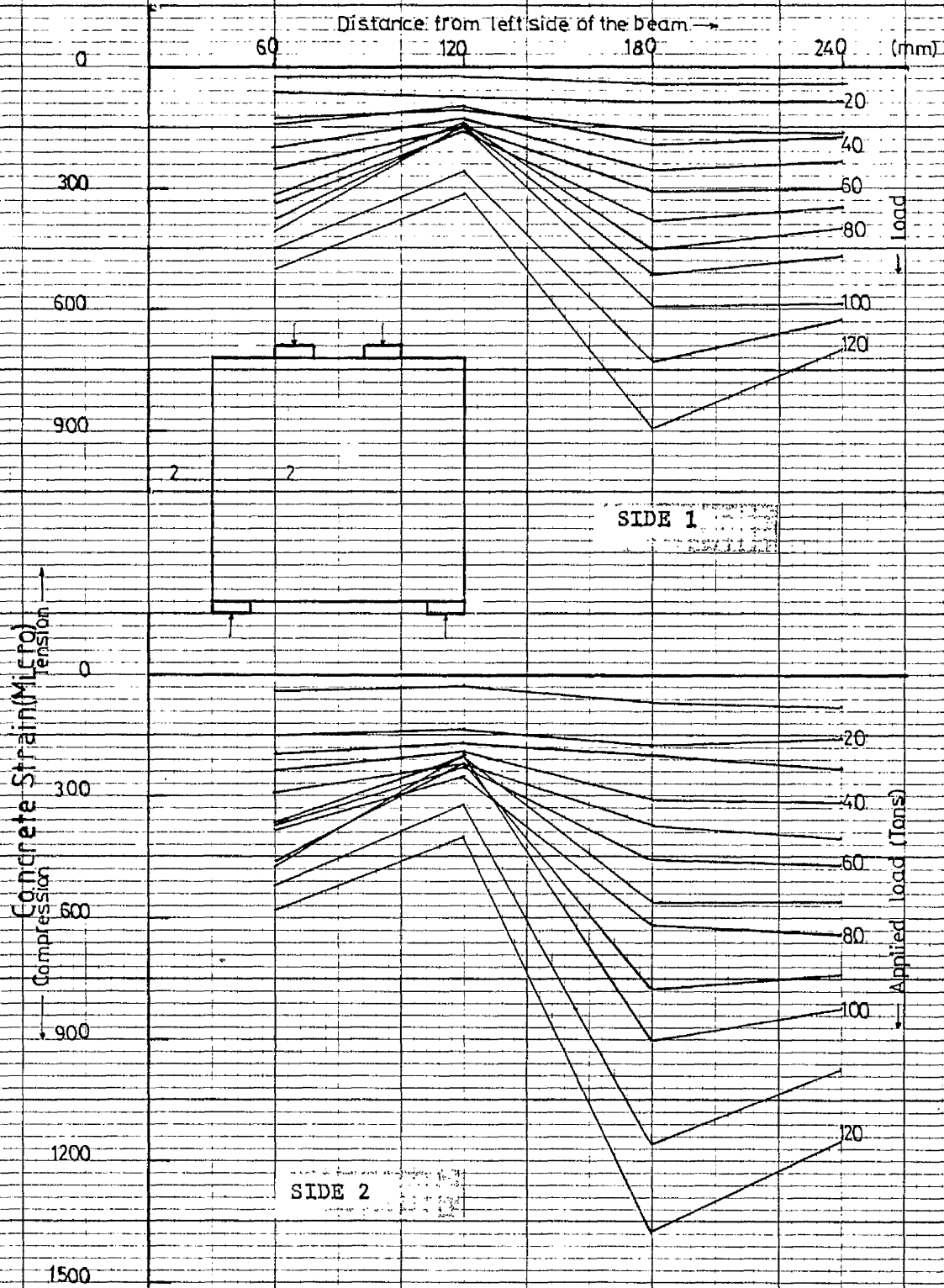


FIG. A1.2b. CONCRETE SURFACE STRAIN (VERTICAL) FOR SECTION 2-2 OF BEAM B2

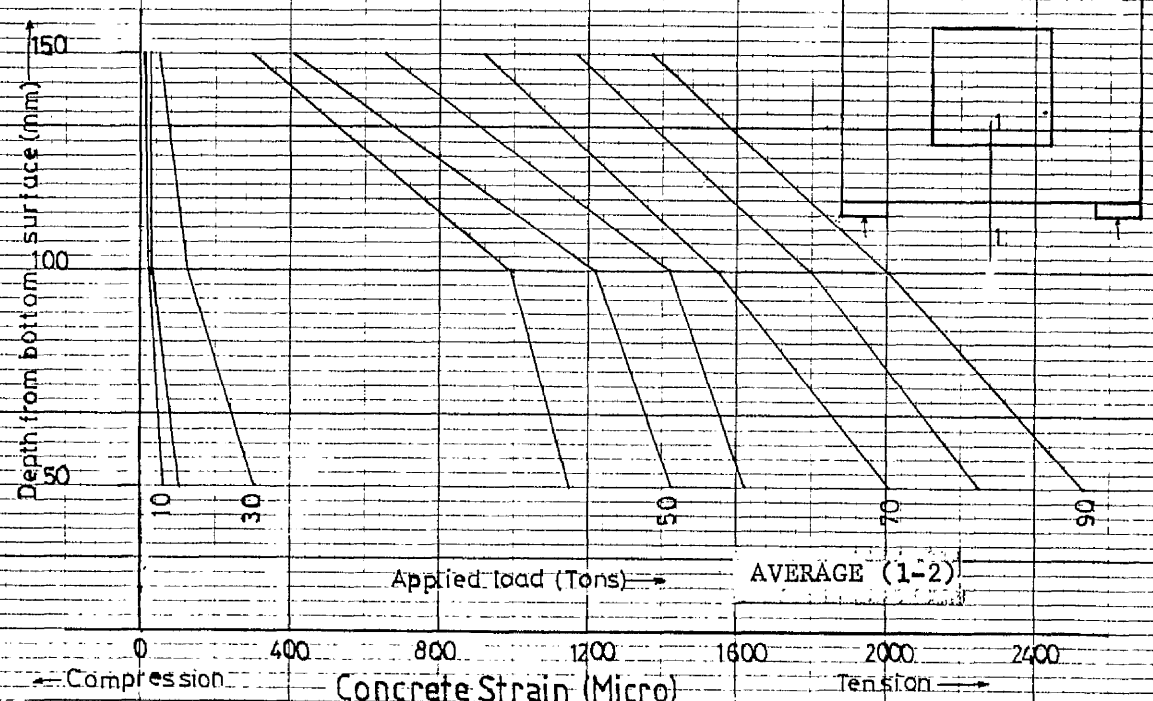
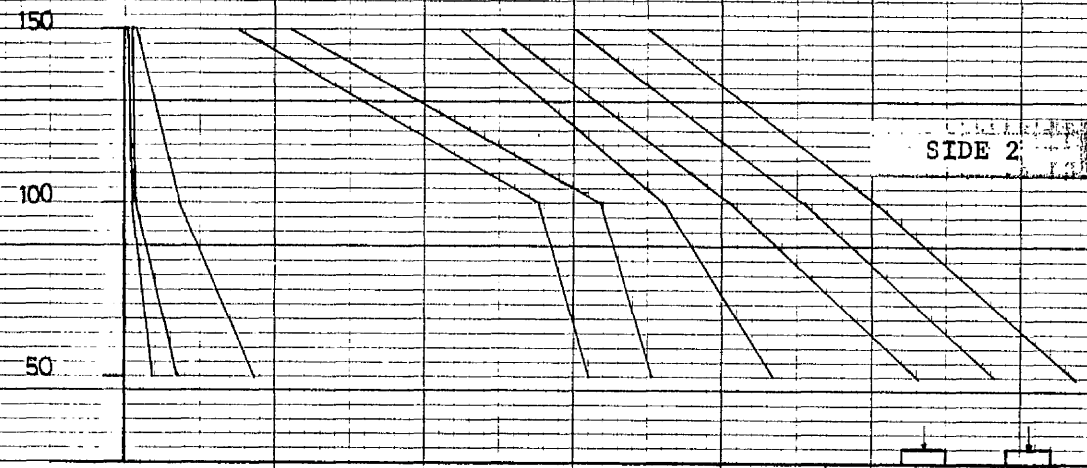
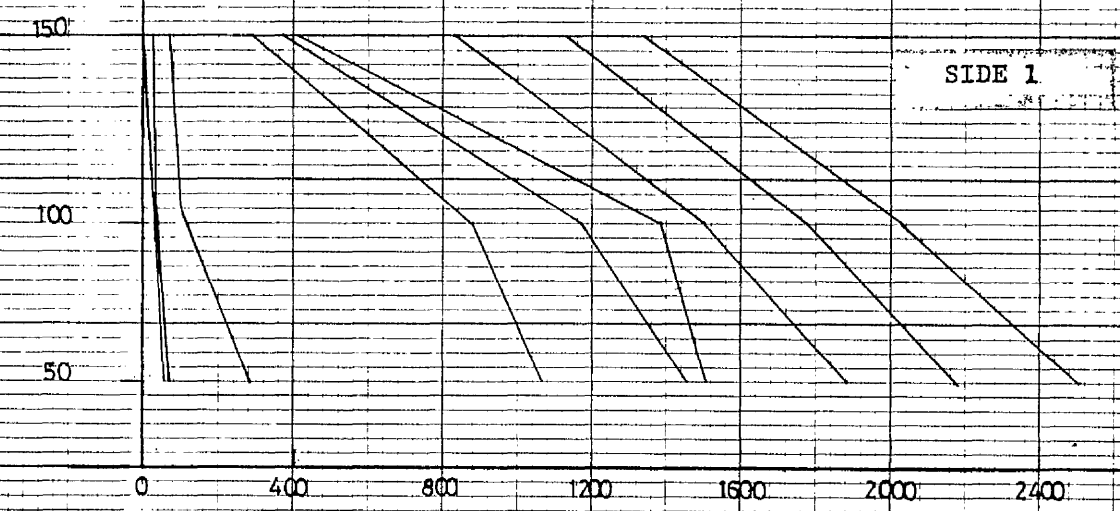


FIG. A1.3a. CONCRETE SURFACE STRAIN (HORIZONTAL) FOR SECTION 1-1 OF BEAM B3.

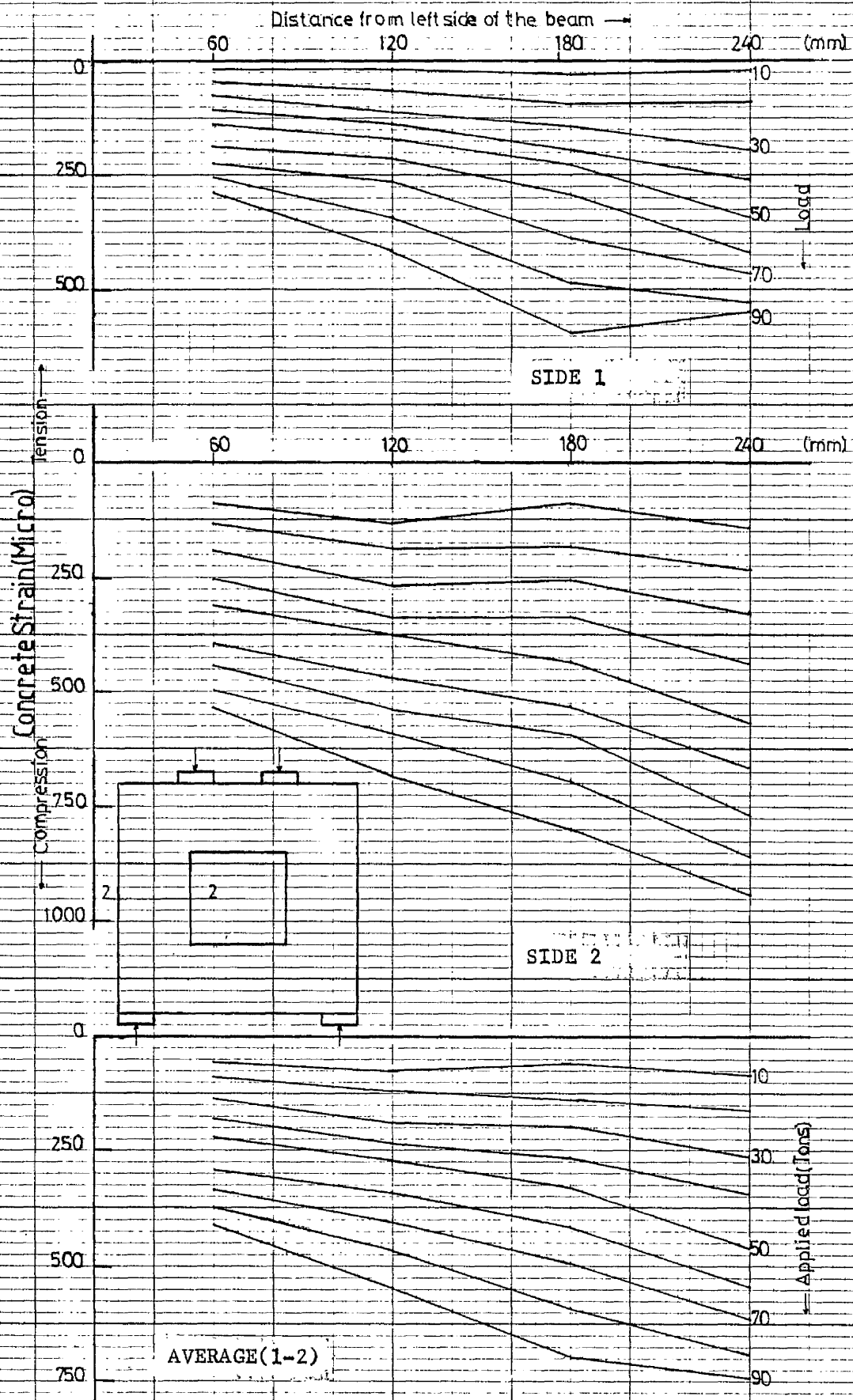


FIG.A1.3b. CONCRETE SURFACE STRAIN(VERTICAL)FOR SECTION 2-2 OF BEAM B3

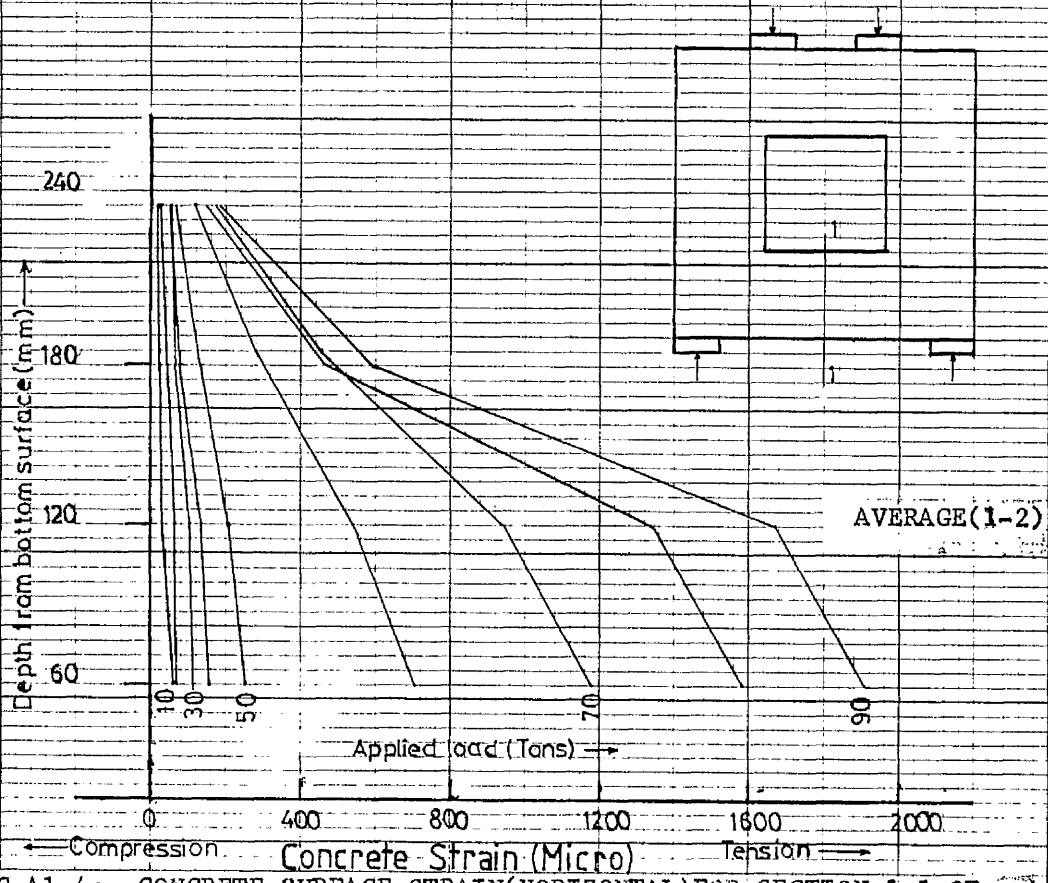
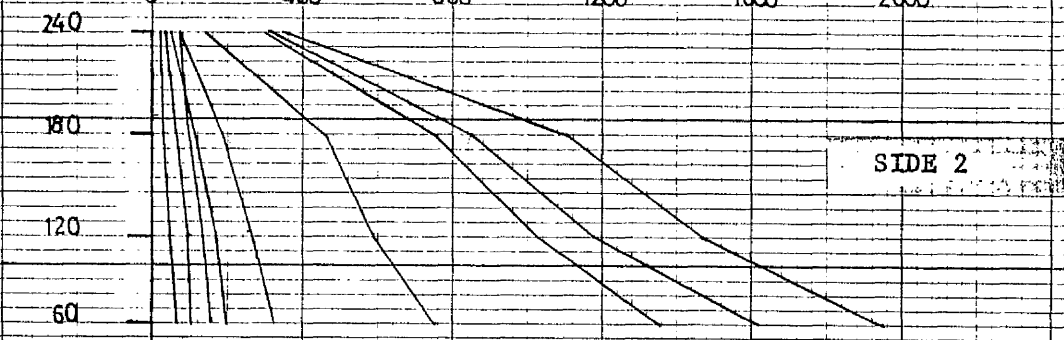
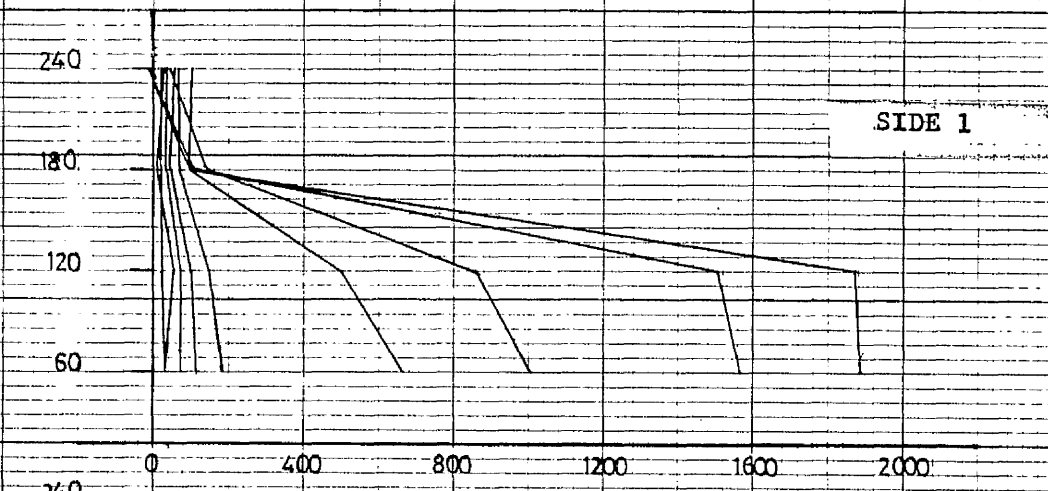


FIG.A1.4a. CONCRETE SURFACE STRAIN(HORIZONTAL)FOR SECTION 1-1 OF BEAM B4.

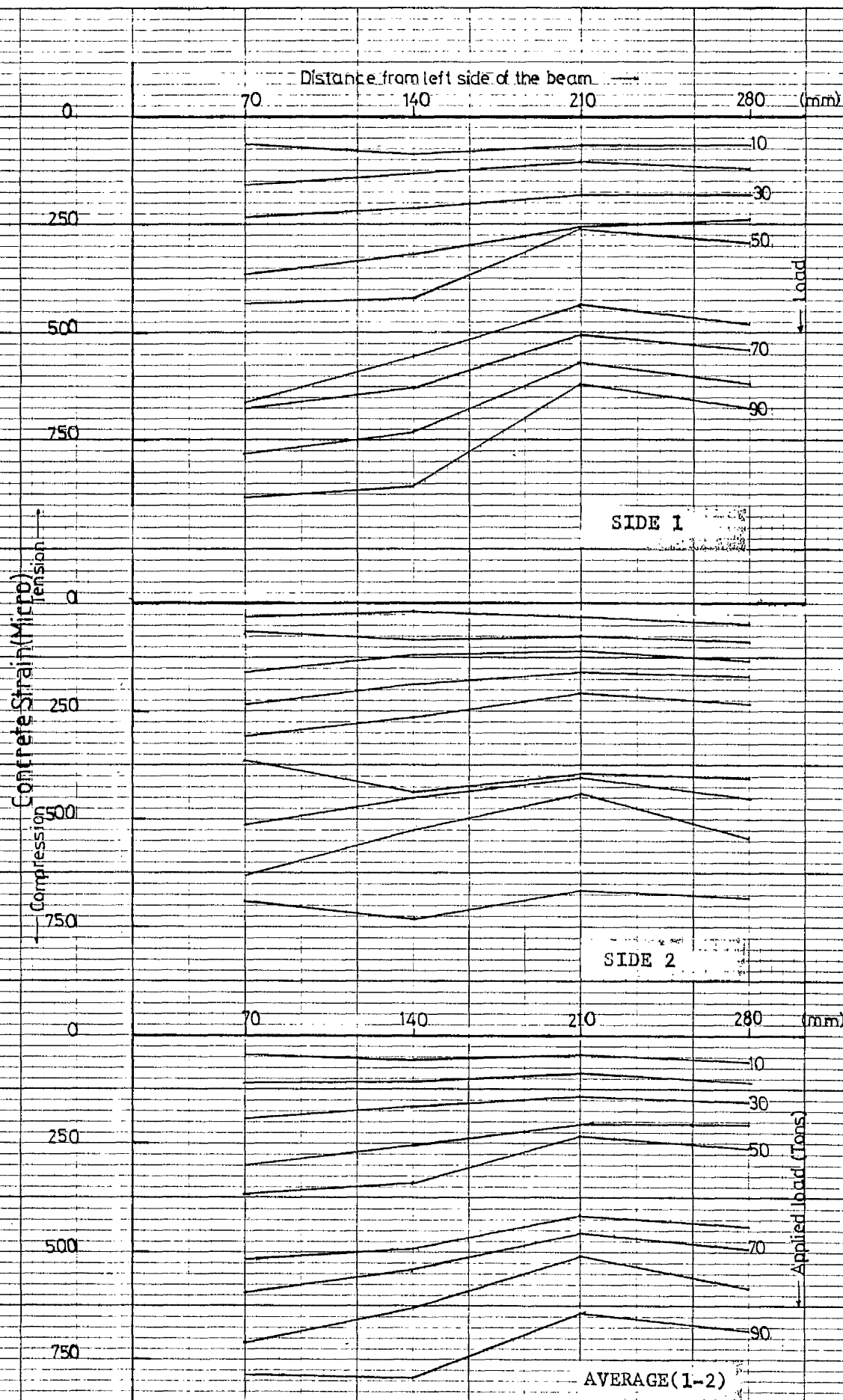


FIG. A1.4b. CONCRETE SURFACE STRAIN (VERTICAL) FOR SECTION 2-2 OF BEAM B4.

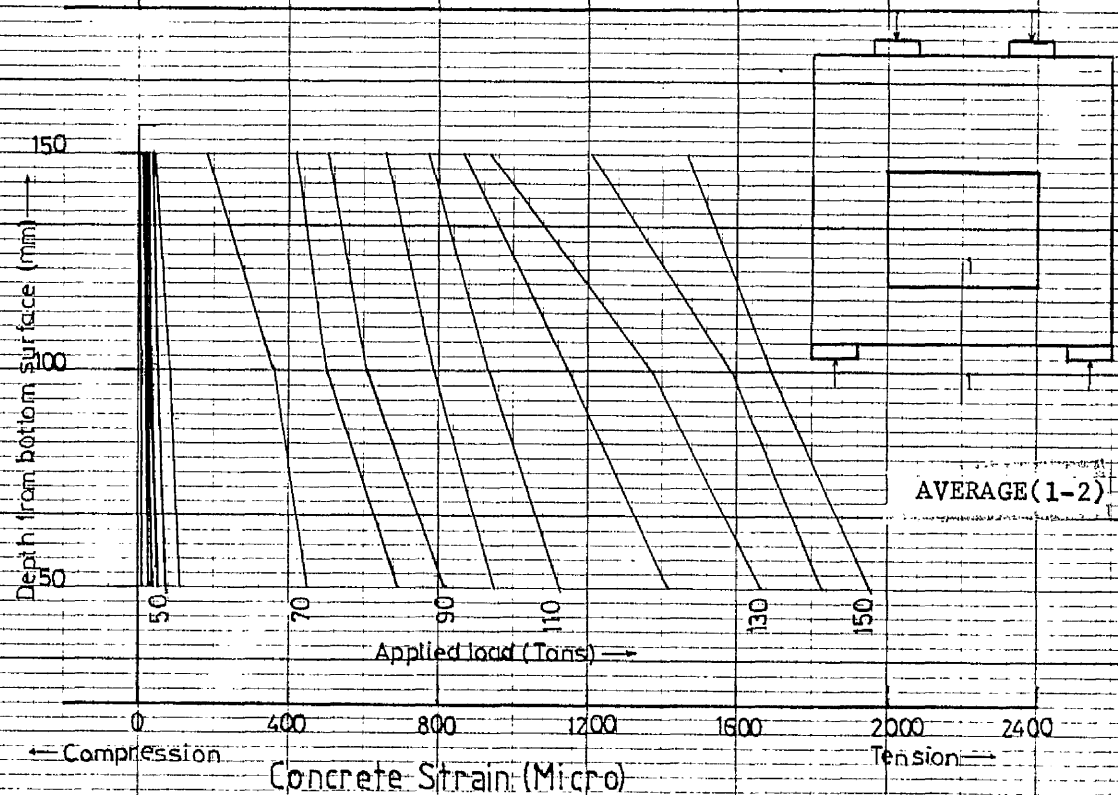
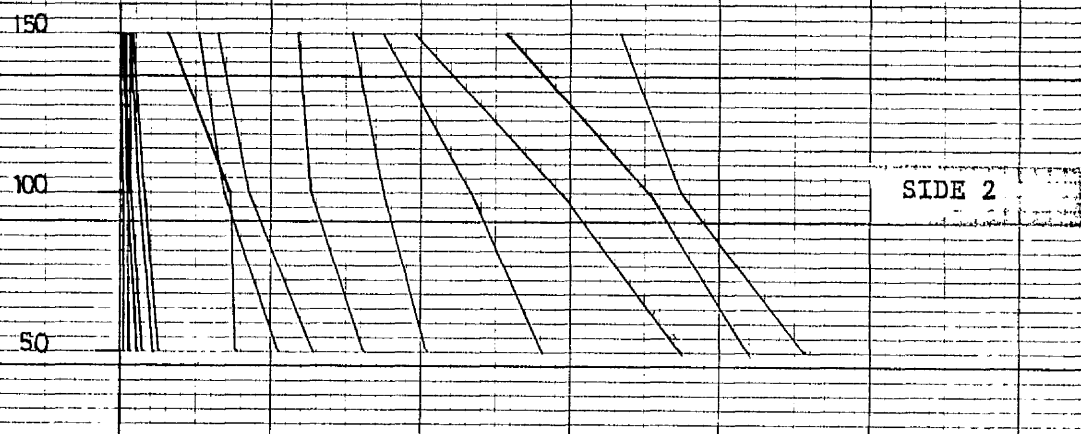
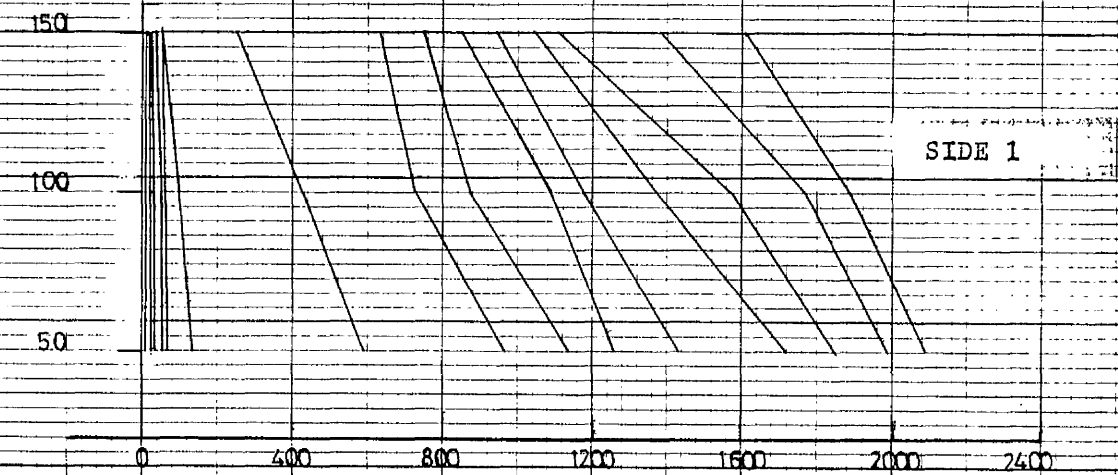


FIG. A1.5a. CONCRETE SURFACE STRAIN (HORIZONTAL) FOR SECTION 1-1 OF BEAM B5.

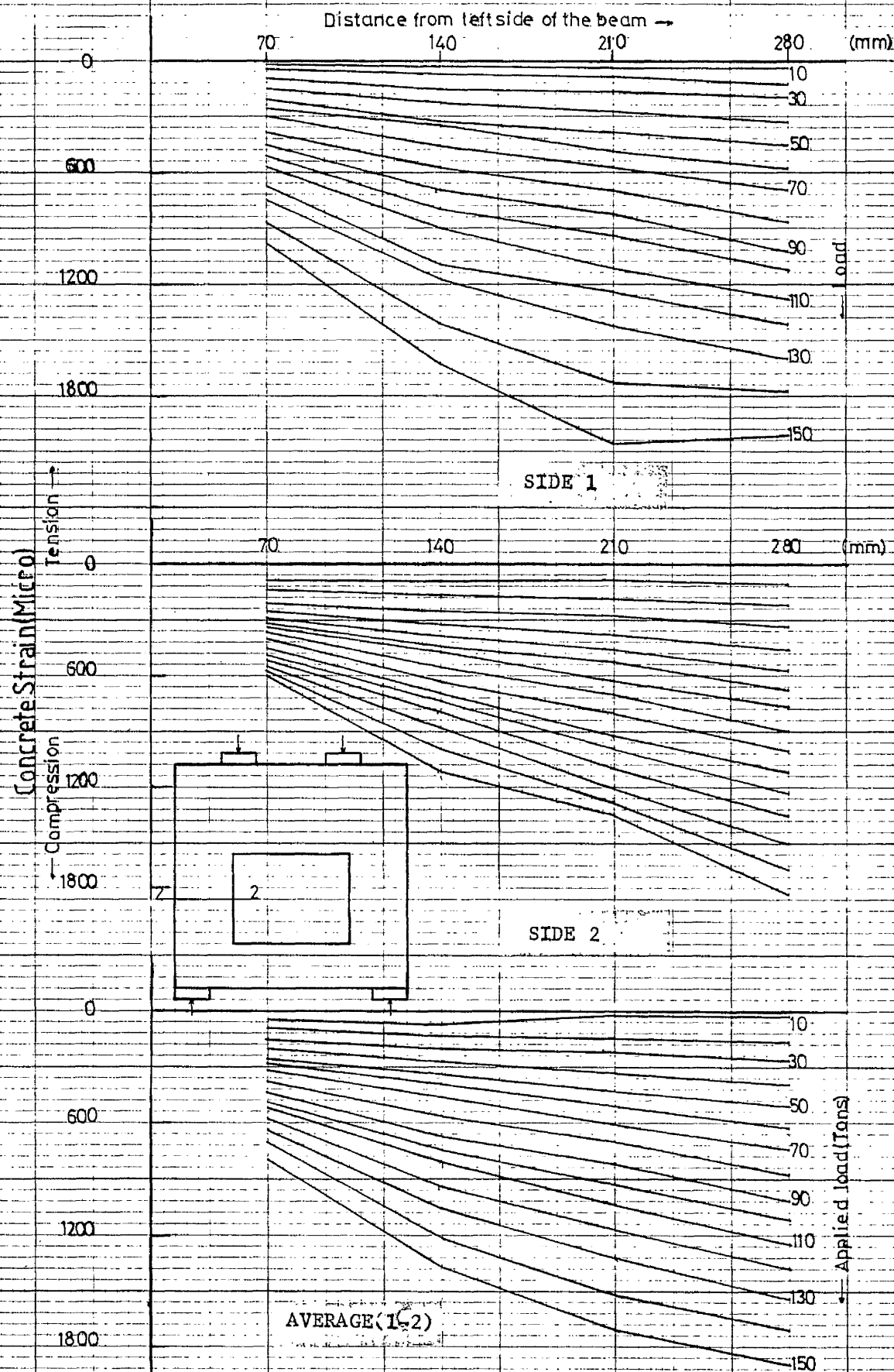


FIG.A1.5b.CONCRETE SURFACE STRAIN(VERTICAL)FOR SECTION 2-2 OF BEAM

B5.

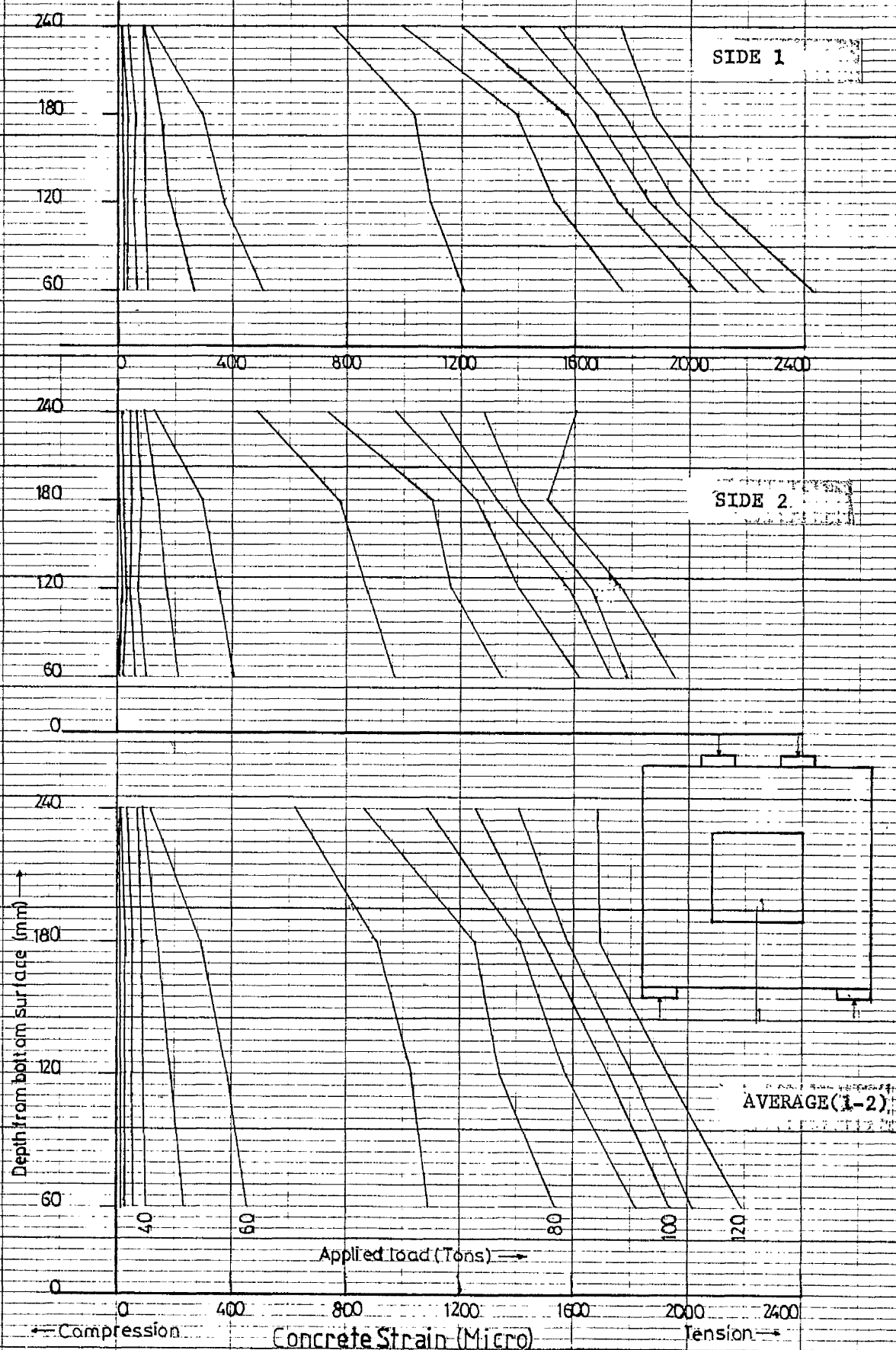


FIG.A1.6a. CONCRETE SURFACE STRAIN (HORIZONTAL) FOR SECTION 1-1 OF BEAM B6.

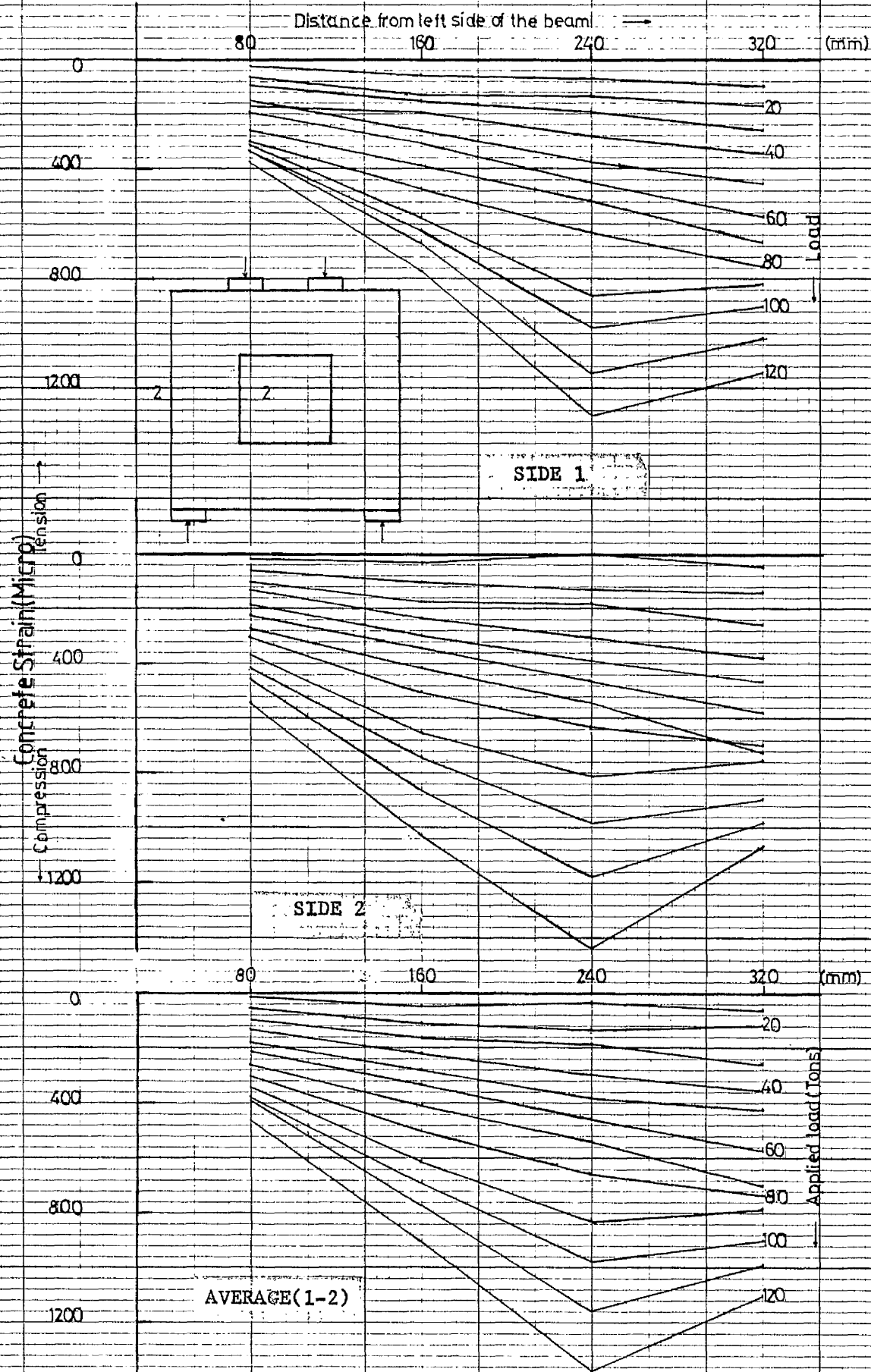


FIG.A1.6b. CONCRETE SURFACE STRAIN(VERTICAL)FOR SECTION 2-2 OF BEAM B6.

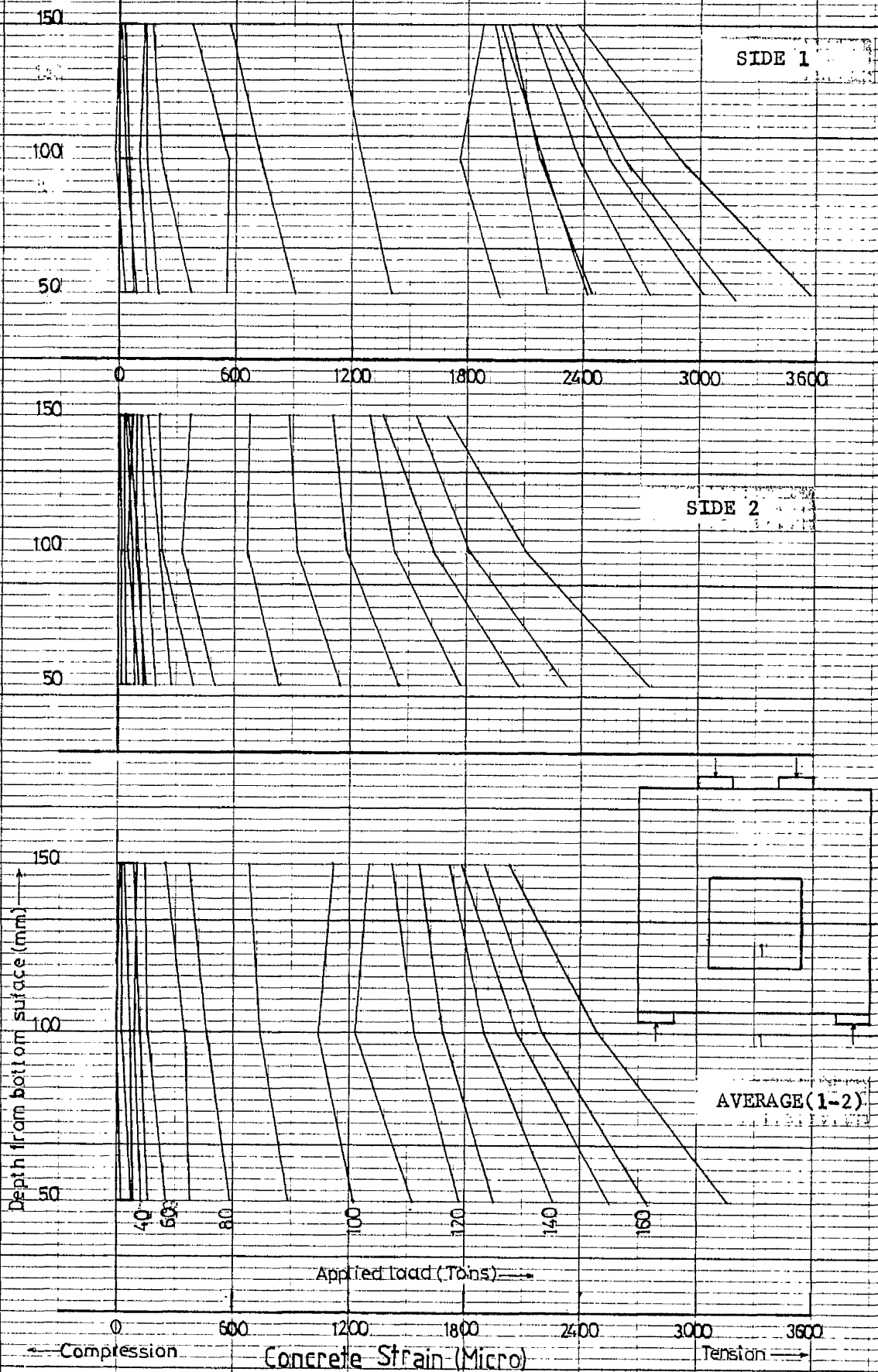


FIG. A1.7a. CONCRETE SURFACE STRAIN (HORIZONTAL) FOR SECTION 1-1 OF BEAM B7.

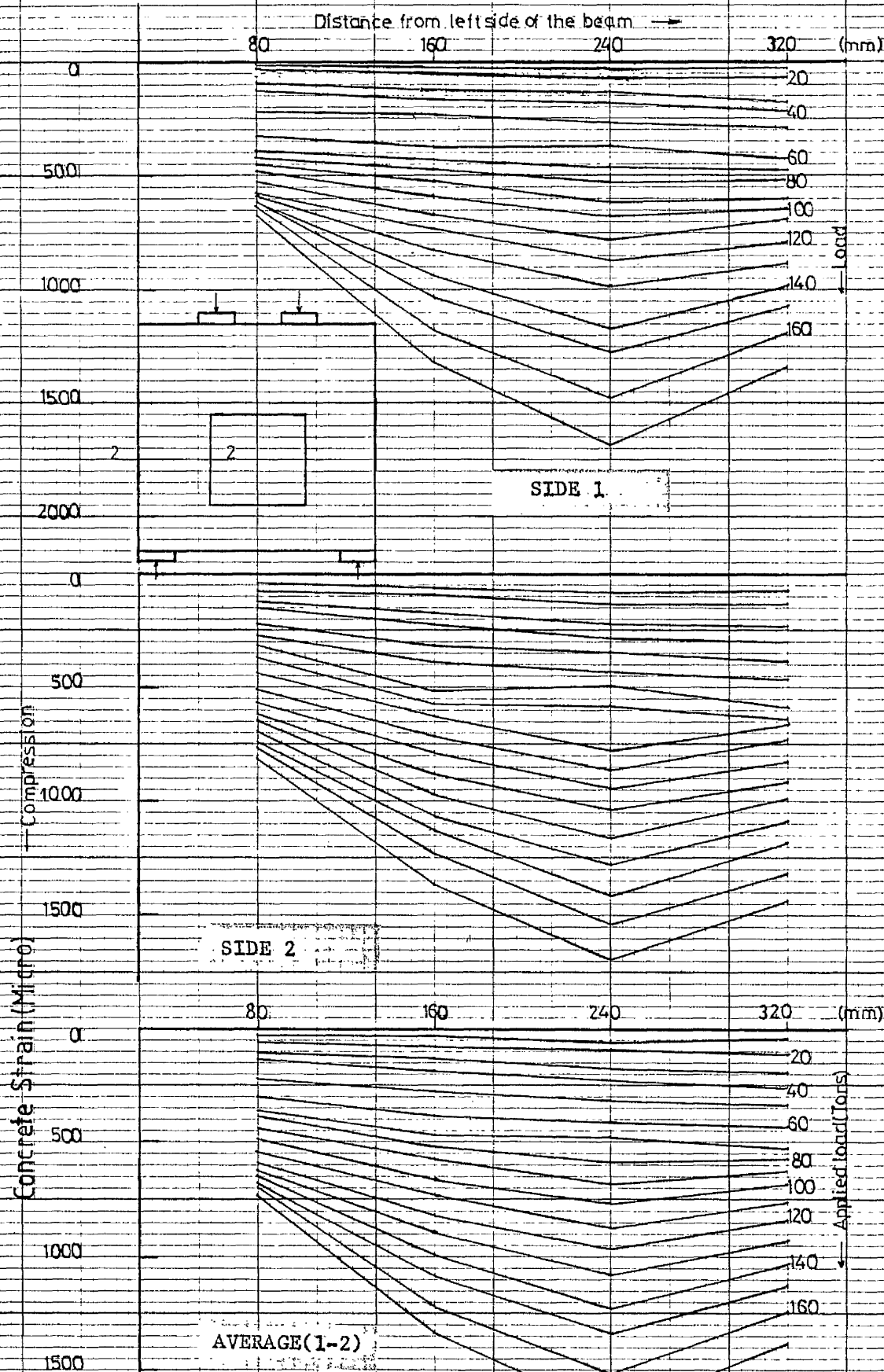


FIG.A1.7b. CONCRETE SURFACE STRAIN(VERTICAL)FOR SECTION 2-2 OF BEAM B7.

APPENDIX 2

STEEL STRAIN DISTRIBUTION ALONG THE BOTTON ROW OF BARS
ABOVE AND BELOW THE OPENING.

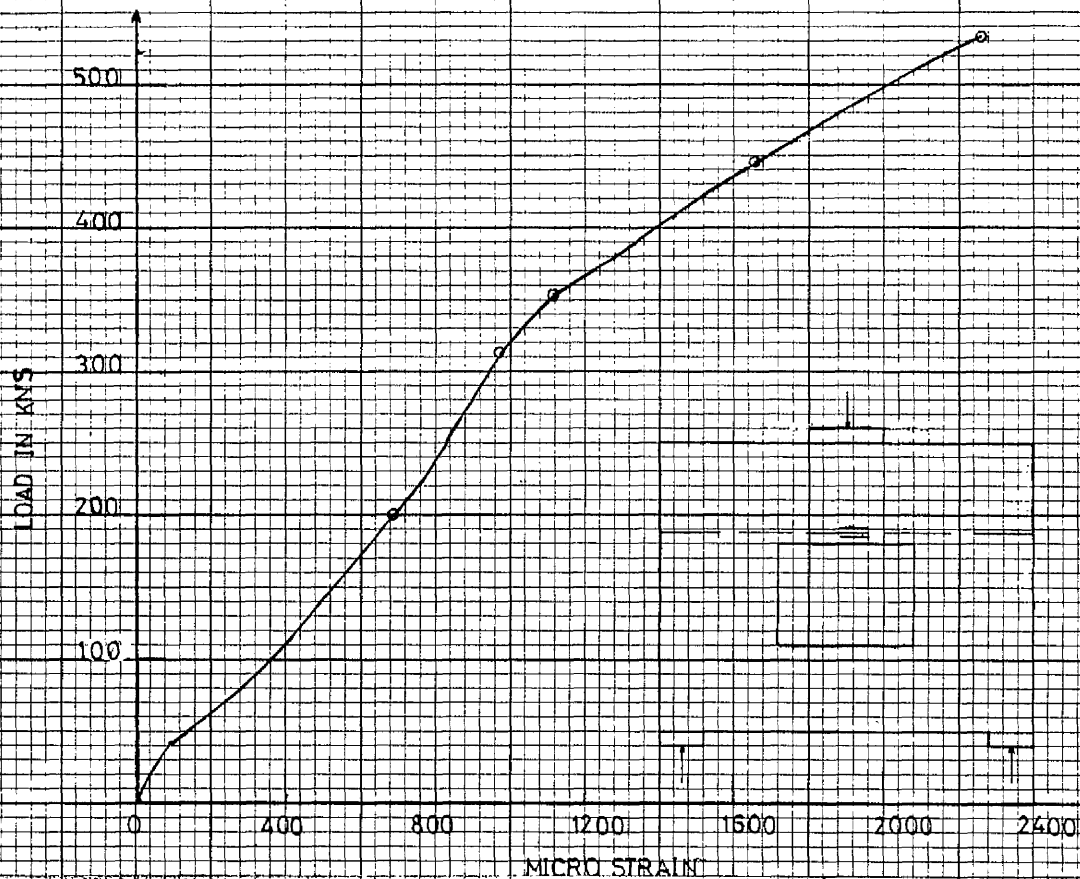


FIG. A2(b).1. AVERAGE STRAIN DISTRIBUTION ALONG THE BOTH BOTTOM BARS (ABOVE THE OPENING) OF BEAM B1.

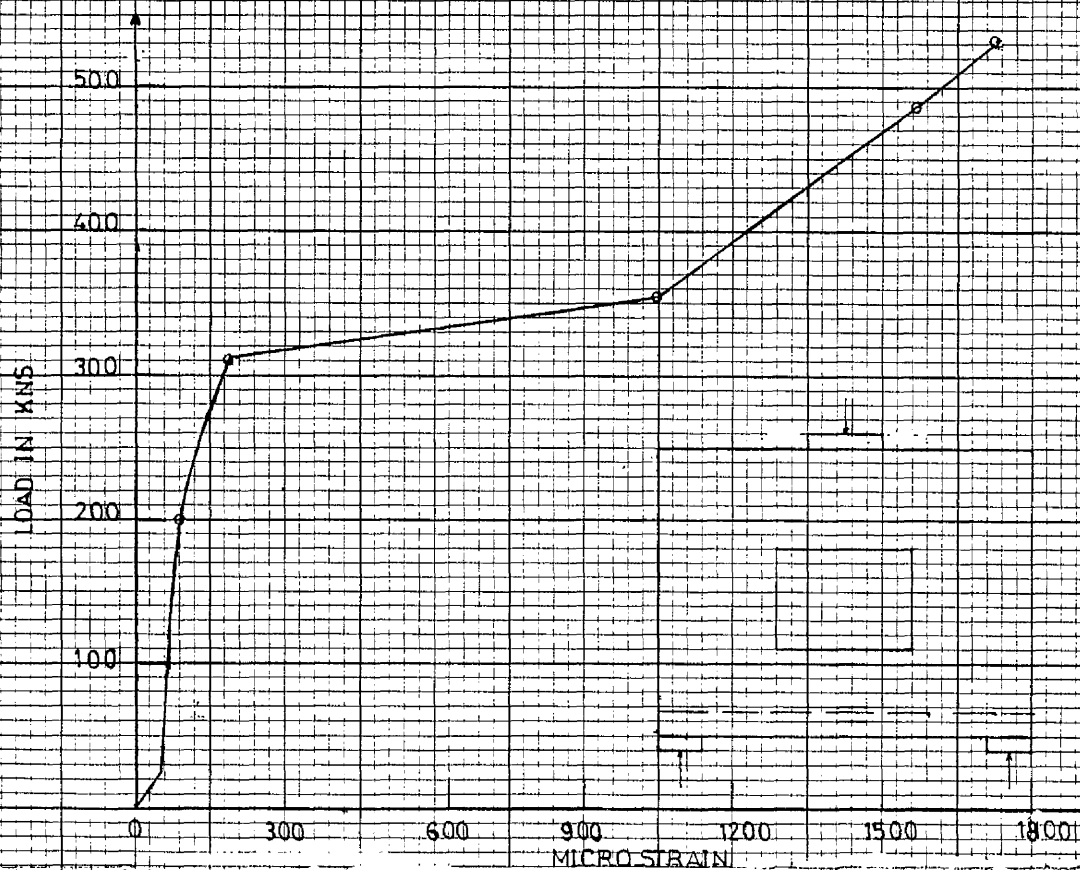


FIG. A2(a).1. AVERAGE STRAIN DISTRIBUTION ALONG THE BOTH BOTTOM BARS (BELOW THE OPENING) OF BEAM 1.

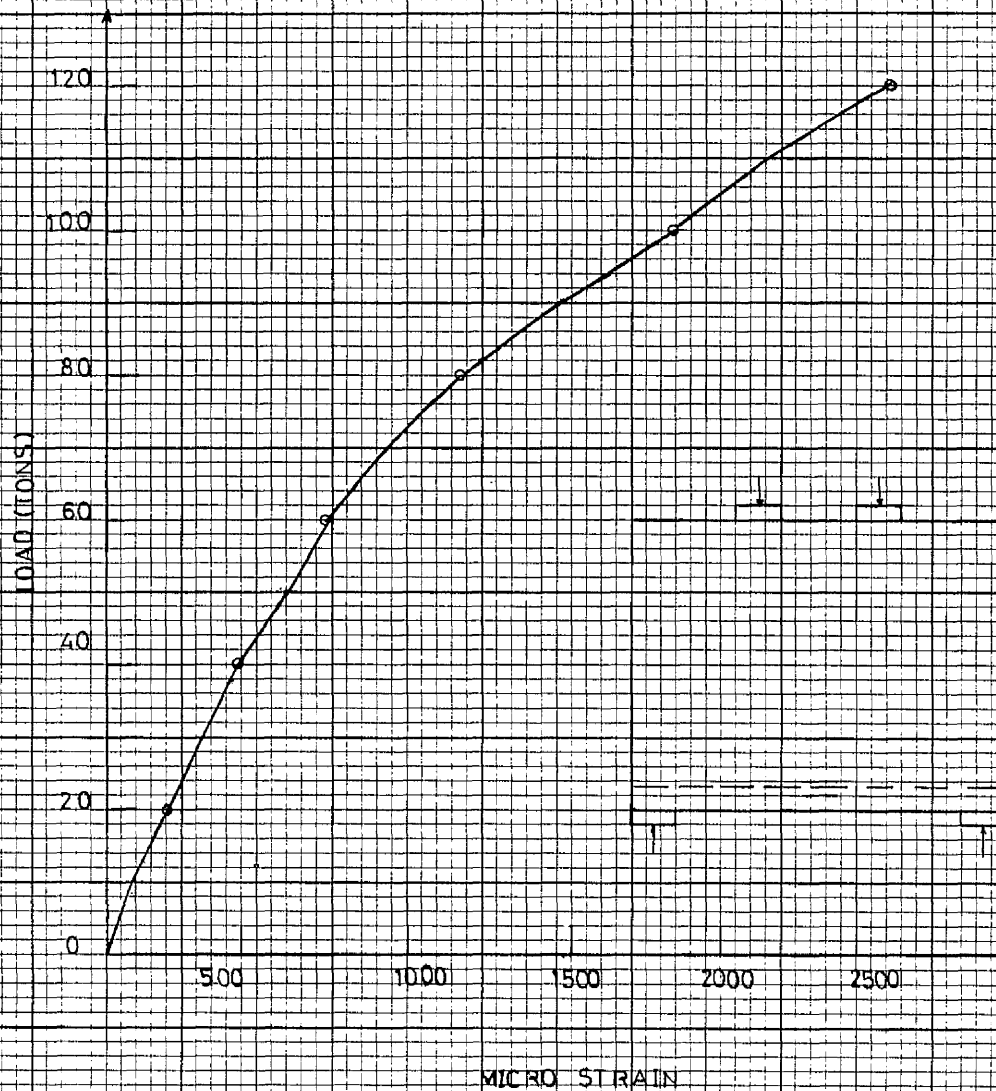


FIG. A2(a). 2. AVERAGE STRAIN DISTRIBUTION ALONG THE BOTH BOTTOM BARS OF BEAM B2.

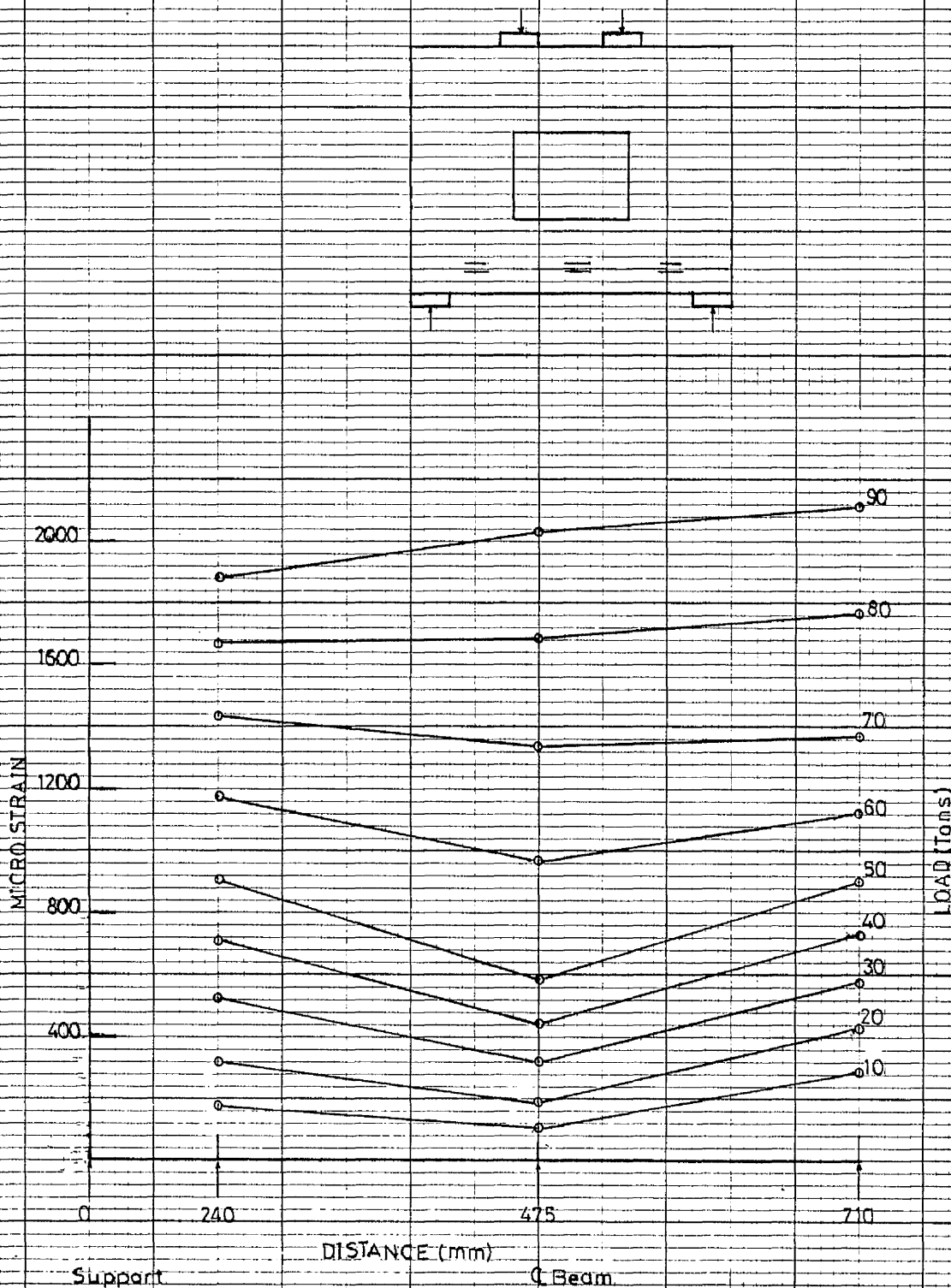


FIG. A2(a).3. AVERAGE STRAIN DISTRIBUTION ALONG THE BOTH BOTTOM BARS (BELOW THE OPENING) OF BEAM B3.

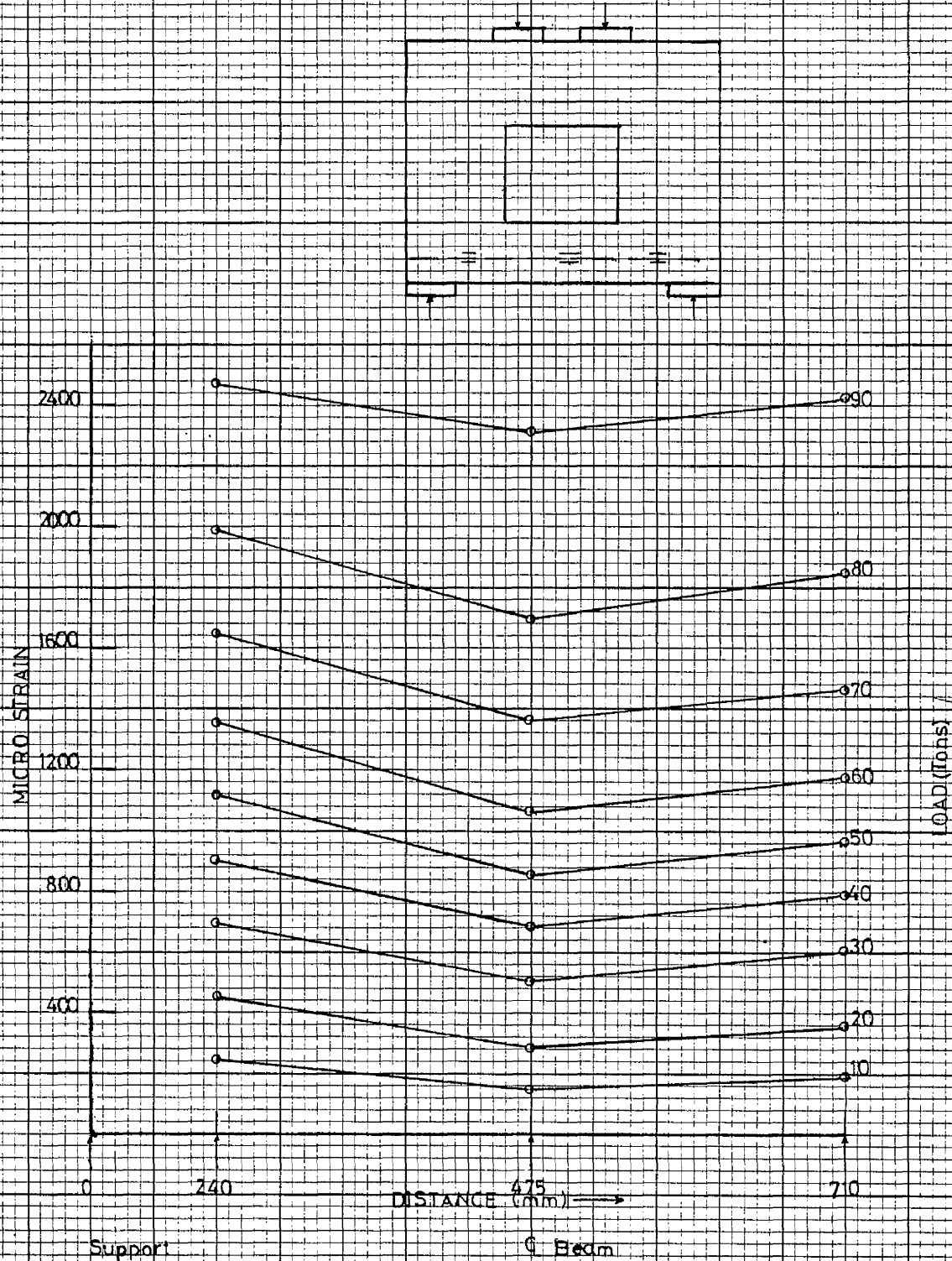


FIG.A2(a).4. AVERAGE STRAIN DISTRIBUTION ALONG THE BOTH BOTTOM BARS (BELOW THE OPENING) OF BEAM B4.

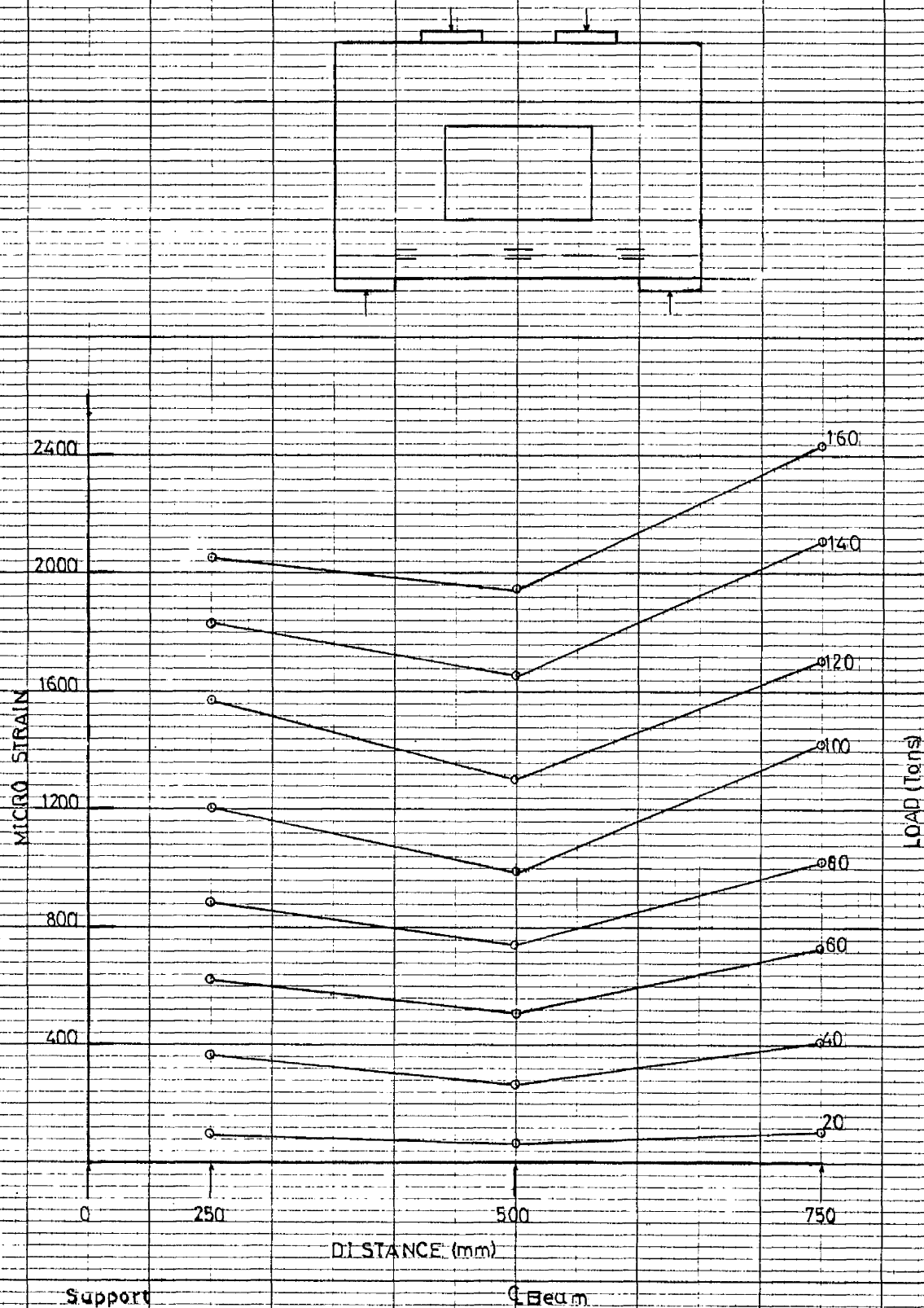


FIG.A2(a).5.AVERAGE STRAIN DISTRIBUTION ALONG THE BOTH BOTTOM BARS
(BELOW THE OPENING) OF BEAM B5.

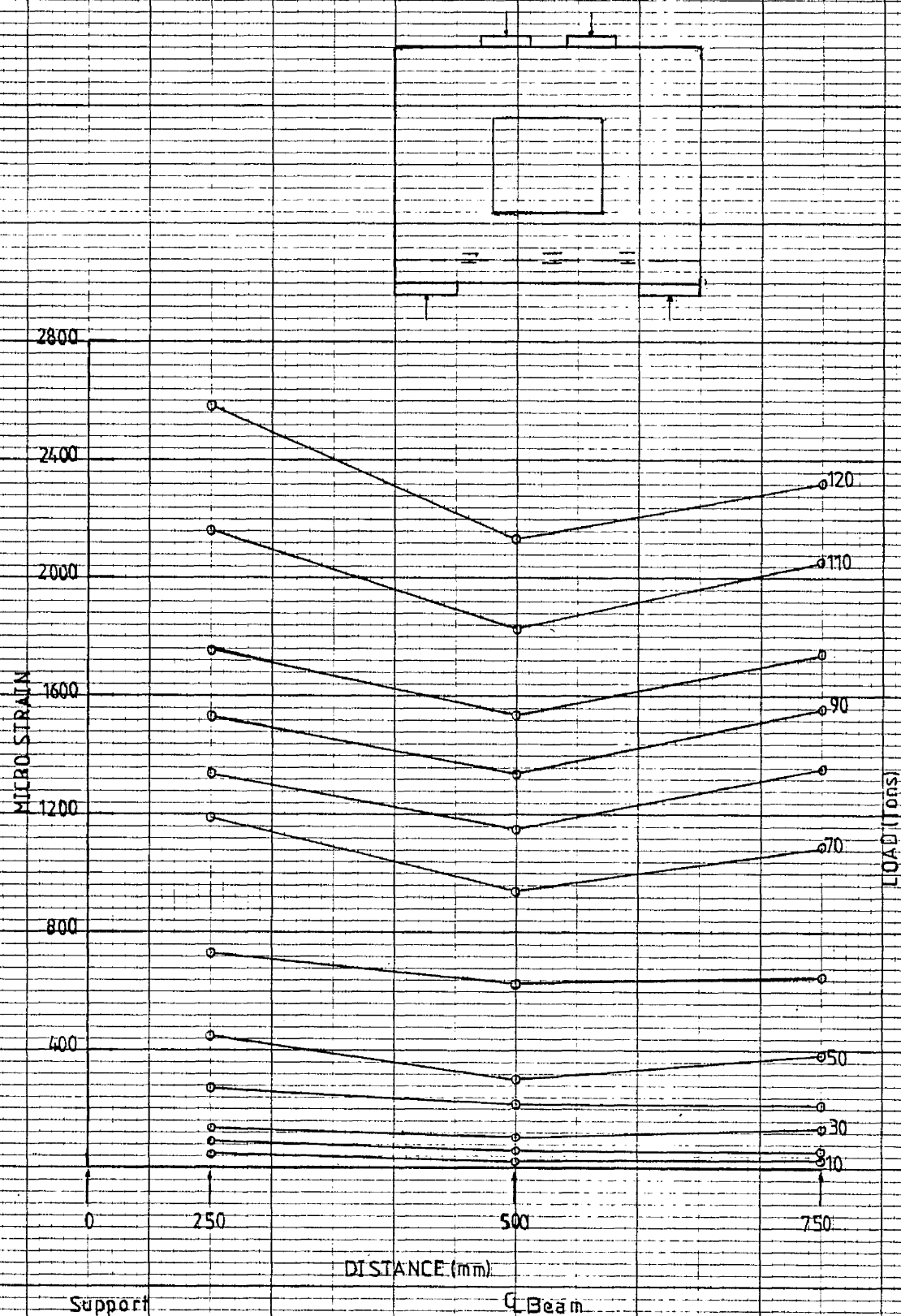
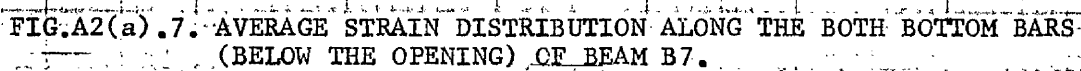


FIG. A2(a).6. AVERAGE STRAIN DISTRIBUTION ALONG THE BOTH BOTTOM BARS (BELOW THE OPENING) OF BEAM B6.



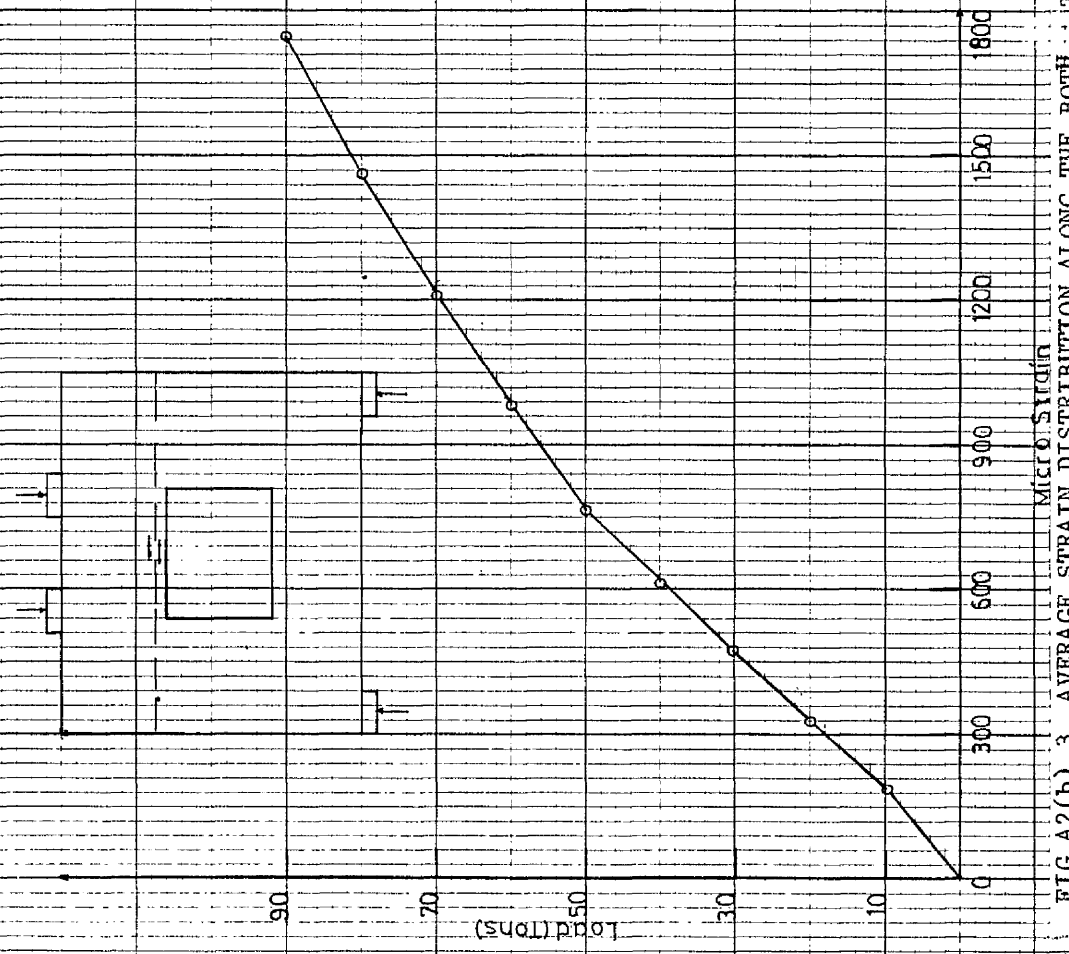


FIG. A2(b). 3. AVERAGE STRAIN DISTRIBUTION ALONG THE BOTH BOTTOM BARS (ABOVE THE OPENING) OF BEAM B3.

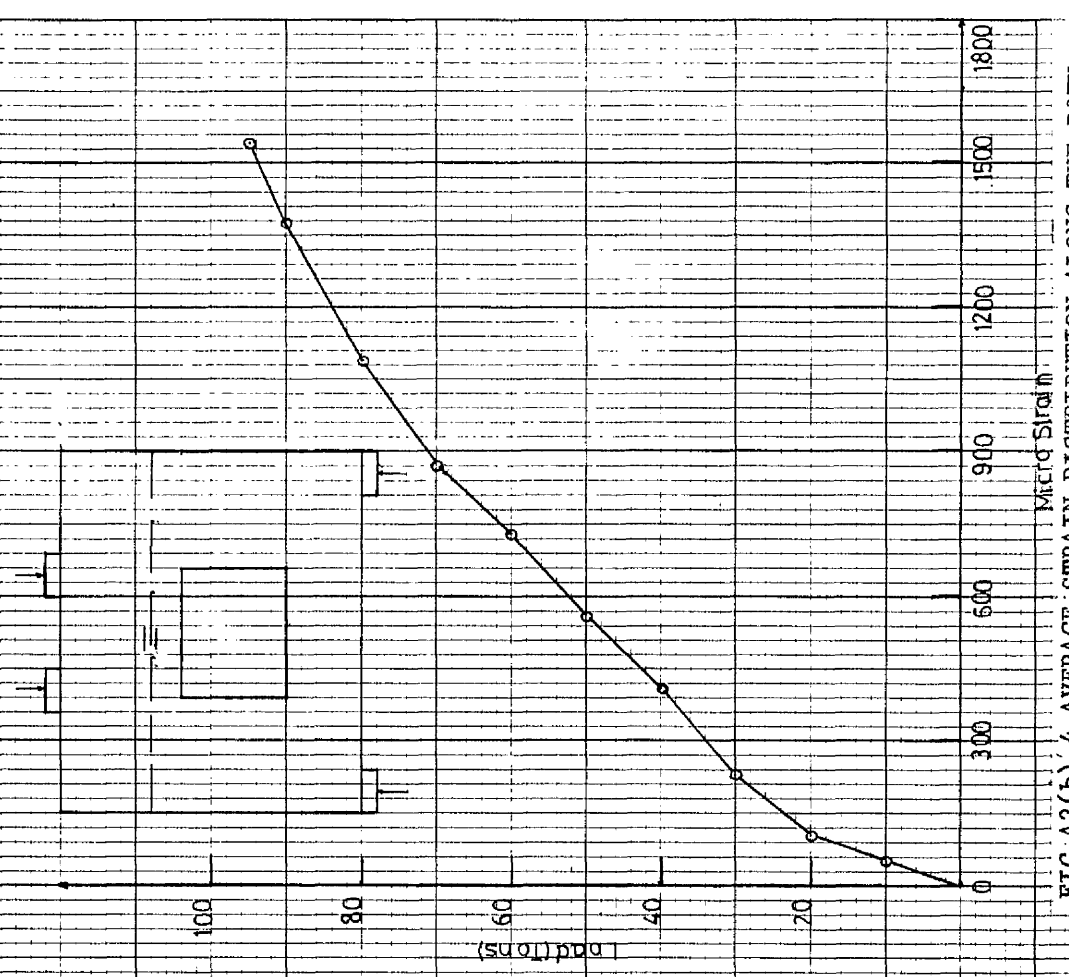


FIG. A2(b). 4. AVERAGE STRAIN DISTRIBUTION ALONG THE BOTH BOTTOM BARS (ABOVE THE OPENING) OF BEAM B4.

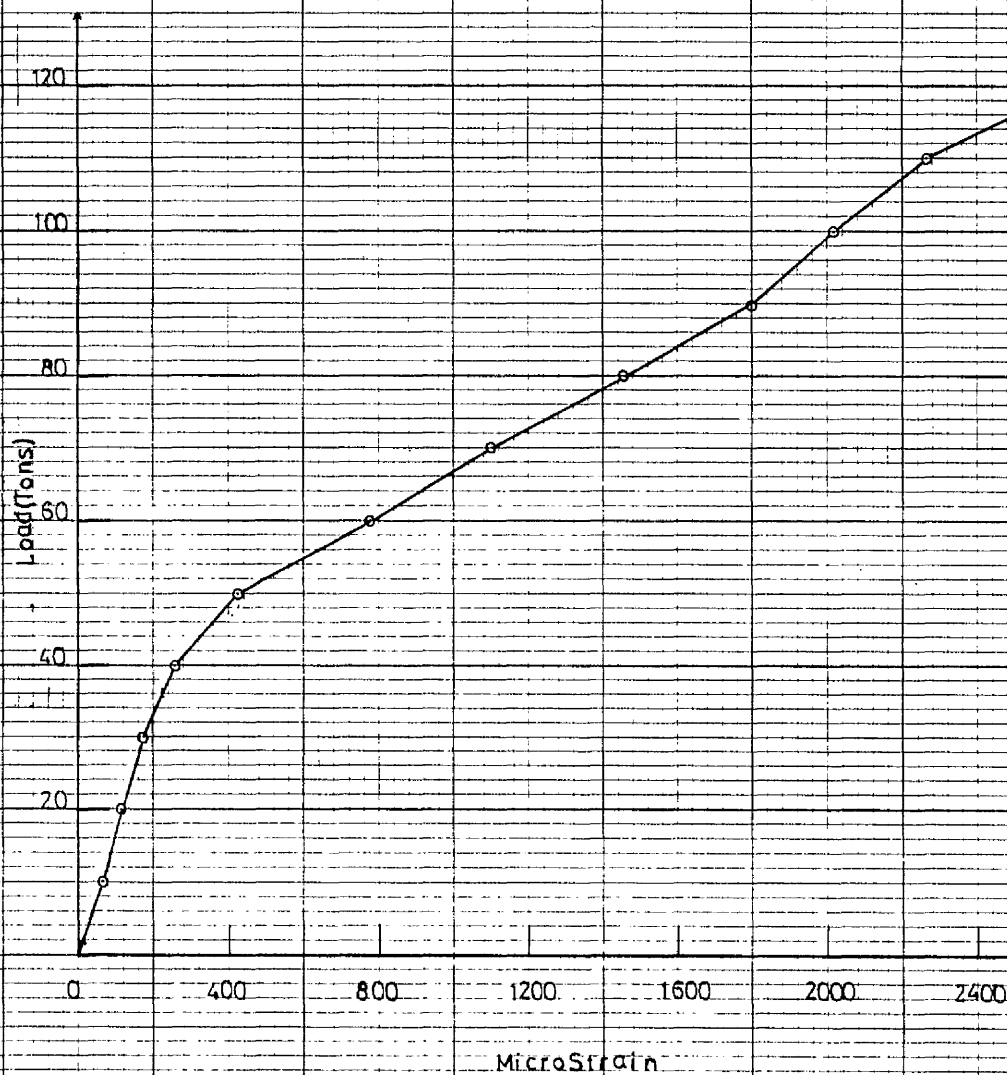


FIG.A2(b).6.AVERAGE STRAIN DISTRIBUTION ALONG THE BOTH BOTTOM BARS
(ABOVE THE OPENING) OF BEAM B6.

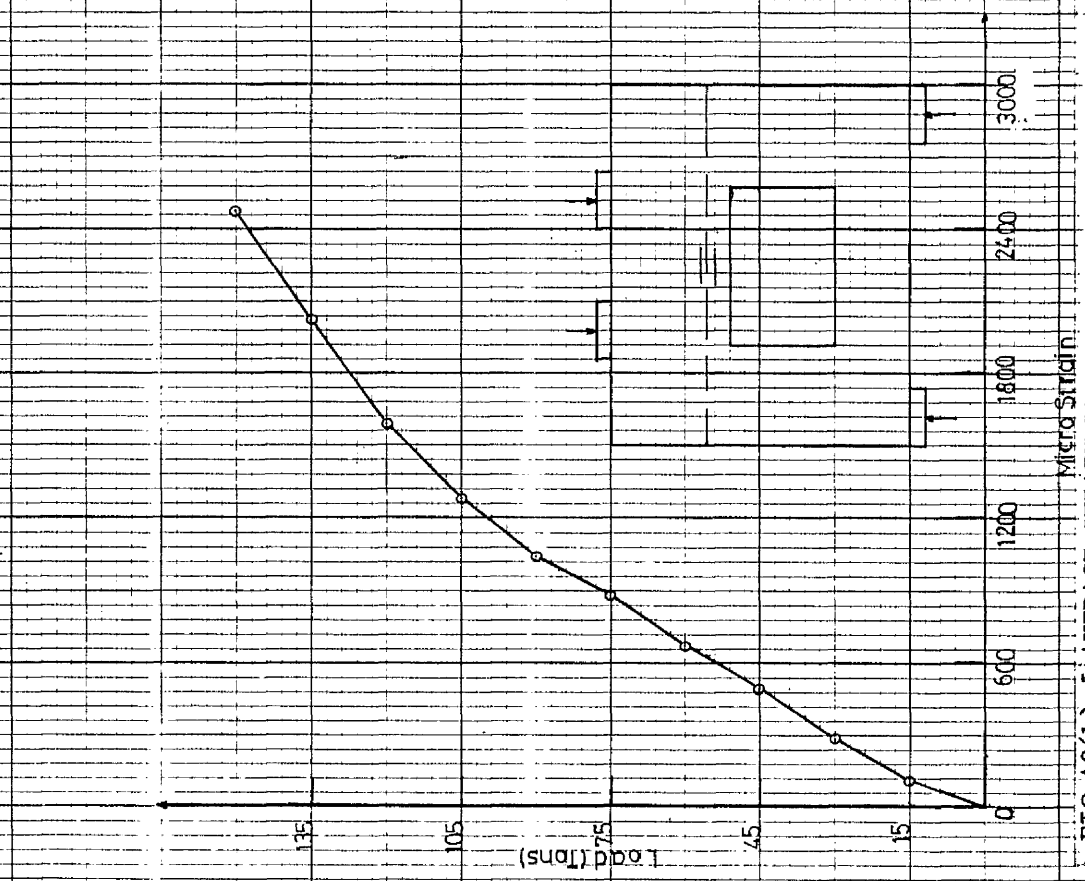


FIG. A2(b). 5. AVERAGE STRAIN DISTRIBUTION ALONG THE BOTTOM BARS (ABOVE THE OPENING) OF BEAM B5

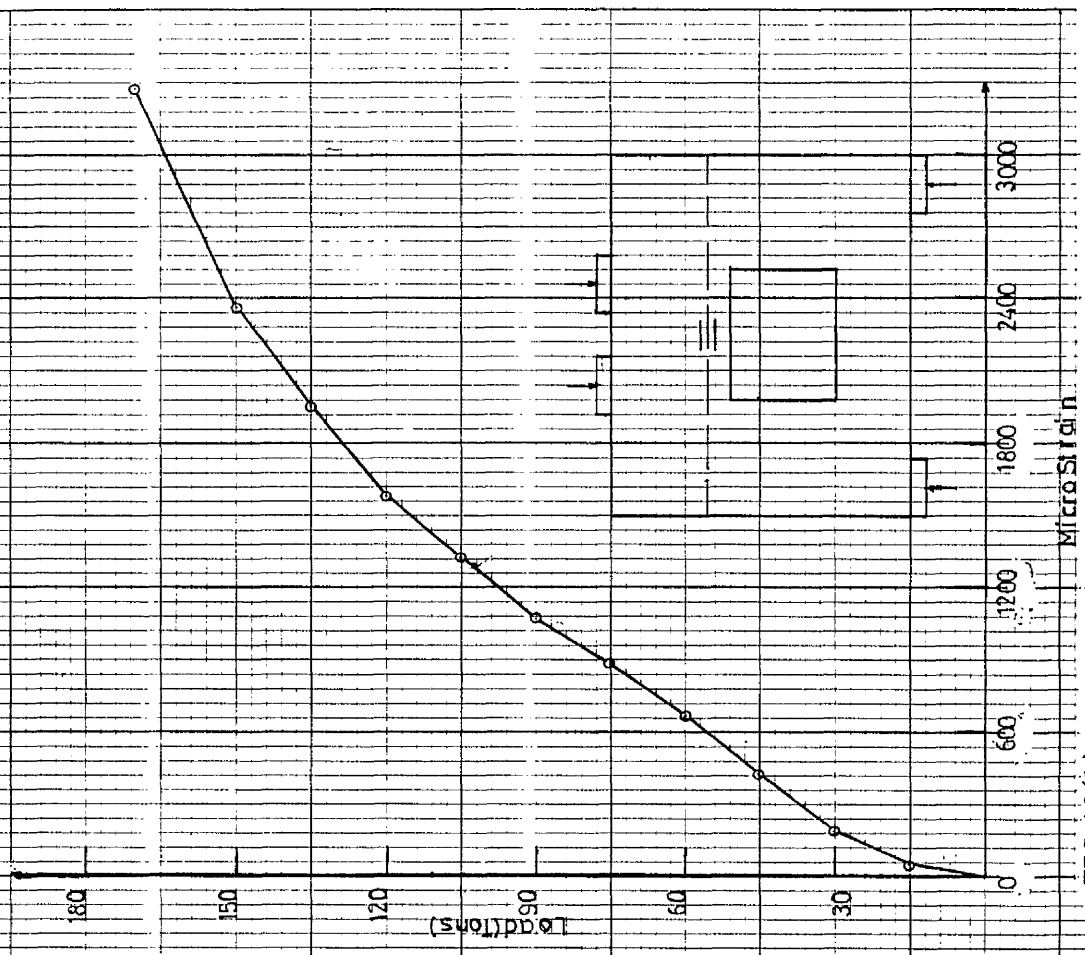


FIG. A2(b). 7. AVERAGE STRAIN DISTRIBUTION ALONG THE BOTTOM BARS (ABOVE THE OPENING) OF BEAM B7

REFERENCES

1. ACI Committee 318 ; "Building Code Requirements for Reinforced Concrete (ACI 318-77)"., American Concrete Institute, Detroit, Michigan 48219. 1977.
2. Comité Européen du Béton-Federation Internationale de la Précontrainte; "International Recommendations for the Design and Construction of concrete structures", Appendix 3 Deep beams, Cement and Concrete Association, London. June 1970.
3. British Standard Institution ; "Code of Practice for the structural use of Concrete (CP110 : Part 1)"., British Standards Institution, London. November 1972.
4. Ove Arup and Partners; "The Design of Deep Beams in Reinforced Concrete". Construction Industry Research and Information Association, London, 1977, CIRIA Guide 2.
5. Kong, F.K. et al.; "The Design of Reinforced Concrete Deep Beams in Current Practice", The Structural Engineer, Vol.53 (No.4), April 1975. Pages 173-180.
6. Kong, F.K. et al.; "Diagonal Cracking and Ultimate loads of Lightweight Concrete Deep Beams", Journal American Concrete Institute, Proceedings Vol. 69 (No.8), August 1972. Pages 513-521.
7. Kong, F.K. and Singh, A. ; "Shear strength of lightweight concrete Deep Beams subjected to Repeated Loading. Shear in Reinforced concrete. Detroit, American Concrete Institute, 1974. ACI-ASCE Special Publication SP-42, Vol. 2. Pages 461-476.

8. Kong, F.K. and Robin, P.J. ; "Shear Strength of Reinforced Concrete Deep Beams". Concrete, Vol.6 (No.3), March 1972, Pages 34-36.
9. Kong, F.K., Robin, P.J. and Cole, D.F. ; "Web Reinforcement effects on Deep Beams". Journal American Concrete Institute, Proceedings, Vol.67 (No.12), December 1970, Pages 1010-1017.
10. Kong, F.K. and Sharp, G.R. ; "Shear Strength of Lightweight Reinforced Concrete Deep Beams with Web Openings". The Structural Engineer, Vol.51 (No.8), August 1973, "Pages 267-275.
11. Booth, E. ; "Deep Beams", Ove Arup Partnership Research and Development Group Technical Paper 11, September 1971.
12. Franz.Dischinger.; "Beitrag zur Theorie der Halbscheibe und des Wandartigen Balkens". International Association for Bridge and Structural Engineering, Zurich, Vol. 1, 1932.
13. Chow, L., Conway, H.D. and Morgan, G.W. ; "Analysis of Deep Beams", Journal of Applied Mechanics, Trans. ASME, Vol. 18 (No.2), June 1951.
14. Chow, L., Conway, H.D. and Winter, G. ; "Stresses in Deep Beams". Proceedings American Society of Civil Engineering (Proc. ASCE), Structural Division, Vol. 78 (Separate No.127) May 1952.
15. Uhlman, H.L.B. ; "The Theory of Girder Walls with Special Reference to Reinforced Concrete Design". The Structural Engineer, Vol. 30 (No.2), August 1952.

16. Guzman, A.M. and Luisoni, C.J. ; "Solution Variacional del problema de la viga rectangular simplemente apoyada de gran altura". Cienciay Technica, Bueonos Aires 111, 119 (1948).
17. Archer, F.E. and Kitchen, E.M. ; "Strain Energy Methods for the Solution of Deep Beams", Civil Engineering and Public Works Review, Vol. 52 (No.618), December 1957.
18. Sundara Raja Iyengar, K.T. ; "Analysis of Deep Beams". Proc. 2nd Congr. Theoretical applied Mechanics, New Delhi (1956).
19. Casewell, J.S. ; "Stresses in short Beams". Engineering 12 and 19, Vol. 178, Nos. 4633-4634, Part 1, Pages 625-628, Part 2, Pages 656-658, November 1954.
20. Kaar, P.H. ; "Stresses in Centrally Loaded Deep Beams", Proceeding Society for Experimental stress Analysis, Vol.15 (No.1), 1957, Pages 77-84.
21. Albritton, G.E. ; "Review of the Literature Pertaining to the Analysis of Deep Beams". Technical report No.1-701, U.S. Army Engineer Waterways Experiment Station, Vicksburg, Mississippi, November 1965.
22. Leonhardt, F. and Walther, R. ; "Deep beams". Wandartige Triger, Deutscher Ausschus Fur Stahlbeton, Bulletin 178, Berlin 1966. CIRIA Translation, January 1970.

23. De-Paiva, H.A.R. and Siess, C.P. ; "Strength and Behaviour of Deep Beams in Shear". Proceeding American Society of Civil Engineers, Journal Structural Division, Vol. 91 (No.ST5), October 1965, Pages 19-41.
24. Kani, G.N.J. ; "Basic Facts Concerning Shear Failure". Journal American Concrete Institute, Proceedings, Vol.63 (No.6) June 1966.
25. Kong, F.K., Robin, P.J., Kirby, D.P. and Short, D.R. ; "Deep Beams with Inclined Web Reinforcement". Journal American Concrete Institute. Proceedings, Vol. 69 (No.3), March 1972, Pages 712-716.
26. Kong, F.K. and Robin, P.J. ; "Web Reinforcement Effects on Lightweight Concrete Deep Beams". Journal American Concrete Institute, Proceedings Vol. 68 (No.7) July 1971, Pages 514-520.
27. Lin, C.K. ; "Ultimate Strength Design of Deep Beams". University of Glasgow, M.Sc Thesis 1979.
28. Loupa, A., Siess, C.P. and New mark, N.W. ; "Strength in shear of Reinforced Concrete Beams". Engineering Experiment Station, Bulletin No. 428, University of Illinois, Urbana III, March 1959.
29. Ramakrishnan, V. and Ananthanarayana, Y. ; "Ultimate Strength of Deep Beams in Shear". Journal American Concrete Institute, Proceeding, Vol. 65 (No.2), February 1968, Pages 87-98.

30. Kong, F.K., Robin, P.J., Singh, A. and Sharp, G.R. ; "Shear Analysis and Design of Reinforced Concrete Deep Beams". The Structural Engineer, Vol. 50 (No.10), October 1972, Pages 405-409.
31. Sharp, G.R. ; "Reinforced Concrete Deep Beams with Web Openings". University of Nottingham, Ph.D Thesis, 1977.
32. Kubik, L.A., ; "Strength and Serviceability of Reinforced Concrete Deep Beams". University of Cambridge, Ph.D Thesis, 1978.
33. Kong, F.K. and Sharp, G.R. ; "Structural Idealization for Deep Beams with Web Openings". Magazine of Concrete Research, Vol. 29 (No.99), June 1977, Pages 81-91.
34. Kubik, L.A. ; "Predicting the strength of reinforced Concrete Deep Beams with Web Opening". Proceedings Institution of Civil Engineers, Vol. 69, Part 2, December 1980, Pages 939-958.
35. ACI Committee Report. "Commentary on Building Code Requirements for Reinforced Concrete (ACI 318-71)". Detroit, Michigan 48219, American Concrete Institute, 1977.
36. Portland Cement Association, "Design of Deep Girder", Concrete Information. No.ST66, 1946.
37. Mosley, W.H. and Bungey, J.H., ; "Reinforced Concrete Design" The Macmillan Press Limited, 1976.

38. Green, D.R., Bhatt, P., Mittra, R.K. and Lin, C.K. ; "Aspects of Serviceability Limit State of Reinforced Concrete Structures". Research Seminar, Cement and Concrete Association Training Centre, September 1977.
39. Row, R.E., Chanston, W.B. and Best, B.C.; "New Concepts in the Design of Structural Concrete". The Structural Engineer, Vol. 43 (No.12), December 1965.
40. Regan, P.E. and Yu, C.W. ; "Limit State Design of Structural Concrete" Chatto and Windus, London 1973.
41. Nielson, M.P. ; "On the Strength of Reinforced Concrete Discs". Copenhagen, Acta Polytechnica Scandinavica, Civil Engineering and Building Construction Series, No.70, 1971.
42. Evans, R.H. and Kong, F.K., ; "Reinforced and Prestressed Concrete". Thomas Nelson & Sons Ltd., 1975.
43. Martin, J.B. ; "Plasticity". M.I.T. Press 1975.
44. Nielson, M.P. ; "Yield Conditions for Reinforced Concrete Shells in the Membrane State". Non-classical shell problems ; IASS Symposium, Warsaw, 1963. Pages 1030-1038.
45. Subedi, N.K., ; "Design of Reinforced Concrete Sections Subjected to Membrane Forces". The Structural Engineer, Vol.53 (No.7) July 1975, Pages 289-292.

46. Morley, C.T. ; "Optimum Reinforcement of Concrete Slab Elements against Combinations of Moments and Membrane Forces". Magazine of Concrete Research, Vol. 22 (No.72), September 1970, Pages 155-162.
47. Clark, L.A. ; "The Provision of Tension and Compression Reinforcement to Resist In-plane Forces". Magazine of Concrete Research, Vol. 28 (No.94). March 1976, Pages 3-12.
48. Phillips, D.V. ; "Non Linear Analysis of Structural Concrete by Finite Element Methods". University of Wales, Swansea, Ph.D Thesis, 1973.
49. ICES-STRU DL II, ; "The Structural Design Language". Engineering User Manual, Vol. 2.
50. B.S. 882 and 1201 : 1965 ; "Specification for Aggregates from Natural sources for concrete". London, British Standards Institution, 1965.
51. Rockey, K.C. et al. ; "Panel for standard Practices for Testing". DOE-TRRL Working Group on Long-term Research into steel Box Girder Bridges, Report of the Panel, January 1975.
52. ELECTMATIC Split Cabinet, 2000 pounds capacity ELECTMATIC split capacity, Universal Testing Machine Model 51, TINUS OLSEN testing machines Company Willow Grove, Penna.

53. Losenhausen 10,000 kN Universal Class A Testing Machine, UHP
1000 type, Mohr & Feblerhaff-Mannheim, Germany, Allemagne.
54. Akthem Al-Manaseer.; "Non-Linear Finite Element Analysis of
Reinforced Concrete Structures." University of Glasgow,
Ph.D Thesis, 1982.

ERRATA

<u>Page</u>	<u>Line</u>	<u>Read</u>	<u>For</u>
1	11	vierendeel	virendeal
1	22	code and in	code. In
6	3	ratio below	ratio is below
40	25	pattern	patterns
48	11	horizontal reinforcement ratios	horizontal ratios
48	13	-do-	-do-
54	7	Weighed	Weighted
54	23	Tor	Tar
61	22	cracks	crack
62	20	they are also	they also
67	4	was	is
71	12	it was based	it based
71	21	it seems that	it seems
73	4	beam	beams
73	21	2	1
75	6	programme	analysis
76	17	can be	was
78	2	equation 5.1 (see ch.5)	equation 5.1
78	21	proposed	above